STUDY REPORT
ON
LATERITIC SOIL FOR ROAD CONSTRUCTION
TECHNICAL
STAGE II

MARCH, 1985

DEPARTMENT OF HIGHWAYS
MINISTRY OF COMMUNICATIONS, THAILAND

JAPAN INTERNATIONAL COOPERATION AGENCY

STUDY REPORT ON LATERITIC SOIL FOR ROAD CONSTRUCTION TECHNICAL STAGE II MARCH 1985

STUDY REPORT
ON
LATERITIC SOIL FOR ROAD CONSTRUCTION
TECHNICAL

STAGE II

MARCH, 1985

DEPARTMENT OF HIGHWAYS
MINISTRY OF COMMUNICATIONS, THAILAND

JAPAN INTERNATIONAL COOPERATION AGENCY

PREFACE

Due to geological conditions in Northeast Thailand, limited suitable rock quarries have caused insufficient road construction materials for a long time. This problem can be solved by stabilizing available local material, lateritic soil, to substitute crushed rock base course.

Many research programmes have been done on lateritic soil-cement stabilization for several years. The first lateritic soil-cement test road was constructed by Siam Cement Company on Highway Rt. No. 24 in Ubonratchatani in Northeast region. Since then, about 1,400 kilometers of soil-cement roads have been constructed in this region. Research evaluation showed that most of the soil-cement roads performed well under low traffic conditions.

Research programme between Thai Government through Department of Highways, Ministry of Communications and Japanese Government through Ministry of Construction, Japan International Cooperation Agency (JICA) and International Engineering Consultants Association (IECA) started from December, 1981 to March, 1984. A test road, with soil-cement base course, was constructed on National Highway Rt. No. 12 between the City of Khon Kaen and Chum Phae District, with an ADT of about 4,000 vpd, in Northeast Thailand. JICA and IECA have provided some necessary equipments for this project.

The study is aimed to obtain further information of the performance of lateritic soil-cement road under heavy traffic.

It is divided into 3 stages:

Stage I : the soil-cement base construction and its performance evaluation

Stage II : the asphaltic concrete surface construction and its performance evaluation

Stage III : the long term performance evaluation.

The Stage I study was the joint research programme and the Report was completed in March, 1984.

Asphaltic concrete surface construction finished in November, 1983. Sensors had been installed on top and inside the surface course, respectively. The performance of surface course such as cracks, roughness and rut depth had been checked. Pavement evaluation had been done by Present Serviceability Index (PSI). Temperature, stresses and strains have been analyzed. The conclusion of Stage II Study is presented in this report. It is hoped that the results of this research project will be valuable for future research and application.

The report is accomplished under the cooperation of Japan International Cooperation Agency (JICA) and Department of Highways. Mr. Yoshiaki Murao, the expert from JICA, provided some technical cooperation to the programme. Dr. Teeracharti Ruenkrairergsa, Department of Highways, provided some guidance and technical review throughout the project. The draft report was prepared by Mr. Wirote Panthawanggoon and reviewed by Dr. Pichit Jamnongpipatkul, Department of Highways. Their hard working are acknowledged.

C. Saligupta

(Chamlong Saligupta)
Director-General
Department of Highways
Ministry of Communications
Thailand

CONTENTS

Page

Page

LIST OF TABLES

LIST OF FIGURES

I. INTRODUCTION

I.1 General

Lateritic soil-cement has been used for road construction in Thailand for almost two decades. However, only in recent years that performance of lateritic soil-cement roads has been extensively studied (Ranananda et al., 1983, Ruenkrairergsa, 1982, 1983).

In order to have a better understanding of the behavior of soil-cement roads, a test section with base course, consisting of lateritic soil treated with varied cement content and two types of thickness, has been constructed. The test section is located on Highway Route No 12 between City of Khon Kaen and Chum Phae District (Fig. I-1). Construction of the lateric soil-cement base and the asphaltic concrete surface of the test section was completed in March and November, 1983, respectively.

During the base course construction, several sensors including strain gages, pressure cells and thermo-couples, were installed beneath the base and subbase course. After the base course construction, but before the surface construction, periodic measurements of stress-strain and deflection under a specified load as well as the temperature variation within the pavement structure were made. The collected data were analyzed and reported in our Stage I report.

During the surface construction in November, 1983, additional strain gages and thermo-couples were installed underneath the surface. The Stage II study, then, began after the

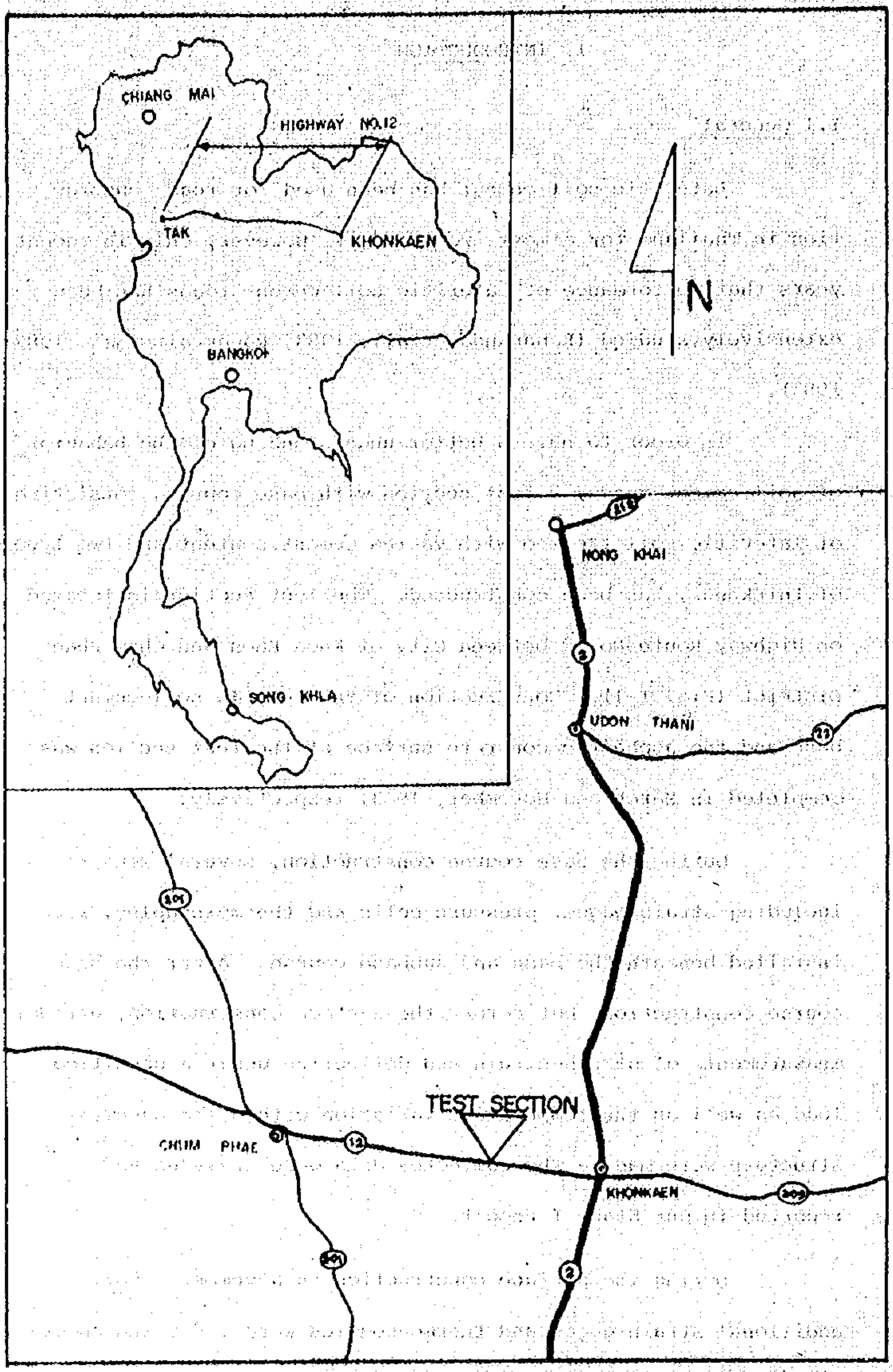

FIG I-1 LOCATION OF TEST SECTION

surface construction.

Flow chart of the study is shown in Figure I-2.

I.2 Purposes of the Study

The objectives of the study is outlined in the Stage I report and is reiterated here as follows:

(1) To study the performance of lateritic soil-stabilyzed with low and high ranges of cement content for being used as a base course of moderately traffic roads.

(2) To study the strength development of the soil-cement base while serving the actual traffic.

(3) To study the induced stress distribution underneath the asphaltic concrete layer.

(4) To study the deflection of surface and soil-cement base under loading.

(5) To study about the probable substitution ratio of soil-cement base as compered to asphaltic concrete.

(6) To check the design method as being employed (CPA method).

(7) To study about the long term performance of the soil-cement road.

I.3 Outline of Stage II Study

Stage II study began after the surface construction in November, 1983. Additional strain gages and thermo-couples were installed for this study.

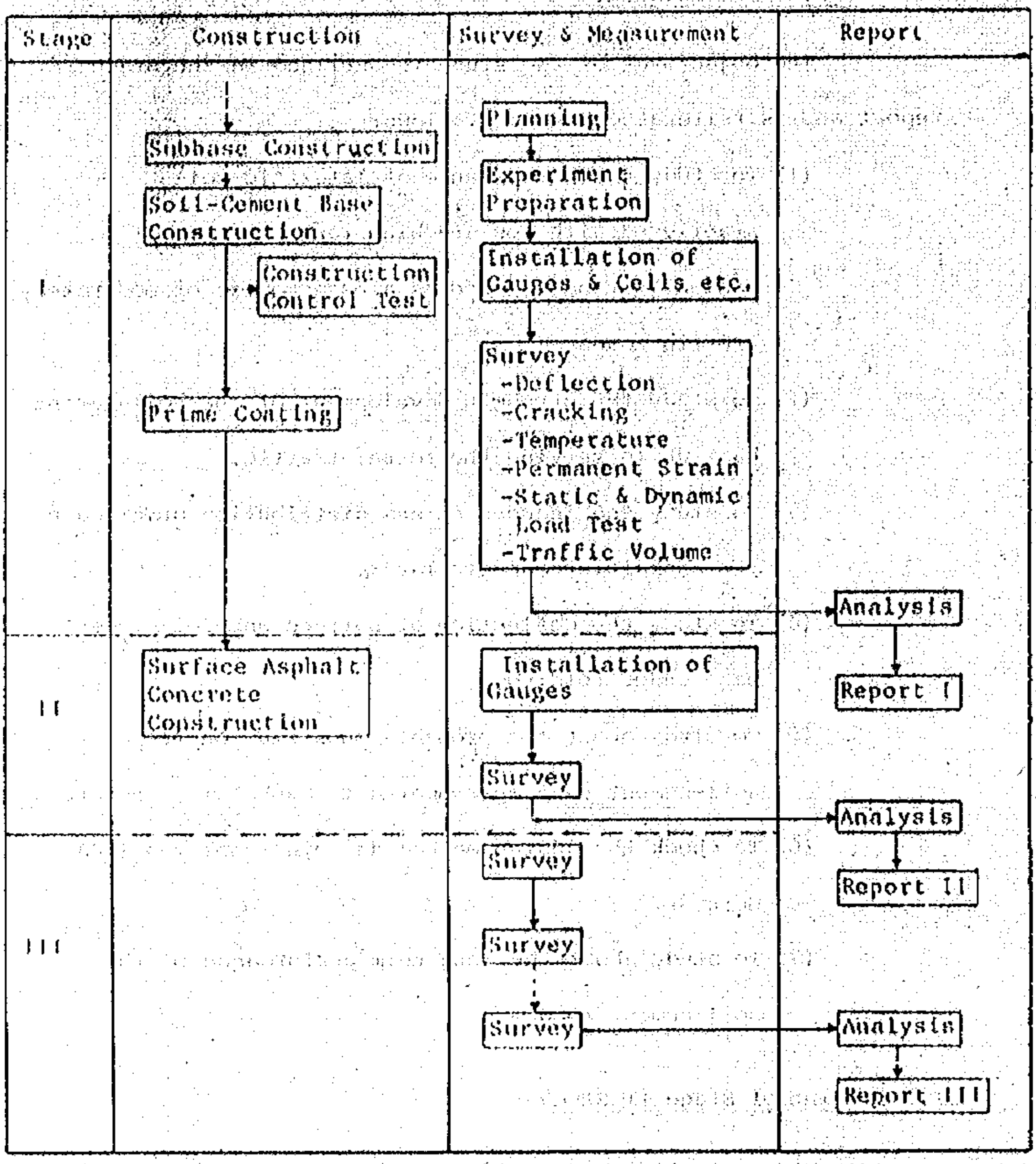

Fig. I-2 Flow Chart of this Study

In this study, as well as, in the Stage I study, the stress-strain variation within the pavement structure under different conditions (for examples, different base thickness, % cement content, loading conditions) was measured using Static Strain Indicator and Dynamic Amplifier with Pen Recorder. The temperature variation within the pavement structure was measured using Pocket Thermometer. The Benkelman Beam deflection was recorded for the surface deflection. Description of the instruments was discussed in detail in our Stage I report.

In addition, Profilometer and Levelling method have been used to measure the roughness and cross-section (rutting depth) of the surface. Selected cored soil-cement samples from the test section have been tested to determine unconfined compressive strength and stress-strain relationship.

I.4 Scope of This Report

In this report, Chapter II summarized the Stage I Report. Chapter III presented the criteria of asphaltic concrete surface including design, construction and the results of material properties. Details of sensors embedments beneath the surface course was mentioned in Chapter IV. Chapter V presented the results of analysis of the measuring data including the results of Deflection, Roughness and Cross-Section Form of Pavement, Crack Results, Temperature Measurements, Static and Dynamic Vertical Stresses, Permanent Strain, Static and Dynamic Horizontal Stresses and Stress-Strain Relationship of Cored Samples. Chapter VI was the conclusion of this report.

II. SUMMARY OF STAGE I REPORT

II.1 Test Road Detail

(1) The typical cross section of the test road is given in Fig. II-1. The pavement structure consists of the subgrade, selected material, subbase, soil-cement base and surface.

The roadway width is 6.5 m., road width is 11.0 m. The Standard crossfall is 2.5 %. The embankment's side slope is 2:1.

(2) The ADT between Khon Kaen and Chum Phae is estimated at 3,000 to 4,000 vehicles in two opposite directions. Large vehicles are supposed to account for 30 percent of all the traffic.

The cement content and thickness varied in 8 test sub-sections. Earth pressure cells, embedment strain gages, and thermo-couples were installed to understand the pavement body behavior (Fig. II-2 and 3).

Lateritic soils were mixed in the field with cements and water by road construction equipment.

II.2 Conclusions in Construction and Test in Stage I

(1) Material Properties. In the design stage, Good Soil and Poor Soil were classified according to their P.I. To develop field strength of 17.6 ksc. (250 psi.), cement contents of 4.3 % and 12.8 % were needed for Good Soil and Poor Soil, respectively. However, during the construction it was not practical to classify field materials as Good Soil and Poor Soil as expected. As a result, only one type of material was used instead of 2 types. The filed material possessed physical properties intermediate

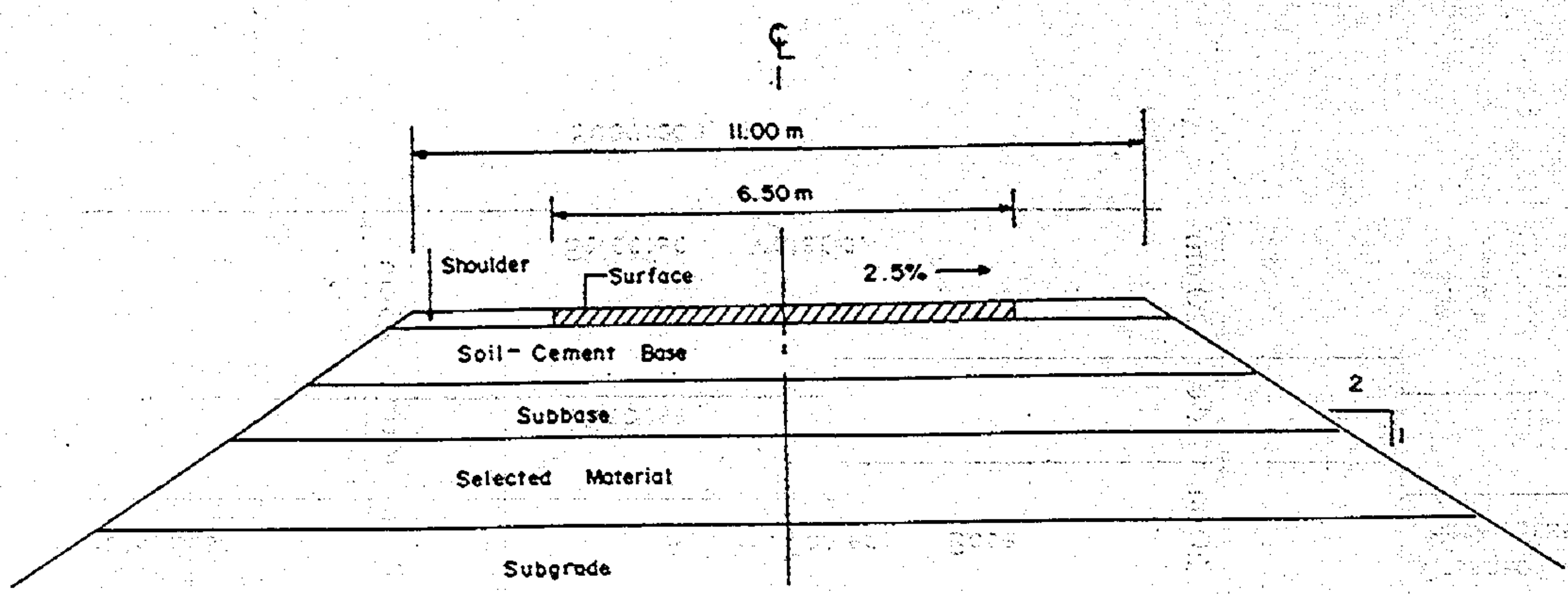

Fig. II-1 Typical Cross Section

Test Condition

Subsection No.	1	2	3	4	5	6	7	8
Material for Base	Poor Soil	Good Soil	Good Soil	Good Soil	Good Soil	Good Soil	Good Soil	Poor Soil
Thickness of Base	15 cm	15 cm	15 cm	15 cm	20 cm	20 cm	20 cm	20 cm
Target Strength(lb/in²)	250	250	350	250	250	350	250	350
Cement Content(%)	12.8	10.0	7.0	4.3	4.3	7.0	10.0	12.8

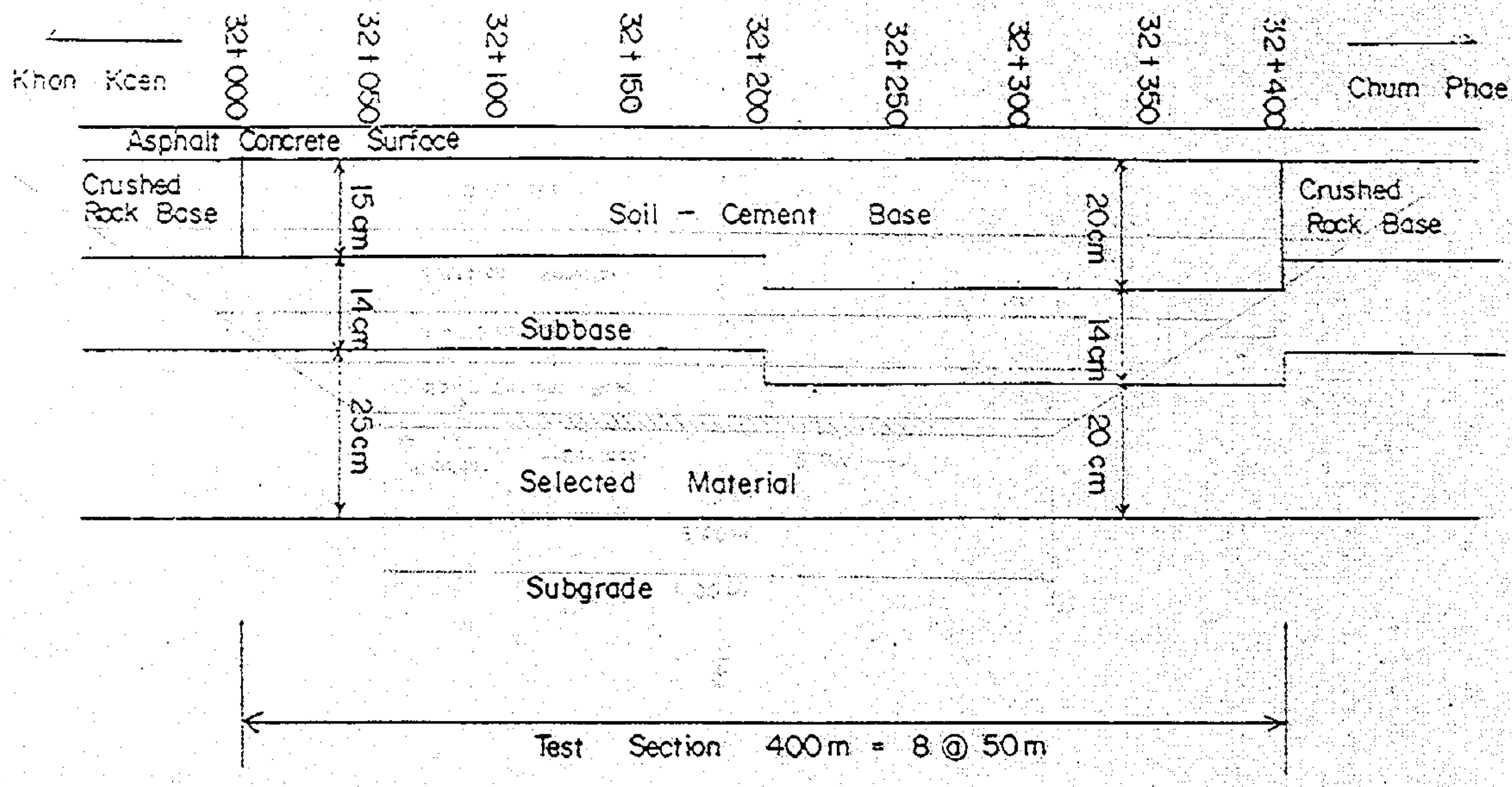

Fig. II-2 Pavement Test Section

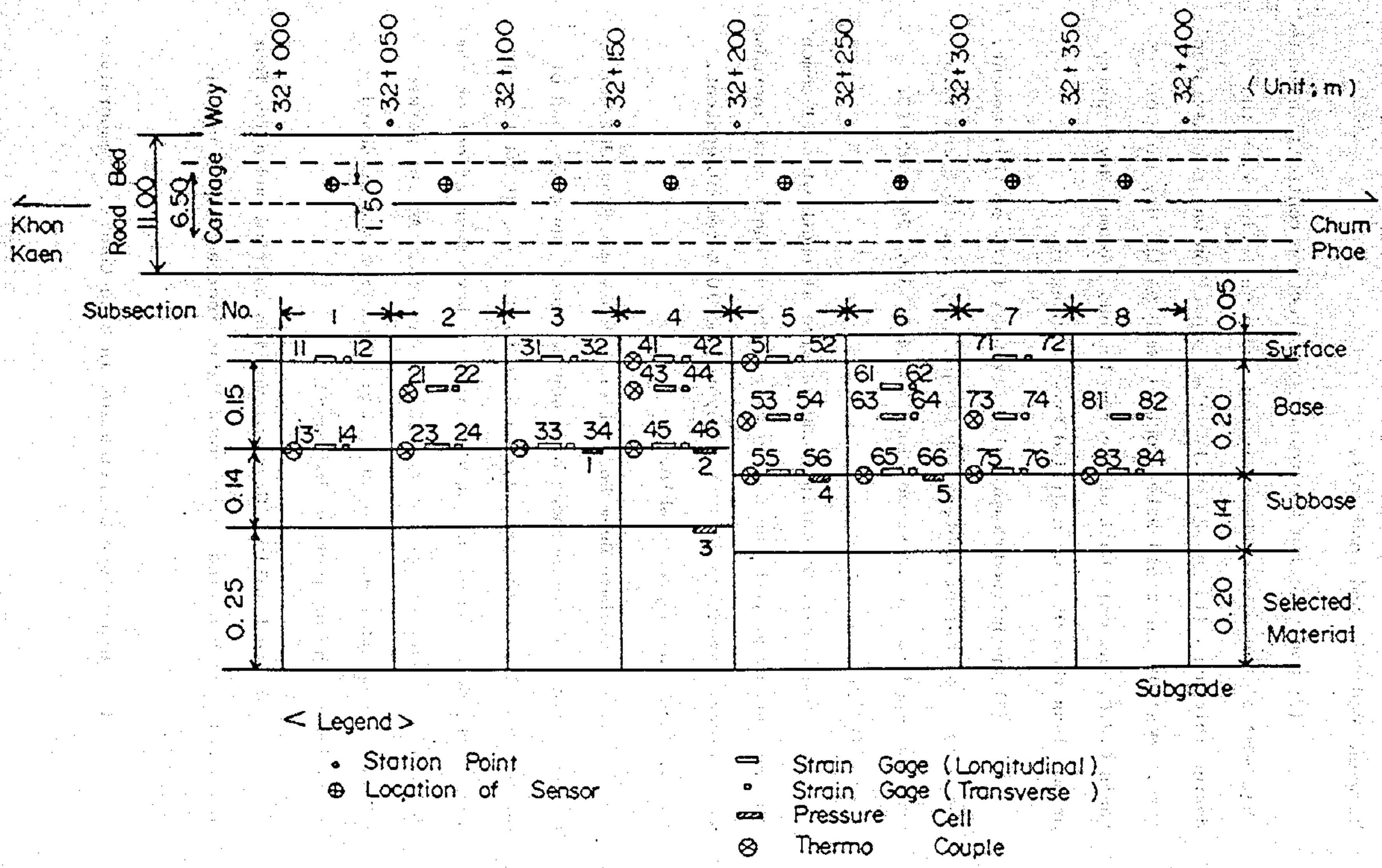

Fig.II - 3 Sensor Embedment Location

between Good Soil and Poor Soil.

(2) Construction Controls. Construction controls indicated that most of the base course thickness were satisfied with the design thickness (15 and 20 cm.). The compaction was not satisfactory. Most of the field water content were on the dry side of Lab's O.M.C. and only half of the samples had maximum dry density of not less than 95 % of Modified Proctor Density.

(3) Unconfined Compressive Strength (UCS) of Soil Cement. The percent of cement contents by weight 4.3, 7.0, 10.0 and 12.8, were designed to use in subsections No. 4&5, 3&6, 2&7 and 1&8, respectively.

In general, unconfined compressive strength of soil-cement samples increased with the curing time. The strength also increased with percent cement up to 10 %. Beyond the 10 % cement content, the strength was unpredictable.

(4) Benkelman Beam Deflection. Benkelman Beam deflection of the surface of soil-cement base course under the axle load of about 12.3 (27,000 lb) varied from 0.10 to 0.30 cm. (0.04 to 0.12 in.). The duration of curing time did not have much effect on the deflection, but the percent cement content did. As the percent cement content increased to 10 %, the deflection and standard deviation of the deflection decreased.

(5) Crack Ratio. Crack survey was carried out after four and a half month curing. The crack ratio increased with cement content.

(6) Temperature Distribution in Base Course. Temperature

distribution was measured on the same day of the crack survey. In general, the temperature decreased with depth from the surface.

(7) Static Vertical Stress. Static vertical stress at the bottom of the base tended to decrease with the increase in cement content, curing time, and base thickness. Load dispersion effects, the ratio of stress at the bottom of base to that at the bottom of subbase, were about five to ten.

(8) Dynamic Vertical Stress. In general, the dynamic vertical stresses decreased with the increase in curing time, cement content, and base thickness. However, there were some exceptions. The relationships with speed peaked within the range of 0 to 10 km/hr. and decreased and flattened as the speed increased.

(9) Accumulated Permanent Strain. Strain gages were embedded on trial both in longitudinal and transverse directions (parallel and perpendicular to center line, respectively). The accumulated strain developed in the gages were recorded. The relation to curing time was divided into 6 stages as follows.

(a) Strain occurring

(b) levelling off

(c) reducing slowly into a tensile condition

(d) reducing rapidly

(e) exceeding the measuring range of the gage

(f) breaking of the gage

(10) Horizontal Stresses Under Static Loading. The horizontal stresses within and the bottom of the soil-cement base showed a tendency for compressive stresses to occur at the upper

part and tensile stresses to occur at the lower part of the base. The transverse stress data were more scattered than the longitudinal ones.

II.3 Conclusion in Supplementary Analysis in Stage I

(1) Comparison of Measured Values with Computed Value by Multi-Layer Elastic Theory. The vertical pressures measured by pressure cells showed higher values than computed values by the multi-layer elastic theory except for No. 4 pressure cell.

It was evident by the multi-layer elastic analysis that the thickness of soil-cement base course influences the vertical pressure at the bottom of base course but it had little influence at the top of subgrade.

(2) Estimate of Elastic Modulus of Soil-Cement Base. It was difficult to value the elastic modulus of soil-cement base course from the measured vertical pressures because the measurements were very scattered.

However, the elastic modulus of soil-cement base course was valued as E = 2,000 to 3,000 kgf./sq.cm. by Multi-Layer elastic analysis, using the adjusted deflections.

(3) Comparison of Measured Values with the Results of Finite Element Analysis. It was confirmed qualitatively that the measured stresses and strains agree with the results of Finite Element Analysis under the condition of cracks in the base course.

(4) Estimate of Durability of Test Road by Shell Design Criteria. The durability of the test road was investigated by the

Shell design criteria and it was considered that the test road is suitably durable.

(5) Proposal to Reduce the Elastic Modulus of Soil-Cement. It was pointed out that even though the elastic modulus was reduced i.e. elastic modulus of soil-cement base was assumed 1,500 kgf./sq. cm., it was considered that the pavement was safe when the base course was 25 cm. thick and the surface was constructed by dense Bitumen Macadam.

III. ASPHALTIC CONCRETE SURFACE

III.1 Types and Composition of Mix

Asphaltic concrete could be classified according to the size of aggregates and amount of asphalt cement use. Each mix design will be suitable for one particular job and objective of the work. Table III-1 shows types of asphaltic concrete and probable amount of asphalt cement (Thum-Umnanysuk,1982).

III.2 Marshall Method of Mix Design

In the Marshall method, test specimen of 2-1/2 in. height x 4 in. diameter, prepared according to a specified procedure, are used. There are three principal features in the mix design (1) bulk specific gravity determination, (2) density, voids analysis, and (3) a stability-test of the compacted test. The stability is the maximum load resistance in pounds which the standard test specimen will develop at 140°F, when tested, and the flow value is the total movement, in unit of 1/100 in. occuring in the specimen between no load and maximum load during the stability test.

To determine optimum asphalt content, the test will be varied by 1/2 % increment of asphalt content, with at least two asphalt contents above and two below optimum. Usually three to five test specimens are prepared for each asphalt content used. Asphalt may be expressed as a percentage by weight of total mix or as a percentage by weight of dry aggregate.

Table III-2 indicates the Marshall Design Criteria, presently adopted by DOH. The criteria were recommended by the

TABLE III-1 TYPES AND COMPOSITION OF ASPHALTIC CONCRETE

DESIGNATION	GRADE A (DENSE GRADE)				GRADE B (COARSE GRADE)					GRADE C (OPEN GRADE)		
	A-1	A-2	A 3	A-4	B-1	B-2	B-3	B-4	B-5	C-1	C-2	C-3
USE	SURFACE BASE	SURFACE BASE	SURFACE BASE	BASE	BASE	SURFACE LEVELING BASE	BASE	BASE	BASE	SURFACE	SURFACE	SURFACE
RECOMMENDED MINIMUM COMPACTED DEPTH FOR INDIVIDUAL COARSE	1"	1 1/2"	2"	3"	1"	1 1/2"	1 1/2"	2"	3"	3/4"	1"	1 1/2"
SIEVE SIZE	PERCENT PASSING BY WEIGHT											
1 1/2"				100					100			
1"			100	80-100				100	75-100			
3/4"		100	80-100	70-90		100	100	75-100	60-85			100
1/2"	100	80-100	—	—	100	75-100	75-100	—	—		100	70-100
3/8"	80-100	70-90	60-80	55-75	75-100	60-85	60-85	45-70	40-65	100	70-100	45-75
#4	55-75	50-70	40-65	45-62	35-55	30-50	30-50	30-50	30-50	45-85	20-40	20-40
#8	35-50	35-50	35-50	35-50	20-35	20-35	20-35	20-35	20-35	5-20	5-20	5-20
#30	18-29	18-29	19-30	19-30	10-22	10-22	5-20	5-20	5-20	—	—	—
#50	13-23	13-23	13-23	13-23	6-16	6-16	3-12	3-12	3-12	-	-	-
#100	8-16	8-16	7-15	7-15	4-12	4-12	2-8	2-8	2-8	-	-	-
#200	4-10	4-10	1-8	1-8	2-8	2-8	1-4	1-4	1-4	1-4	1-4	1-4
ASPHALT CEMENT CONTENT % BY wt. TOTAL MIX	3.5-7.0				3.0-6.0					3.0-6.0		

TABLE III-2 MARSHALL DESIGN CRITERIA

Traffic Category	Heavy		Medium		Light	
Number of compaction blows each end of specimen	75		50		35	
Test property	Min	Max	Min	Max	Min	Max
Stability, all mixtures	750	—	500	—	500	—
Flow, all mixtures	8	16	8	18	8	20
Percent air voids						
Surfacing or levelling	3	5	3	5	3	5
Base	3	8	3	8	3	8
Percent voids in mineral aggregate (VMA)	Depends on nominal maximum particle size of aggregate used					

Asphalt Institute in 1962. Figure III-1 shows relationship between Minimum Voids in Mineral Aggregates (V.M.A.) and nominal maximum size of the compacted Dense-Graded Paving Mixture.

III.3 Design of the Test Section Surface

The surface of the test section consists of 5-cm. thick asphaltic concrete layer. The asphaltic concrete is designed using Marshall Method Laboratory tests are performed on a dense-graded asphaltic concrete mix to be used for the heavy traffic category. The aggregates used in the mix is shown in Fig.III-2, having the maximum nominal size 1/2 in. Figure III-3 shown the results of the tests following DOH'S practice, the asphalt content, as determined for the median of the limits for percent air voids, is used as the initial design value which is checked and adjusted to conform with other criteria.

From Figure III-3, the asphalt content providing 4 % air voids (median of 3-5 % range for the surface mix, Table III-2) is 5.2 %. At this asphalt content, other properties of the mix as determined from Fig. III-3 are as follow.

Density	99.7 % of optimum
Stability	2200 lbs.
Flow	11
Percent Voids in Mineral Aggregates	15

It will be noted that the stability value exceeds the minimum of 750 lbs. that the flow value is within the range of 8-16 and the percent voids in mineral aggregates exceed the

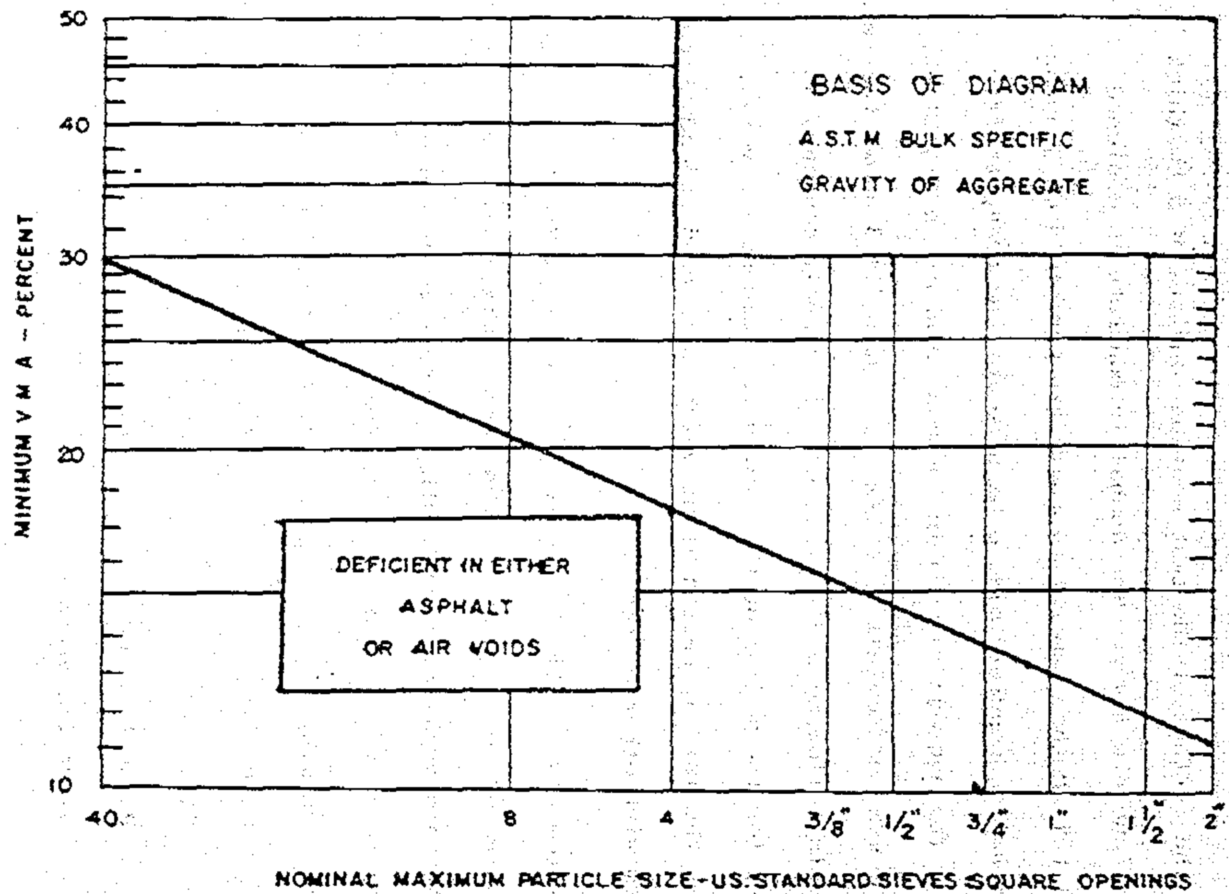

Figure III-1 Relationship Between Minimum Voids in Mineral Aggregate (V.M.A.) and Nominal Maximum Particle Size of the Aggregate for Compacted Dense-Graded Paving Mixtures

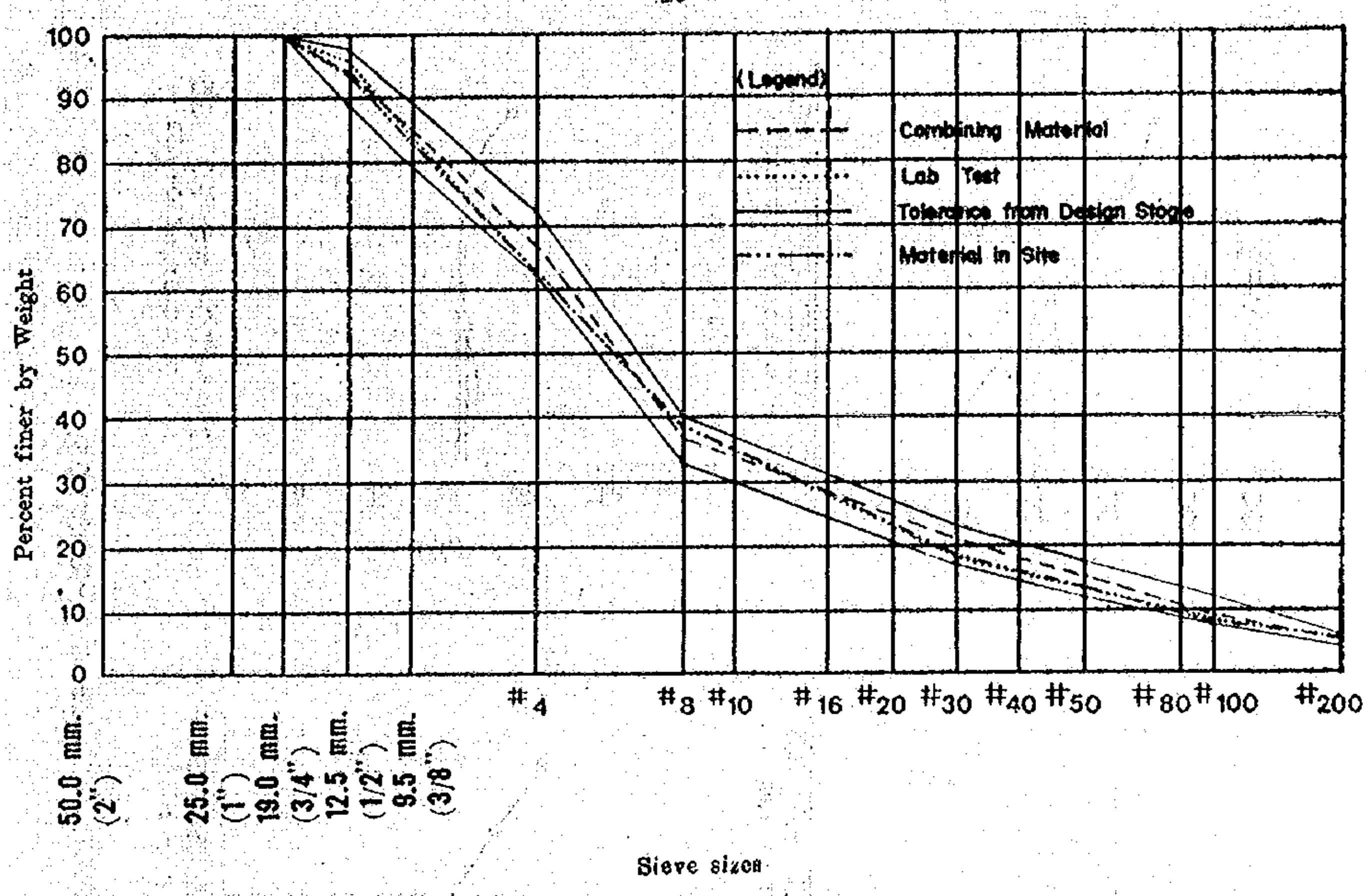

a) Sta. 31+825 — 32+600 , Right Lane

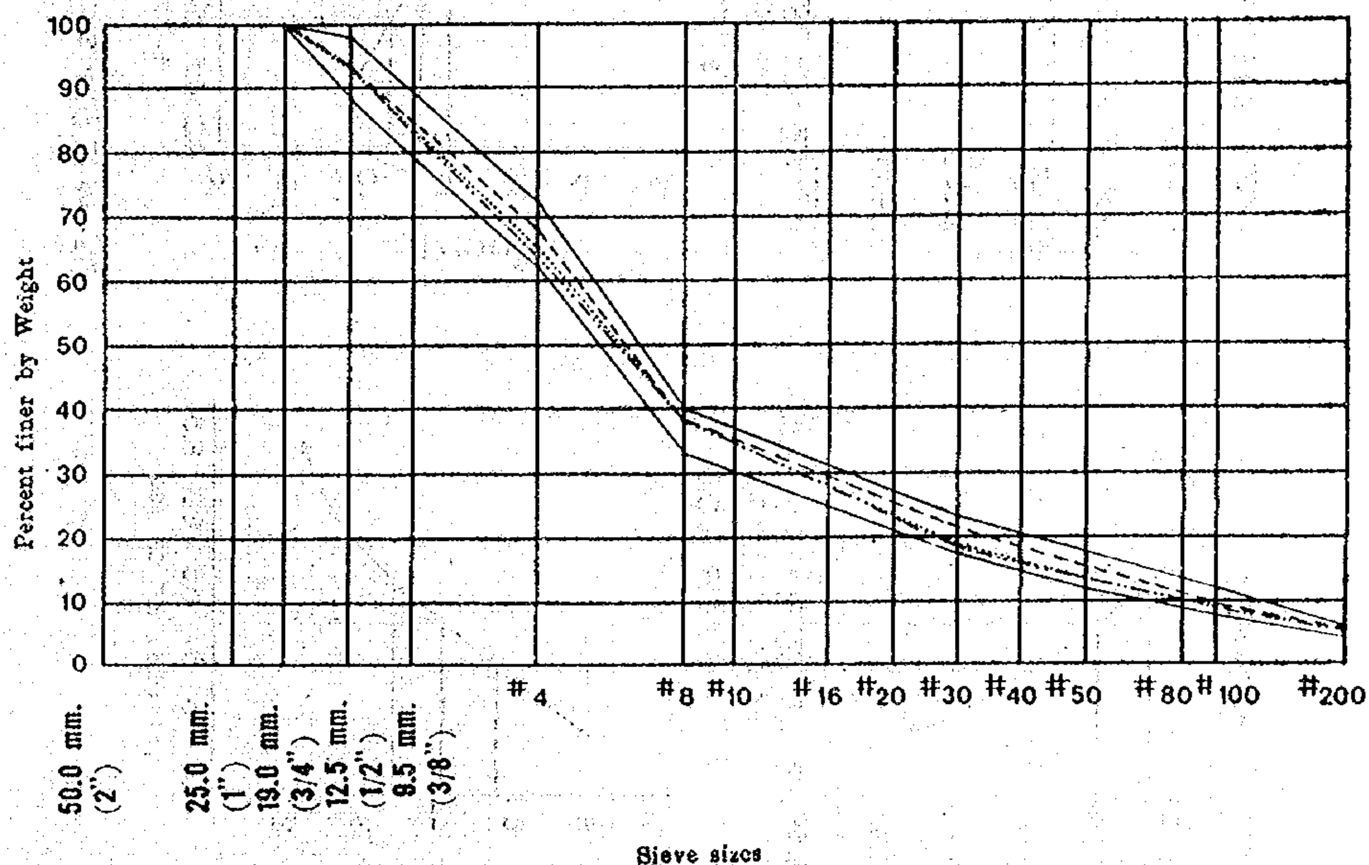

b) Sta. 31+700 — 32+675 , Left Lane

Fig. III-2 Gradation of Aggregate (After-construction)

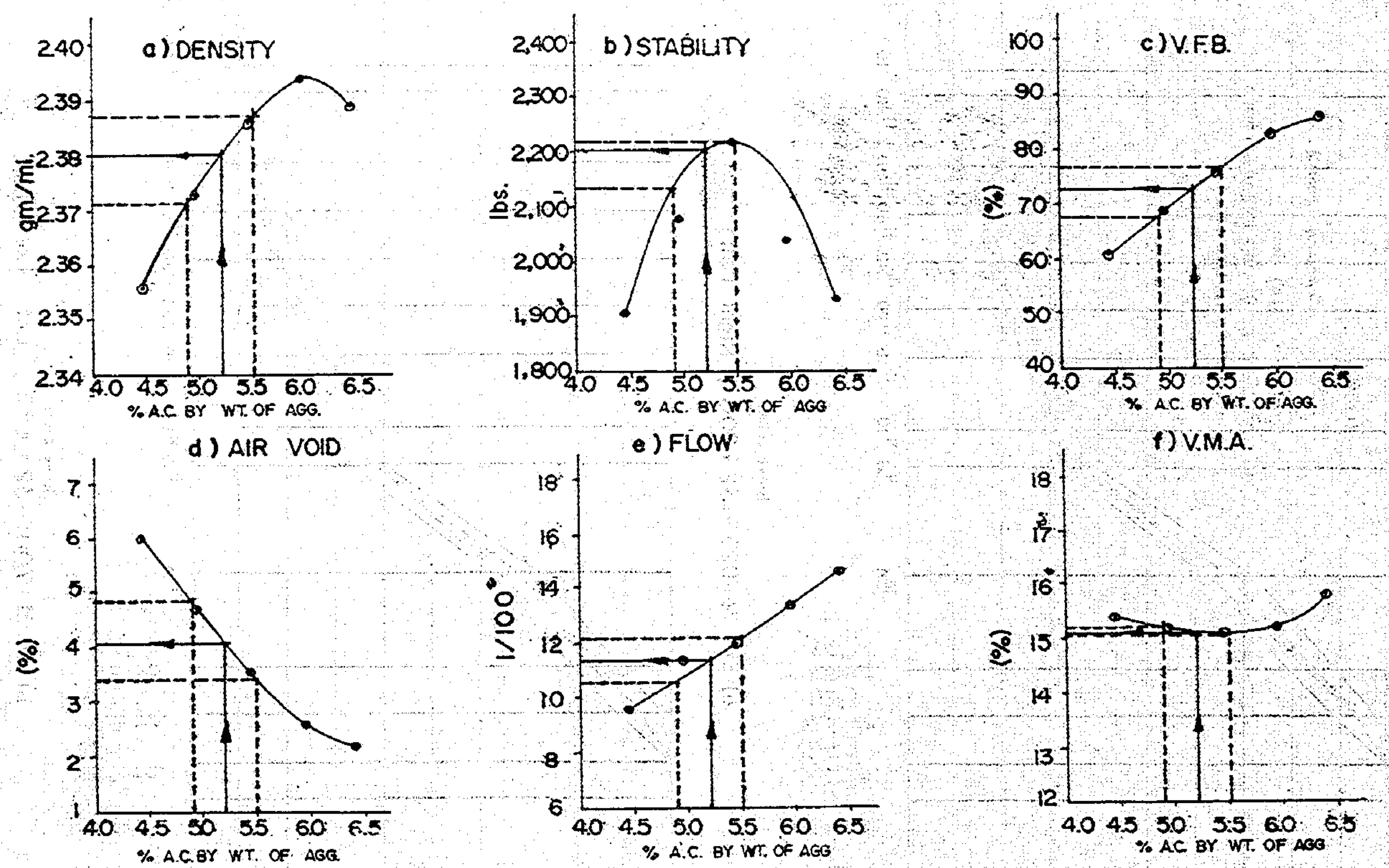

Fig. III - 3 Pre-construction Material Properties.

minimum of 14. The percent voids in the total mix is within the limits. Thus, the mix design have all test properties within the allowable limits.

There are some tolerance in the plant-mix design as follows

Aggregate passing	No. 4	and greater		= 5 %
	No. 8	"	"	= 4 %
	No. 30	"	"	= 3 %
	No. 200	"	"	= 1 %

Bitumen : 0.3 %

As a result the range of asphalt content allowed for the plant mix is between 4.9 and 5.5 %.

The properties of the mix for the design range are still within the allowable limits as indicated in Fig. III-3.

III.4 Surface Construction

III.4.1 Equipment

Followings are the list of equipments used for the surface construction.

- 1 continuous type asphaltic concrete plant
- 4 dump trucks
- 1 paver
- 2 steel rollers
- 1 self-propelled pneumatic tire roller

III.4.2 Plant Mix

In the plant mix, the amount of aggregates and asphalt cement content are controlled within the design range to specified temperature, 325 ± 15°F. for the aggregates and 333 ± 15°F. for the asphalt cement. The range of mixing temperture are 290-320°F.

III.4.3 Construction Procedure

The hot mix is hauled from the plant by dump trucks as spreaded at the test site by paver. Immediately after the spreading, compaction is performed. Followings are steps of compaction.

(1) Initial or Breakdown Rolling. Steel rollers used to compact the mix. The compaction is required until the smoothness and neatness of the surface are obtained. The smoothness and neatness of the surface are checked by using straightedge. Temperature during compaction must not be lower than 250°F.

(2) Second Rolling. Rubber tire roller is applied while the mix is still hot (temperature is in the range of 170 ± 15°F.). This steps mill induce maximum density to the asphaltic concrete surface.

(3) Finished Rolling. The surface must be made smooth using the steel rollers while the mix is still warm (temperature should be 140 ± 15°F.).

After the compaction, the surface is cured for 16 hours before open to traffic.

III.4.4 Properties of the Mix After Construction

The properties of Lab-compacted and field-compacted samples as compared with the properties in the design range are presented in Fig. III-4. It is indicated that field densities of both lanes are lower than the design range. However, they are greater than 98 % Maximum Density. The % Air Voids and V.M.A. of the field-compacted samples are greater and lower than the design range, respectively.

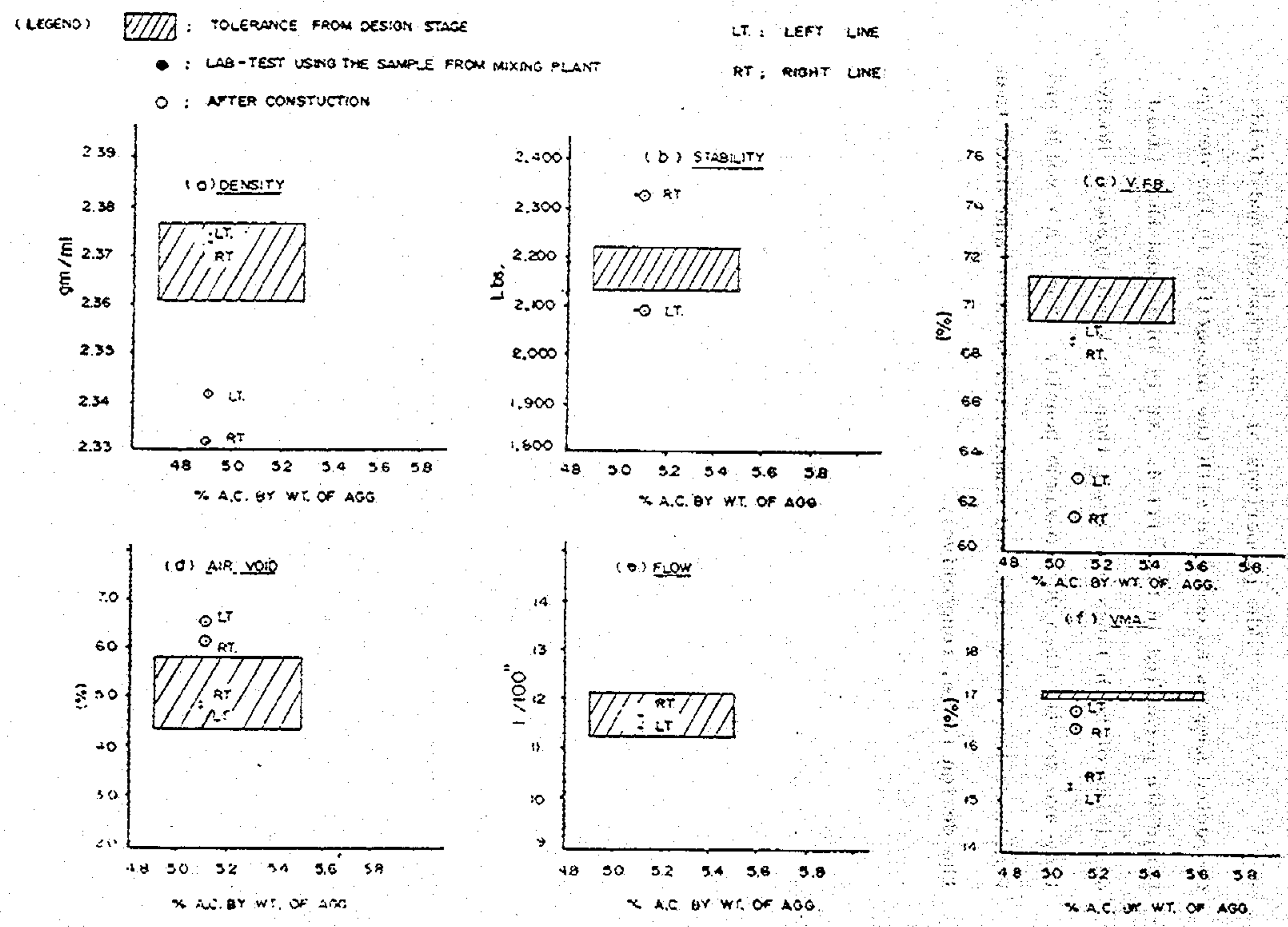

Fig. III-4 After - Construction Material Properties

IV. SENSOR INSTALLATION

IV.1 Types of Sensors and Their Locations

Sensors, which were installed within the pavement structure of the test section, are pressure cells, strain gages and thermo-couples. Specification of these sensors are included in Appendix A.

Locations of Sensors are shown in Fig. II-3.

IV.2 Steps of Sensor Installation

IV.2.1 Stage I Study In the Stage I study, the sensors were installed within and under the soil-cement base course. Details of the installation was discussed in our Stage I report.

IV.2.2 Stage II Study Only strain gages and thermo-couples were installed beneath the asphaltic concrete surface in the subsection nos. 1, 3, 4, 5 and 7.

The steps of installation are as follow.

(1) Before overlaying asphaltic concrete surface, tacking coat was done by using asphaltic cement. Then, wooden form was placed at the embedment location, as shown in Fig. IV-1 (a). Then wooden form was firmly fixed on the base course.

(2) After overlaying asphaltic concrete surface, the wooden form was removed to provide the strain gage space. Fig. IV-1 (b) shows the section of asphaltic concrete overlaying stages. This step was done while the asphaltic was still hot.

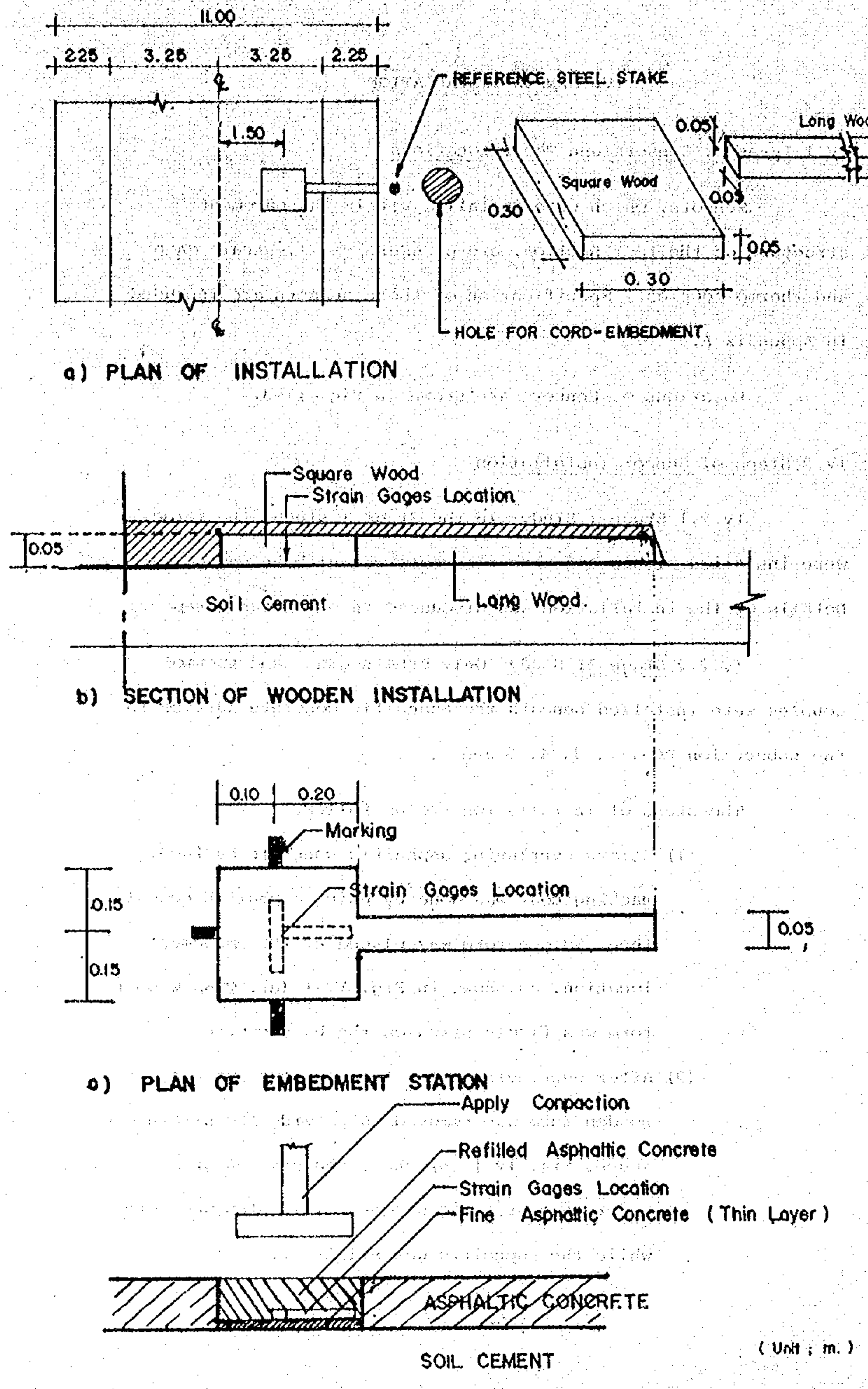

Fig. IV-1 The Steps of Sensor Installation

(3) Within the providing space, thin layer of fine asphaltic concrete was used to level the surface of base course. Installed location was marked on the levelling surface. Fig. IV-1 (c) shows plan of embedment location.

(4) Two strain gages were installed at the specified location. Asphaltic concrete was spreaded and compacted in the space. Fig. IV-1 (d) shows this step.

Steps (2), (3) and (4) were done as quickly as possible to obtain the homogeneity of the asphaltic concrete surface course.

Cord embedment was done by digging a ditch along the side slope embankment and collecting the cord in the hole as shown in Fig. IV-1 (a).

IV.3 Measuring Instrument and Method

The measuring instrument and method were descriped in detail in our Stage I report and is reproduced in Appendix B of this report.

V. RESULTS

V.1 DEFLECTION

V.1.1 Recorded Deflection

Benkelman Beam Deflection Method has been used to measure the surface deflection of the test section. The method was described by Ruenkrairergsa (1982). In our studies, the loads being used varied from the standard loads of 18,000 lbs. (8.036 tons) as shown in Table V.1-1. As a result, The recorded deflection was in error to some degrees. The recorded data is then multiplied by a correction factor which is simply the ratio of the standard load and the actual load.

Table V.1-2 shows the average surface deflection and standard deviation of each subsection measured at different period as compared with the soil-cement base deflection. Also, In the same table, presents the deflection of surface constructed on crushed rock base.

V.1.2 Deflection-Service Time

The surface course deflection is plotted against service time in Fig.V.1-1. It is indicated that the deflection tends to increase with the service time. However, from the period of 7 to 10 months, The deflection decreases. It is difficult to see the relationship at relatively short service time, since variation of climate particularly raining will exert large influence on the recorded deflection.

In the same figure, surface course deflection of crushed rock base is also plotted against service time. It can be seen

TABLE VI-1 BENKELMAN BEAM TRUCK'S WEIGHT

WEIGHT , kg.	DATE		
	DEC.20 & 21, 83	MAY 7, 84	AUG. 7, 84
FRONT WHEELS	3,234	3,138	3,637
REAR WHEELS	10,585	8,659	8,697
TOTAL	13,875	11,797	12,327

TABLE V.I-2 AVERAGE OF DEFLECTION AND STANDARD DEVIATION

(Unit, mm.)

		Cement Content (%)	Base Thickness (cm)	Base Course			Surface												Ratio of Base Course to Surface			
				Mar.23 to May 16.1983 *			Dec.21, 1983 *			Mar.3, 1984 *			June.28, 1984 *			Aug.6, 1984 *						
				$\overline{X}_0$	$\measuredangle_0$	n0	$\overline{X}_1$	$\measuredangle_1$	n1	$\overline{X}_2$	$\measuredangle_2$	n2	$\overline{X}_3$	$\measuredangle_3$	n3	$\overline{X}_4$	$\measuredangle_4$	n4	$\frac{\overline{X}_0}{\overline{X}_1}$	$\frac{\overline{X}_0}{\overline{X}_2}$	$\frac{\overline{X}_0}{\overline{X}_3}$	$\frac{\overline{X}_0}{\overline{X}_4}$
Soil - Cement Base Subsection No.	1	12.8	15	1.01	0.374	14	0.18	0.0292	10	0.24	0.0379	4	0.266	0.0556	6	0.189	0.0538	12	5.6	4.2	3.8	5.4
	2	10.0	15	0.87	0.214	19	0.14	0.0360	10	0.17	0.0200	4	0.190	0.0535	6	0.172	0.0383	12	6.2	5.1	4.6	5.1
	3	7.0	15	1.03	0.389	19	0.22	0.0366	10	0.27	0.0549	4	0.249	0.0526	6	0.289	0.0891	12	4.7	3.8	4.1	3.6
	4	4.3	15	1.14	0.366	19	0.15	0.0284	10	0.17	0.0297	4	0.201	0.0853	6	0.161	0.0614	12	7.6	6.7	5.7	7.1
	5	4.3	20	1.26	0.465	19	0.32	0.0743	10	0.33	0.0901	4	0.383	0.1797	6	0.345	0.0071	12	3.9	3.8	3.3	3.7
	6	7.0	20	1.04	0.381	18	0.28	0.1209	10	0.26	0.0494	4	0.292	0.1144	6	0.252	0.1009	12	3.7	3.8	3.6	4.1
	7	10.0	20	1.03	0.358	18	0.21	0.1205	10	0.26	0.0609	4	0.257	0.1083	6	0.203	0.0441	12	4.9	4.0	4.01	5.1
	8	12.8	20	1.01	0.412	14	0.14	0.0221	10	0.20	0.0992	4	0.229	0.1492	6	0.168	0.0668	12	7.9	5.0	4.4	6.0
Crushed Rock Base			15				0.28	0.0454	10				0.334	0.0698	40	0.321	0.096	36				

Note;

*	Indicates the measuring date
$\overline{X}$	Average Value
$\measuredangle$	Standard Deviation
n	Number of measuring point or time

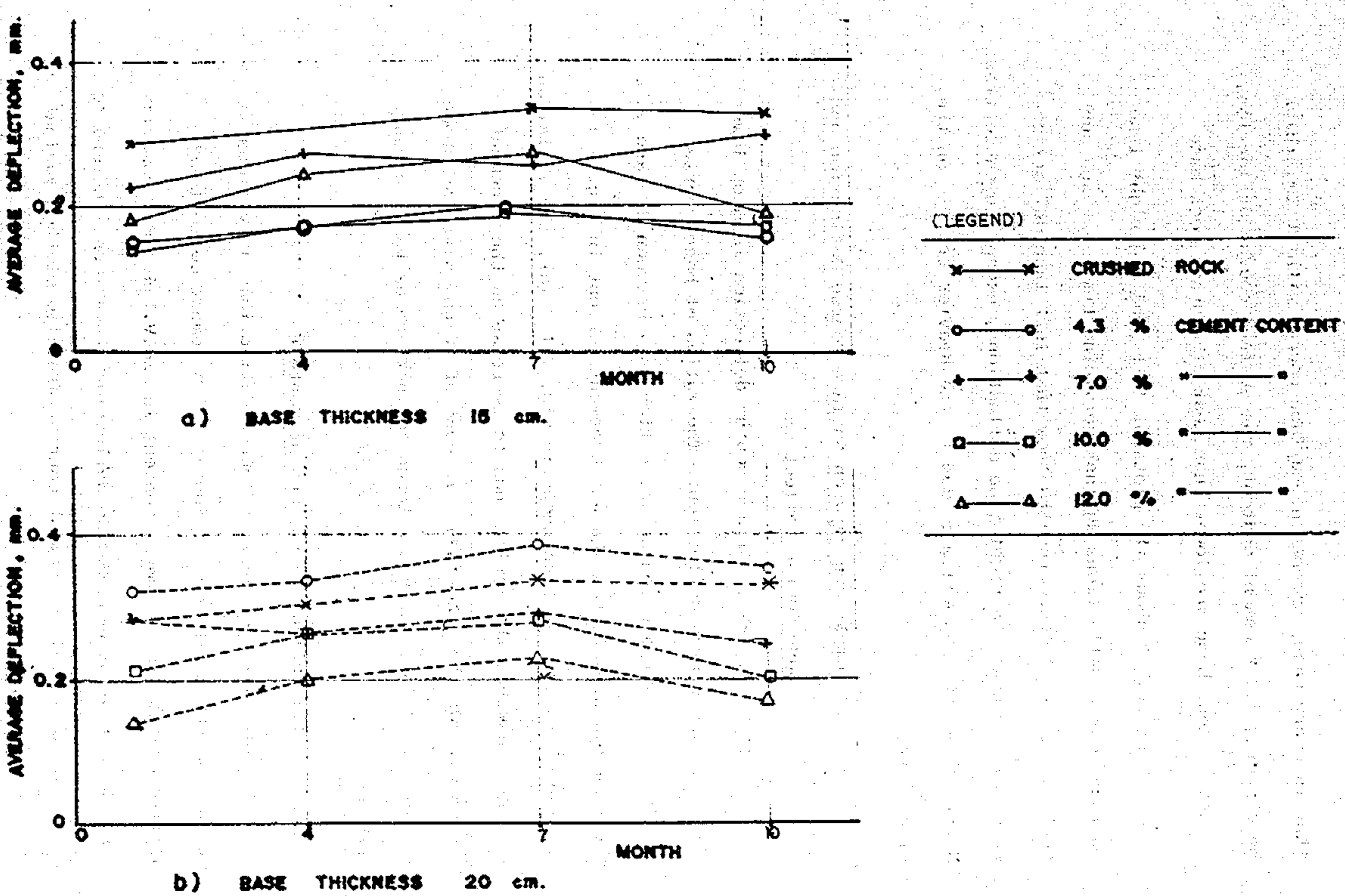

Fig V.1-1 DEFLECTION VS. TRAFFIC SERVICE TIME that in every case, except the surface course with 20 cm.-thick base having 4.3 % cement content, the surface course deflections of soil cement base are lower than that of crushed rock base.

Fig.V.1-2 shows the plots of left lane and right lane surface course deflections against servicing time for each subsection. Most of these results show that left lane deflection were smaller than the right lane deflections, except in subsection No.8. These effects would be due to the heavier traffic on the right lane.

V.1.3 Comparison Between Surface Course Deflection and Base Course Deflection

In every case, surface course deflection is much lower than the base course deflection. The ratios of base course deflection to surface course deflection vary between 3.3 and 7.7. These ratios are plotted against % cement content in Fig. V.1-3. In case of 15 cm. base, as shown in Fig. V.1-3 (a), the variation is high. However the ratio tends to decrease as the % cement increases. On the other hand, in case of 20 cm. base, as shown in Fig. V.1-3 (b), the ratio tends to increase as the % cement increases.

V.1.4 Deflection VS. Cement Content

The ratios of surface course deflections at various % cement content to the deflection at 4.3 % cement content are plotted against the % cement content in Fig.V.1-4. For comparison, the ratios of base course deflection at various % cement to the deflection at 4.3 % cement content are also plotted against

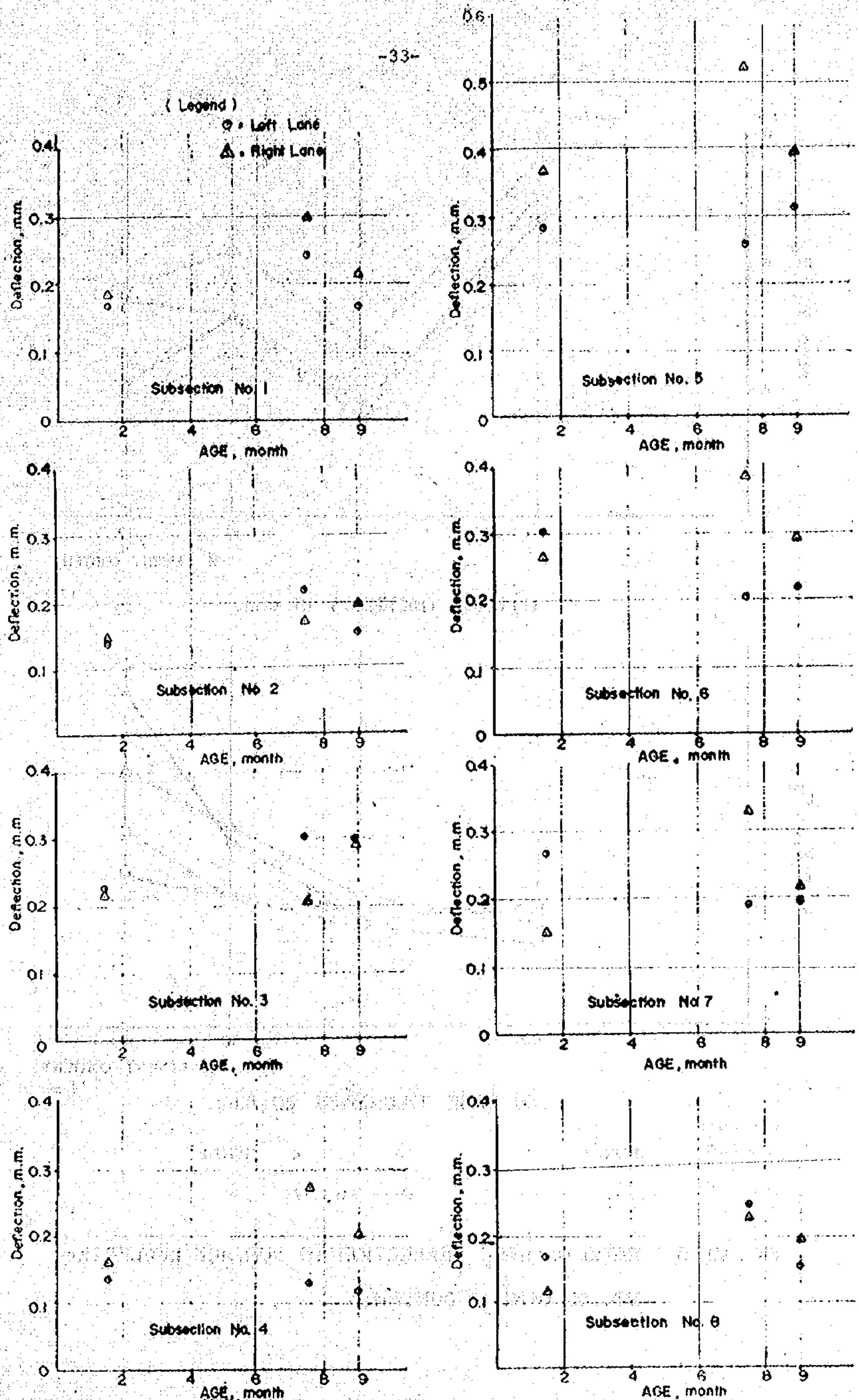

FIG. V.I-2 AVERAGE DEFLECTION VS. AGE

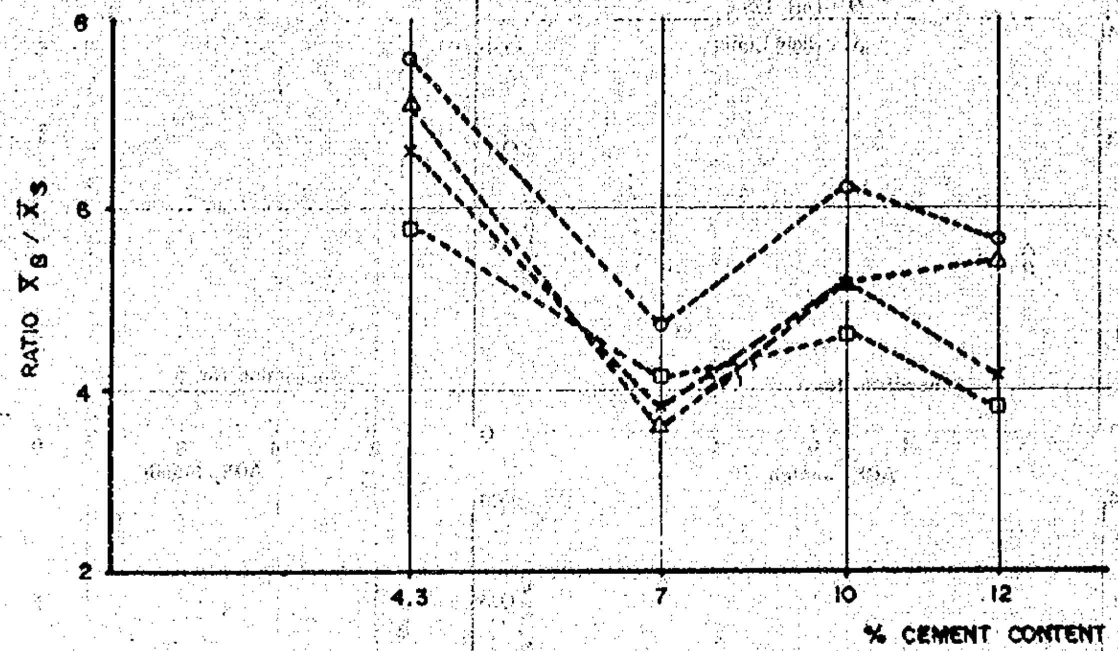

a) BASE THICKNESS 15 c.m.

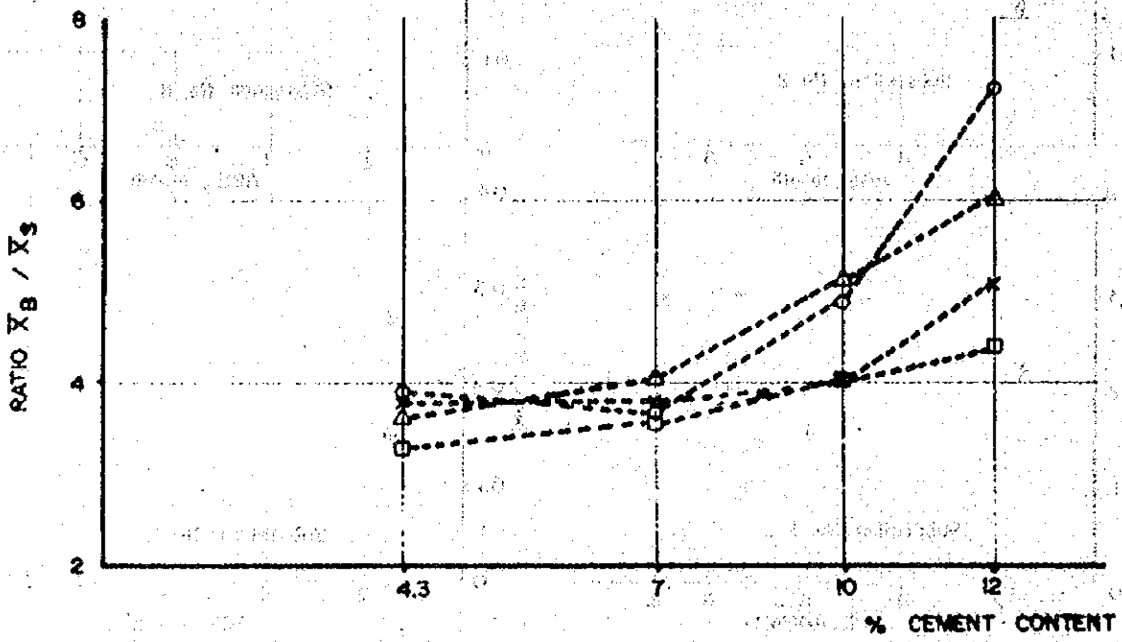

b) BASE THICKNESS 20 c.m.

(LEGEND)

O-------O 1 MONTH		X-------X 4 MONTH	
□-------□ 7 "		△-------△ 10 "	

FIG. V.I-3 RATIO OF BASE DEFLECTION TO SURFACE DEFLECTION VS. % CEMENT CONTENT

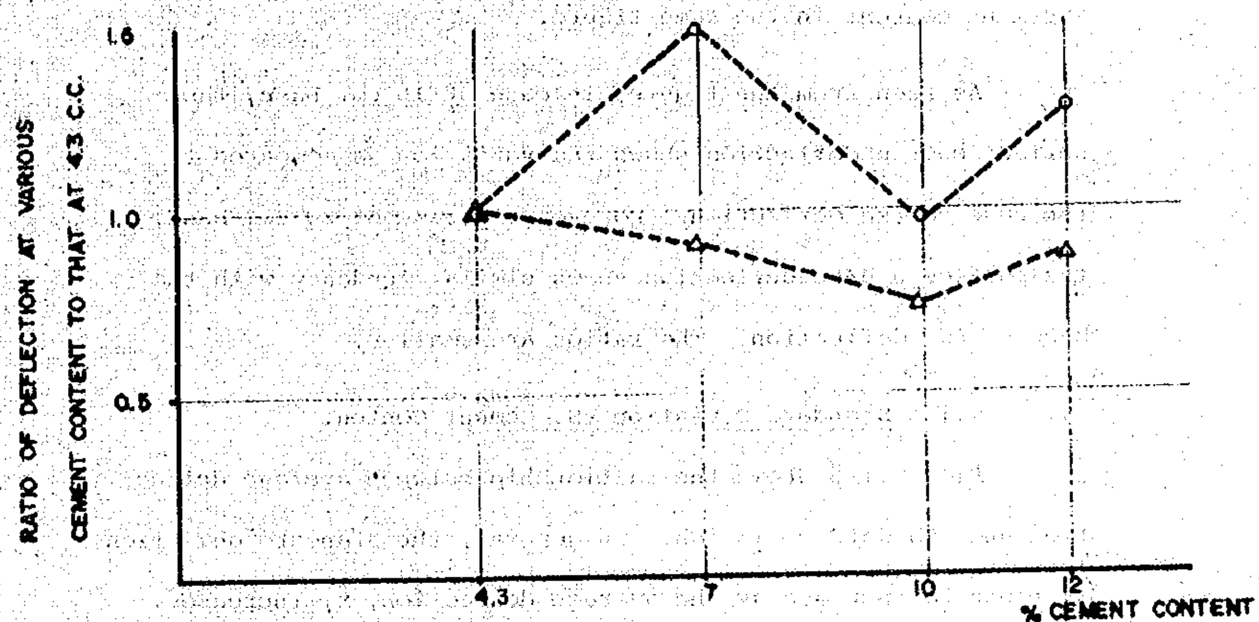

a) BASE THICKNESS 15 cm.

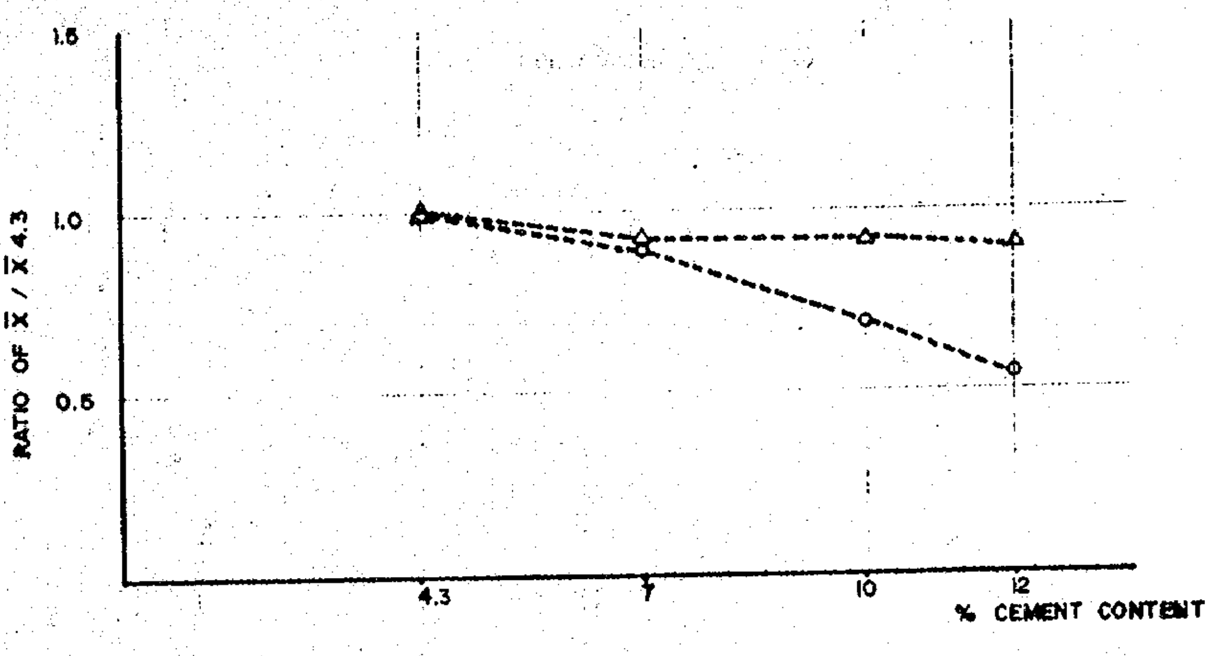

b) BASE THICKNESS 20 cm.

(LEGEND)

o-----o SURFACE COURSE DEFLECTION   △-----△ BASE COURSE DEFLECTION

FIG. V.1-4 RATIO OF DEFLECTION VS. %CEMENT CONTENT

% cement content in the same figure.

As seen from the figure, in case of 15 cm. base, the surface course deflection shows the variation as compared to the base course deflection. However, in case of 20 cm. base, the surface course deflection shows similar tendency with the base course deflection. The ratios are smaller.

V.1.5 Standard Deviation VS. Cement Content

Fig. V.1-5 Shows the raltionship between average deflection and standard deviation. In general, the standard deviation, σ, tends to increase as the average deflection, $\bar{x}$, increases. There is a board relationship between these two parameters, as shown below

$$\sigma = 2/3\ \bar{x} - 0.093$$

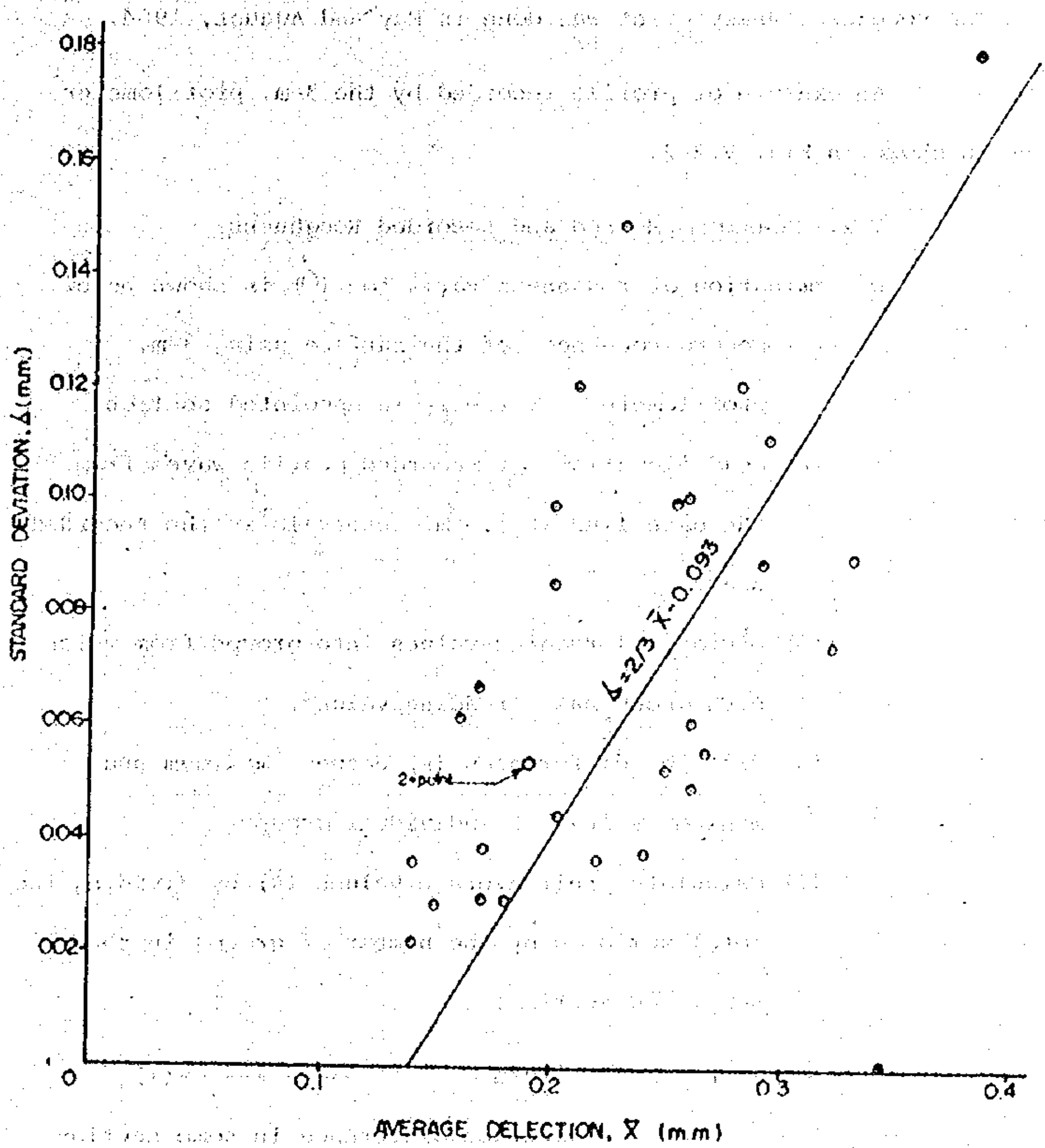

FIG. V.I – 5 STANDARD DEVIATION VS. AVERAGE DEFLECTION

V.2 ROUGHNESS OF SURFACE COURSE

3-m. profilometer, of "Intergrating Irregularity Recorder, Type KKY-3T" manufactured by Tokyo Tanifuji Co.,Ltd. with the auto-reading device, was used to measure roughness (Fig.V.2-1). The roughness measurement was done in May and August, 1984.

An example of profile recorded by the 3-m. profilometer is shown in Fig. V.2-2.

V.2.1 Measuring Method and Recorded Roughness

Determination of roughness variation (σ) is shown below.

(1) Record roughness of the surface using 3-m. profilometer for the whole appointed section.

(2) Read elevations of recorded profile waves from the base line at 1.5 m. intervals in the recorded chart.

(3) Divide all reading-values into groups from which each group has 6 reading values.

(4) Find the differences (R) between maximum and miniumu values of individual groups.

(5) Calculate their average values ($\bar{R}$) by dividing the total sum of R by the number of groups in the appointed section.

$$\bar{R} = \Sigma R/n \qquad \text{-------------(1)}$$

where $\bar{R}$ = average difference in some section

ΣR = measured individual difference of each group

n = number of group

(6) Compute the roughness deviation (σ) using the

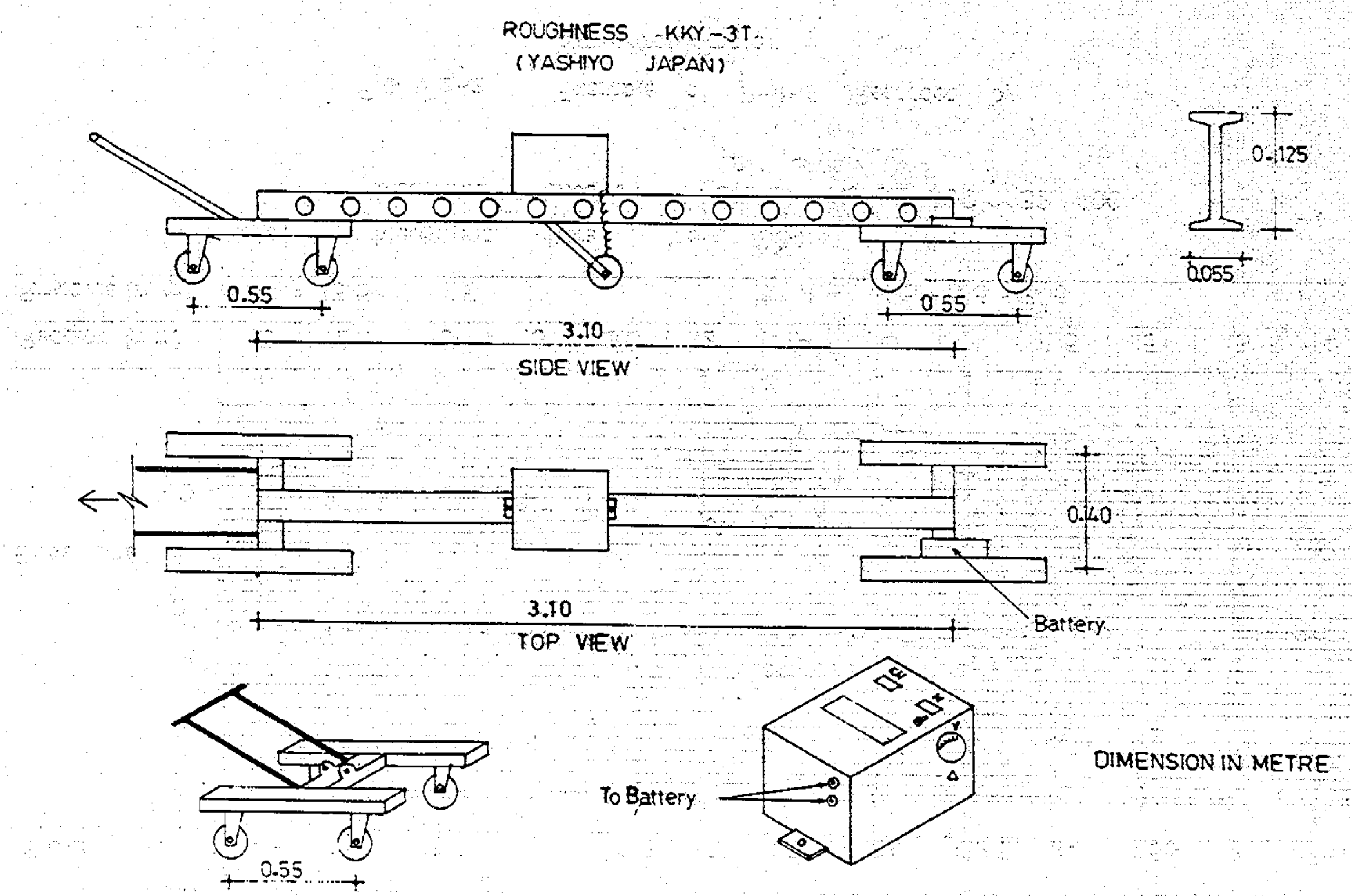

Fig. V.2-1 Profilometer

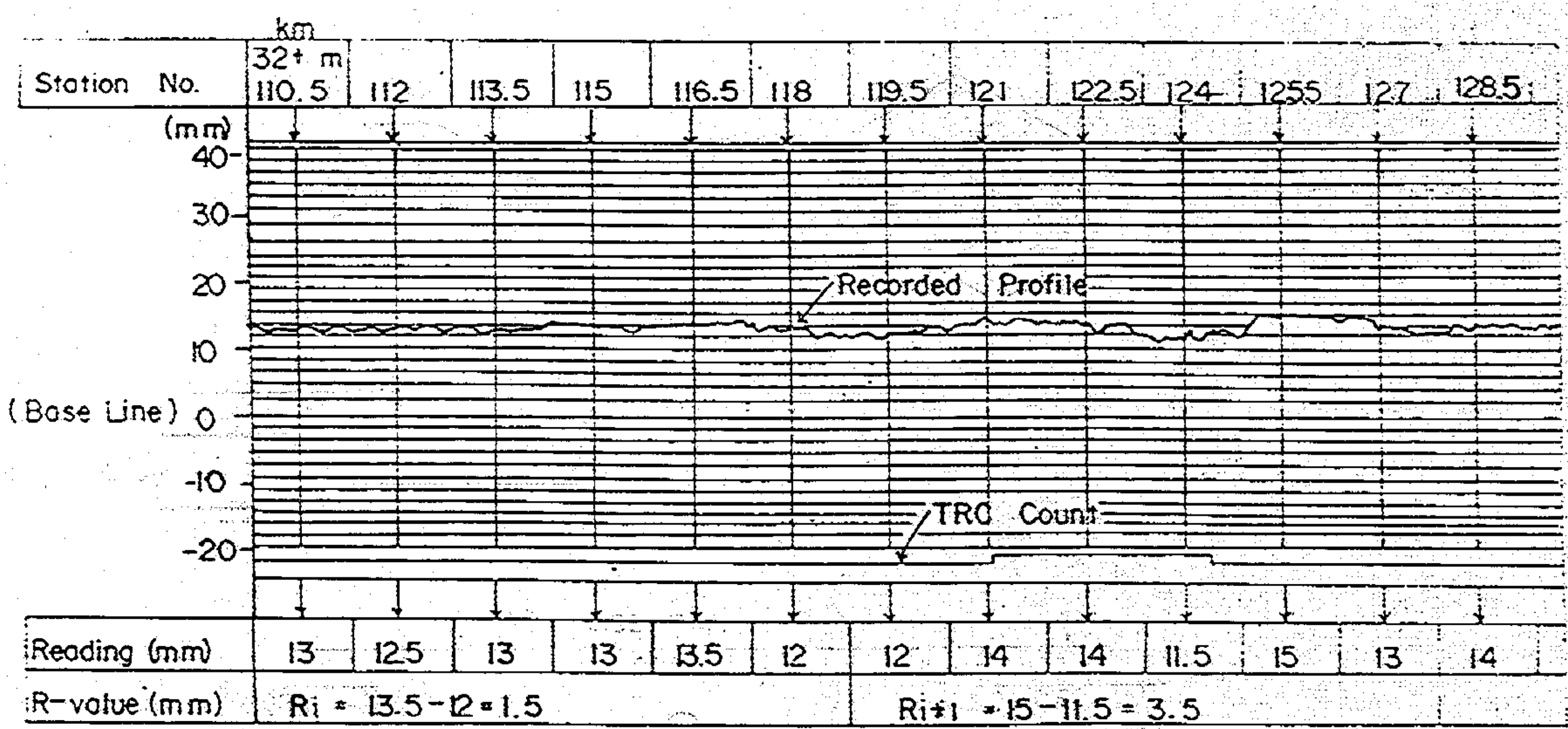

(Note) : Measuring Date : May 1984

: Measured Location : Station No. 32+000 ~ 32+400
Left Lane / OWP

Fig. V.2-2 Example of Profile Recorded by
3m - Profilometer

equation below.

$$\sigma = \bar{R}/C \qquad \text{------------(2)}$$

where C = Coefficient fixed in accordance with measurements involved in the group in case that the number of measurement involved in a group is 6, C is 2.53

Table V.2-1 shows calculated roughness deviation for each subsection.

V.2.2 Roughness Deviation

The roughness deviations from OWP in both lanes are averaged for each subsection and plotted in Fig. V.2-3 in general, the roughness deviation for each subsection is relatively low particularly in subsections No.2,5,6 and 7. The deviations at 9-month old are also compared in the same figure. In all cases but subsection No.3, the roughness deviations at 9-month old are greater than those at 6-month old.

The roughness deviation can be used to indicate the serviceability. Table V.2-2 shows the relationship between the roughness index and service index as proposed by Koono (5).

V.2.3 Roughness Index

Roughness Index (RI) is calculated using the equation below.

$$RI = \Sigma ai/L \quad (cm./km.) \qquad \text{----------(3)}$$

where Σai = Accumulated deviation of the measuring wheel in one direction of either up or down by recording counter (cm.)

L = Measured distance (km.)

Table V.2-3 presents the calculated Roughness Index for the whole soil-cement section. The Roughness Index can be used to

Table V.2-1 Recorded Roughness Deviation

(Unit; m.m.)

Measuring Date	Age	Measured Location		Sub-Section No. 1	2	3	4	5	6	7	8	Average
May 1984	6 months	Right Lane	OWP.	1.66	1.11	1.82	1.54	1.34	0.91	1.26	1.42	1.38
			IWP.	0.55	0.71	1.11	1.15	0.67	0.63	0.83	0.71	0.80
		Left Lane	IWP.	1.70	1.34	0.87	0.95	1.07	0.75	0.87	0.99	1.07
			OWP.	0.95	0.87	0.99	1.15	0.91	1.46	1.19	1.98	1.19
		Average		1.22	1.01	1.20	1.20	1.00	0.94	1.04	1.28	1.11
Aug. 16 1984	9 months	Right Lane	OWP	1.54	1.23	1.74	1.66	1.38	1.07	1.58	1.19	1.42
			IWP.	1.34	0.83	0.79	1.03	1.07	1.26	1.42	1.62	1.17
		Left Lane	IWP.	1.86	1.19	0.95	0.99	1.03	0.91	1.30	1.82	1.26
			OWP	0.82	1.26	1.03	1.15	0.67	1.03	1.03	1.36	1.04
		Average		1.39	1.13	1.13	1.21	1.04	1.07	1.33	1.50	1.22

Note ; Age ; Count from the Surface course construction in November 1983

OWP ; Out Wheel Path

IWP Inner Wheel Path

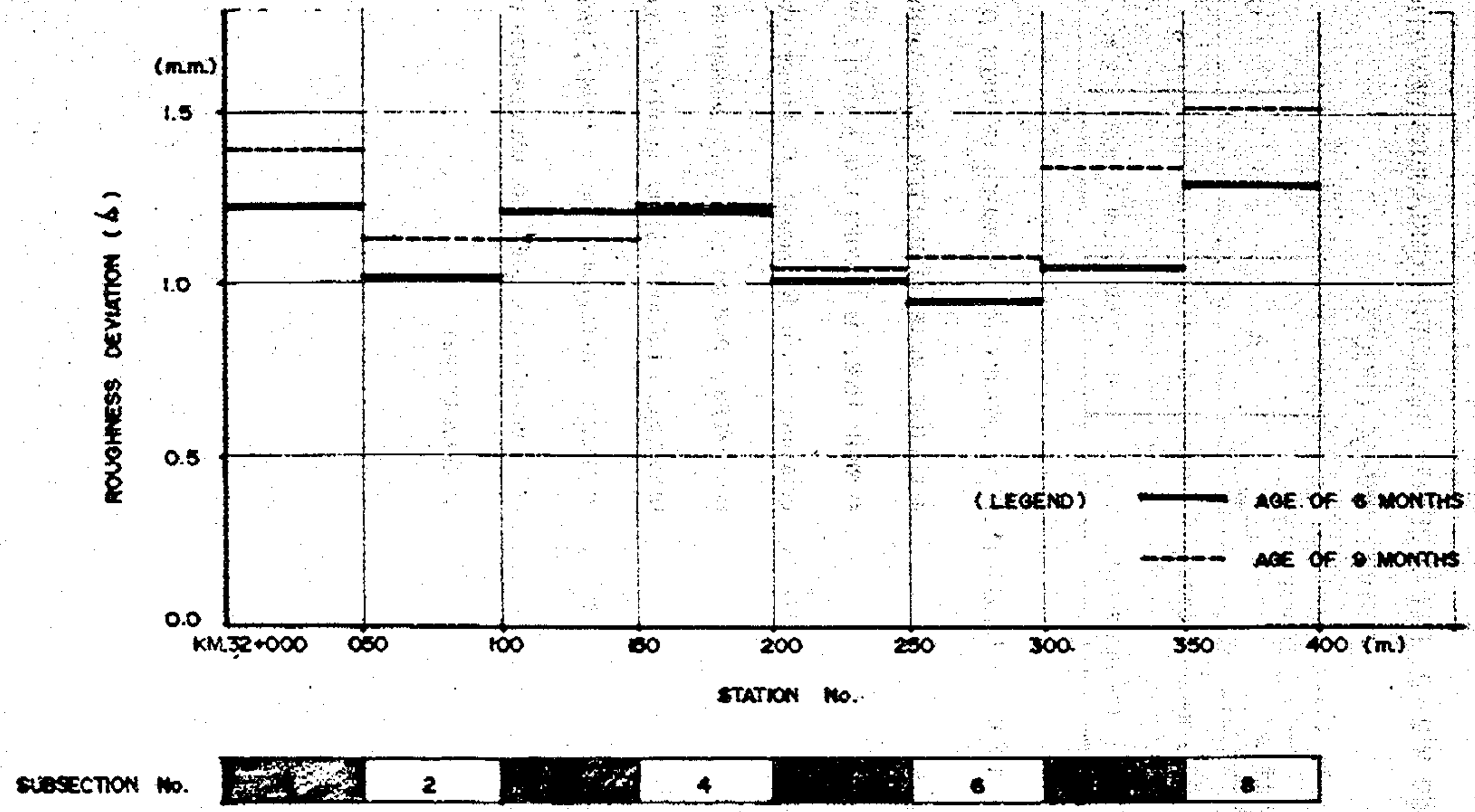

FIG. V.2-3 ROUGHNESS DEVIATION OF EACH SUBSECTION

TABLE V.2-2 RELATIONSHIP BETWEEN ROUGHNESS DEVIATION AND SERVICE INDEX (KOONO)

(UNIT ; m.m.)

SERVICE INDEX / MEASURING INSTRUMENT	A	B	C	D
STRAIGHT EDGE	0 - 1.15	1.16 - 1.75	1.76 - 2.60	2.61 -
3-m. PROFILOMETER	0 - 1.50	1.51 - 2.40	2.41 - 3.70	3.71 -

NOTE. A, B ; IT IS DIFFICULT TO DISTINGUISH BETWEEN A AND B IN DAYTIME, HOWEVER SPOTTING HEAD-LIGHT OF A CAR IN NIGHT TIME, B LOOKS LIKE A LITTLE WORSE THAN A

C ; COMPARING WITH A AND B, C LOOKS LIKE WORSE IN ROUGHNESS, PASSING BY A CAR, VIBRATION CAUSED BY UNEVENNESS (ROUGHNESS) IS SLIGHTLY FELT.

D ; ROUGHNESS IS CLEARLY BAD AT SIGHT, PASSING BY A CAR, VIBRATION CAUSED BY UNEVENNESS (ROUGHNESS) IS CLEARLY FELT

Table V.2 - 3 Recorded Roughness Index

Unit; (c.m./km)

Measuring Date			May '84	Aug. 16 '84	
Age (months)			6	9	
Measured Location	Right Lane	OWP.	90.90	113.63	
		IWP.	60.60	50.50	
	Left Lane	IWP.	53.03	60.60	
		OWP.	63.49	58.79	

evaluate the surface condition as shown in Table V.2-4.

Fig. V.2-4 shows the relationship between the roughness deviation (σ) and roughness index (RI). The broad relation is derived from these data, is shown below.

$$\sigma = 0.0095\ RI + 0.5 \qquad (4)$$

Table V.2-4 EVALUATION OF RI

RI (cm/km.)	EVALUATION
0 ~ 50	Excellent
50 ~ 100	Very Good
100 ~ 200	Good
Over 200	Bad

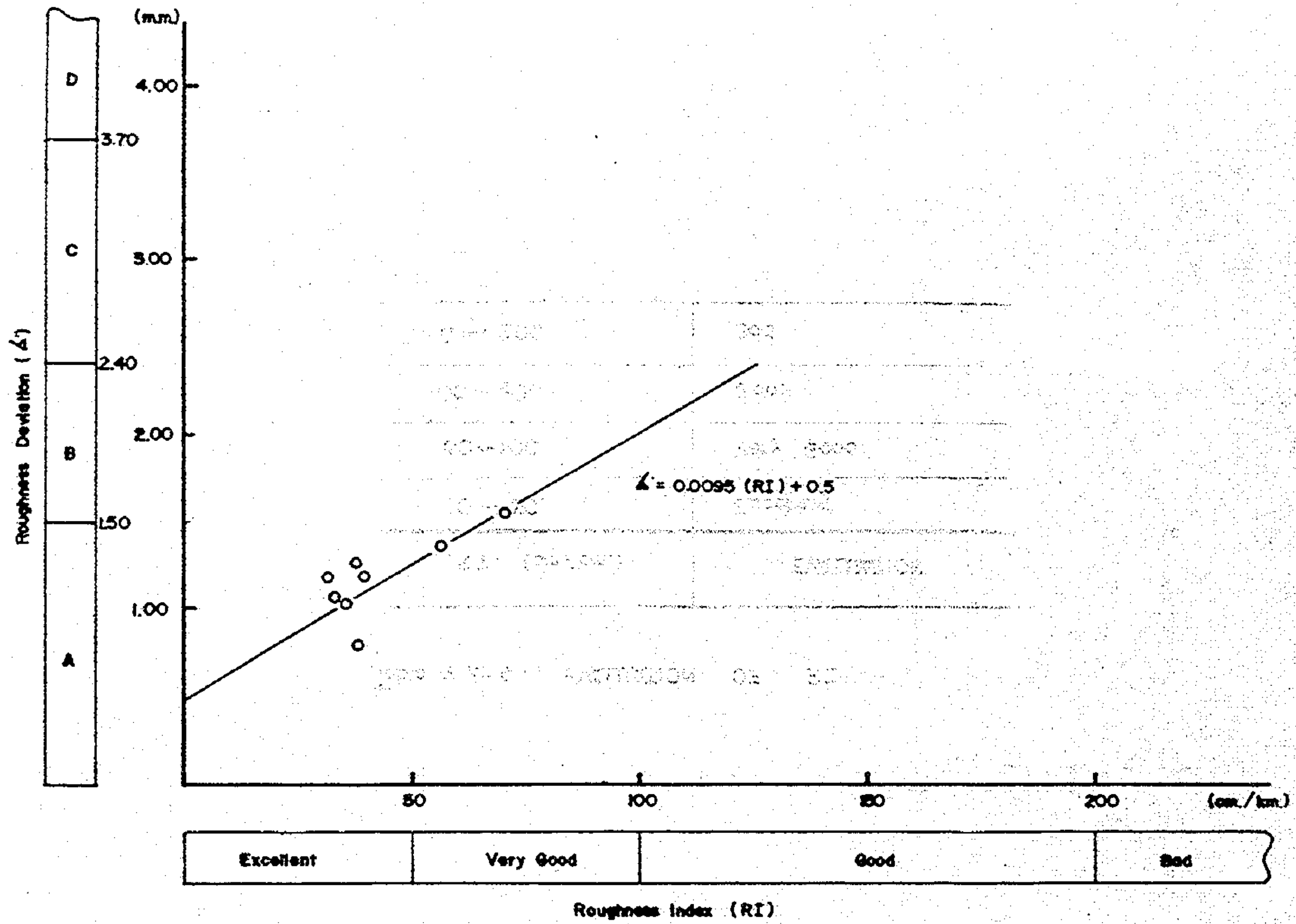

Fig. V.2-4 Roughness Index (RI) and Roughness Deviation (σ')

V.3 CROSS SECTIONAL FORM

V.3.1 Measuring Method

The cross sections of all test subsections were surveyed in August, 1984 by levelling method. The line of measurement was 10 m. apart. The measuring interval was 20 cm.

Fig. V.3-1 shows the average cross sections for each subsection. In the same figure, the designed crossfall of 2.5 % is also shown.

V.3.2 Deviation from the Design

The deviation from the design on each surveyed line is calculated using the equation below.

$$\bar{Y} = \sum Yi/n$$

$\bar{Y}$ = the deviation on each surveyed line

$\sum Yi$ = vertical deviation in absolute, mm.

n = number of measured point

The deviation for the test section are calculated and plotted in Fig. V.3-2. The average deviation in the left lane of subsection 1 is the lowest, about 3.6, and in the right lane of subsection 2 is the highest, about 18.9 mm.

V.3.3 Rut Depth

Rut depth for each subsection is determined from the cross-section plot presented in Fig. V.3-1. The results are summarized in Table V.3-1. The measured rut depth of the test section ranged from 0 to 3 mm. which is relatively low.

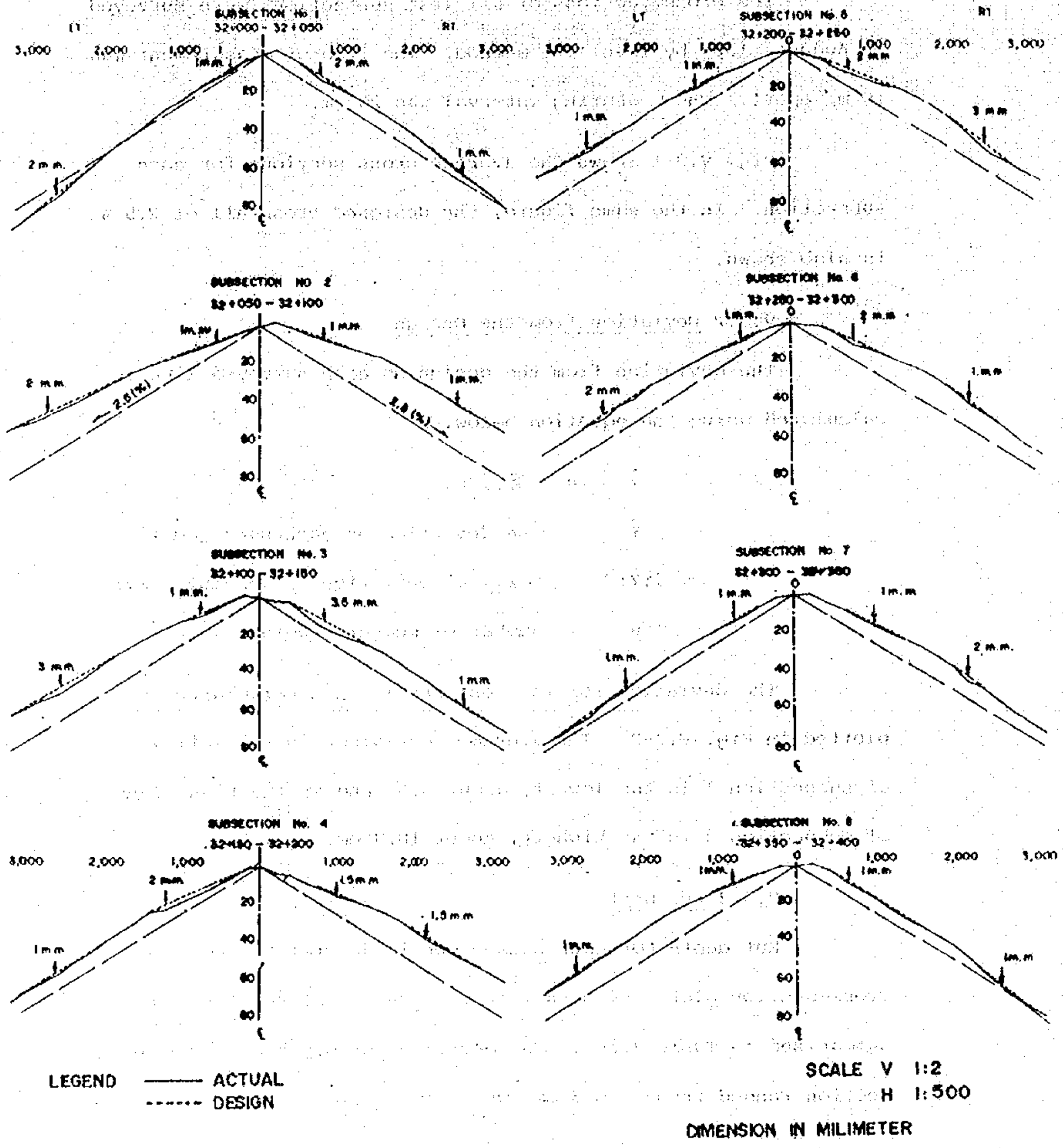

FIG. V.3-1 CROSS-SECTION

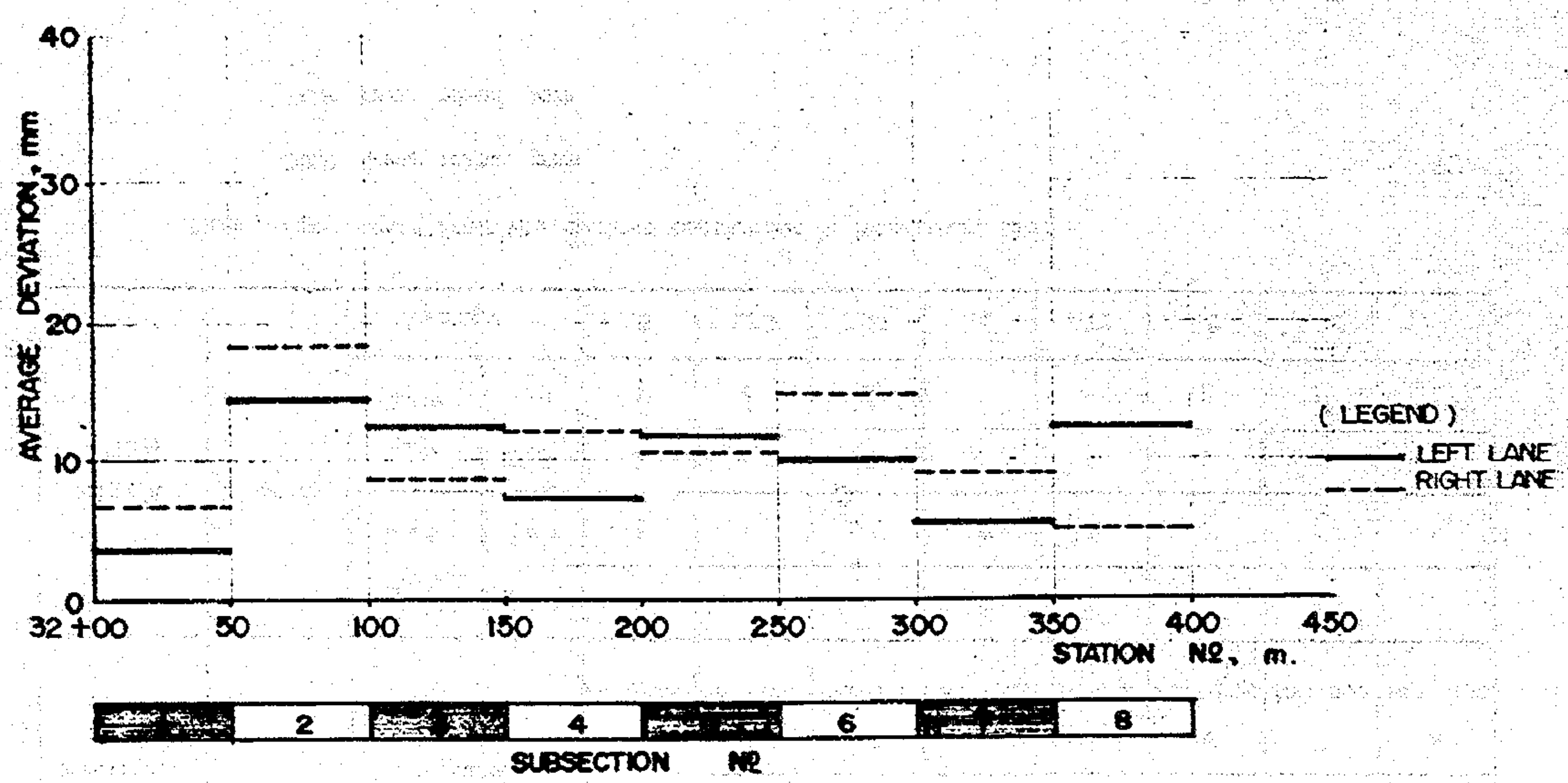

Fig. V.3-2 AVERAGE DEVIATION

Table V.3-1 Rut Depth

(Unit, m.m.)

Measuring Date	Age	Measured Location		Subsection No. and Station No. 32+___							
				1 000-050	2 050-100	3 100-150	4 150-200	5 200-250	6 250-300	7 300-350	8 350-400
Aug 16 1984	9 month	Right Lane	OWP	1	1	1	1.5	3	1	2	1
			IWP	2	1	3.5	1.5	2	2	1	1
		Left Lane	OWP	2	1	1	2	1	1	1	1
			IWP	1	2	3	1	1	2	1	1
		Average		1.5	1.25	2.13	1.5	1.75	1.5	1.25	1

Note; Age count from the surface constuction in November, 1983

OWP Outer wheel path

IWP Inner wheel path

V.4 CRACK RESULTS

V.4.1 Recorded Cracks

Crack survey was carried out on May 8, 1984, 6 months after surface construction. It was observed that most of the cracks were longitudinal. Lane joint crack was remarkable in subsections 2 and 4. Edge crack close to shoulder was remarkable in subsections 3, 7 and 8.

The investigated area was divided into 1.0 x 1.0 m. square meshes. The meshes in which cracks developed were recorded according to the classification in Table V.4-1. The classified cracks of all subsections are presented in Fig. V.4-1. The crack area and crack ratio were then determined. The crack ratio was calculated using the equation below.

$$\text{Crack ratio } (\%) = \frac{\text{Crack Area } (m.^2) \times 100}{\text{Investigated area } (m.^2)} \quad \text{-----------} (1)$$

Result of the calculation are presented in Table IV.4-2.

V.4.2 Crack Ratio VS. Cement Content

The relationship between crack ratio and cement content is plotted in Fig. V.4-2. The crack ratio in every subsection is less than 7% and tends to increase as the cement content. However, as the cement content over 10 %, the crack ratio decreases.

In the Table V.4-2 is shown the plot between the crack ratio of all subsections including the results of before and after surface construction. In all cases, the crack ratio of base course is higher than that of the surface course, ranging from 3 % to 73 %.

Table V. 4-1 Crack Classification

Classification	Example	Sign	Cracked Area
Cracks of more than two lines			1.00 m^2
One line crack of completed or more than half.		○	0.30 m^2
One line crack of less than half		△	0.15 m^2

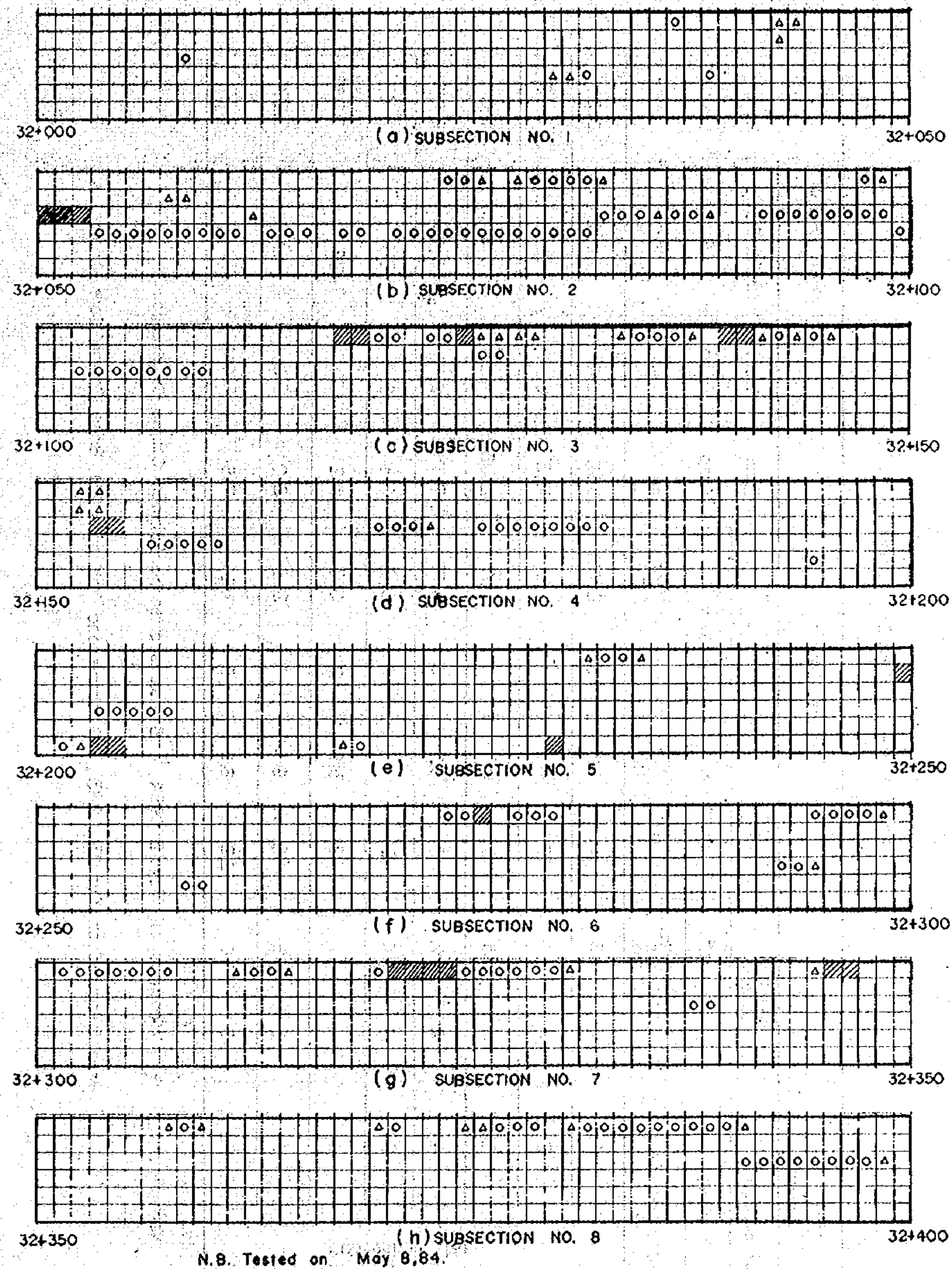

Fig. V.4-1 Classified Crack.

TABLE V. 4-2 CRACK RATIO

Measured Location		Surface Course *								Base Course **	
Classification		▨		○		△		Total Area (m^2)	Crack Ratio R_s (%)	Crack Ratio R_b (%)	R_s/R_b
Unit Area		1.00 m^2		0.30 m^2		0.15 m^2					
Number and Area		Number	Area (m^2)	Number	Area (m^2)	Number	Area (m^2)				
Subsection No.	1	0	0	4	1.2	5	0.75	1.95	0.7	20.2	0.03
	2	3	3	47	14.1	8	1.2	18.3	6.1	0.4	15.25
	3	5	5	19	5.7	9	1.35	12.05	4.0	10.9	0.37
	4	2	2	17	5.1	5	0.75	7.85	2.6	5.4	0.24
	5	4	4	9	2.7	4	0.6	7.3	2.4	3.3	0.73
	6	1	1	13	3.9	2	0.3	5.2	1.7	22.8	0.07
	7	6	6	18	9.4	4	0.6	16.0	5.3	19.4	0.27
	8	0	0	22	6.6	8	1.2	7.8	2.6	30.6	0.08

Note ; * Measured on May. 8 1984, 6 months after the Surface Course Construction

** Measured on Aug. 13 1983, 4 months and half after the Base Course Constuction.

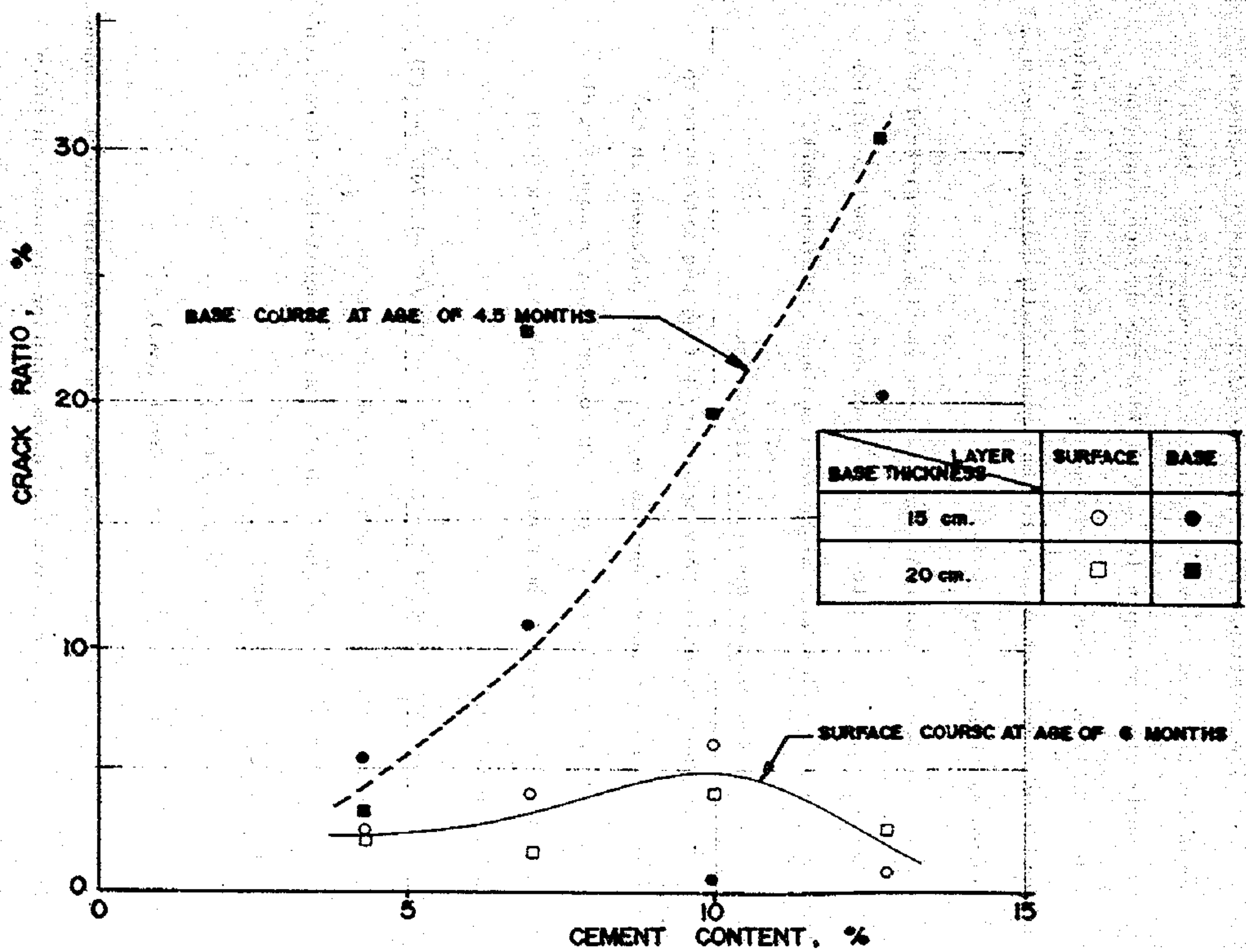

Fig. V.4-2 RELATIONSHIP BRTWEEN CEMENT CONTENT AND CRACK RATIO

V.4.3 Crack Ratio and Roughness Deviation

The relationship between the crack ratio and roughness deviation are used to evaluate the surface condition. Ministry of Construction of Japan (6) has divided the surface condition into 7 different classes according to the crack ratio and roughness deviation. For each class, the maintenance alternative is recommended as shown in Fig. V.4-3.

The data obtained from the test section are plotted in the same figure. It indicates that the surface is in good condition although subsection No.2 might need surface treatment work.

V.4.4 Present Serviceability Index

The concept of Serviceability Rating was introduced to evaluate the smoothness and riding ability of pavement in the AASHO Test Road (7). Based on this concept, Japan Road Association (6) has proposed the Present Serviceability Index (PSI) equation below.

$$PSI = 4.53-0.518\log \sigma - 0.371\sqrt{C} -0.174D^2 \text{-----} (2)$$

where PSI = Present Serviceability Index

σ = Roughness deviation in Lognitudinal Direction (mm.)

C = Crack ratio (%)

D = Average rut depth (cm.)

Japan Road Association has also recommended the maintenance for the PSI calculated from the above equation as shown in Table V.4-3.

PSI of all test subsections are calculated and presented in Table V.4-3 and Fig. V.4-4. The PSI can be used to evaluate

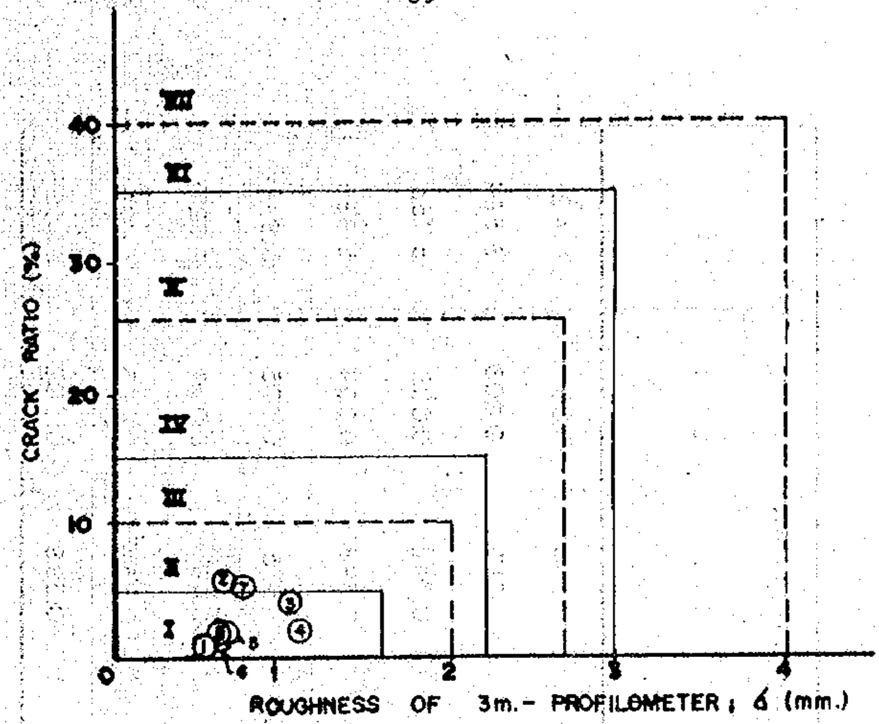

CLASS I Do nothing.

II Surface treatment or do nothing.

III Surface treatment.

IV Overlay or surface treatment

V Overlay.

VI Whole reconstruction or overlay with partial reconstruction or overlay

VII Whole reconstruction or overlay with. partial reconstruction.

Note ; ① Subsection No. 1

Fig V 4-3 Maintenance Alternetive for Asphalt Pavement with Crack Ratio and Roughness Deviation.

Table V4-3 Present Serviceability Index (PSI)

Sub Section No.	Roughness Deviation Δ (mm.)	Crack Ratio C (%)	Rut Depth D (c.m)	Calculation Process			PSI
				0.518 Log Δ	0.371 $\sqrt{C}$	0.174 D^2	
1	1.39	0.7	0.150	0.074	0.310	0.004	4.142
2	1.13	6.1	0.125	0.027	0.916	0.003	3.584
3	1.13	4.0	0.213	0.027	0.742	0.008	3.753
4	1.21	2.6	0.150	0.043	0.598	0.004	3.885
5	1.04	2.4	0.175	0.009	0.575	0.005	3.941
6	1.07	1.7	0.150	0.015	0.484	0.004	4.027
7	1.33	5.3	0.125	0.064	0.854	0.003	3.609
8	1.50	2.6	0.100	0.091	0.598	0.002	3.839

Note ; $PSI = 4.53 - 0.518 \text{ Log } \Delta - 0.371 \sqrt{C} - 0.174 D$

Crack survey was done in May, 1984

Data of Roughness and Rut Depth were collected in August, 1984

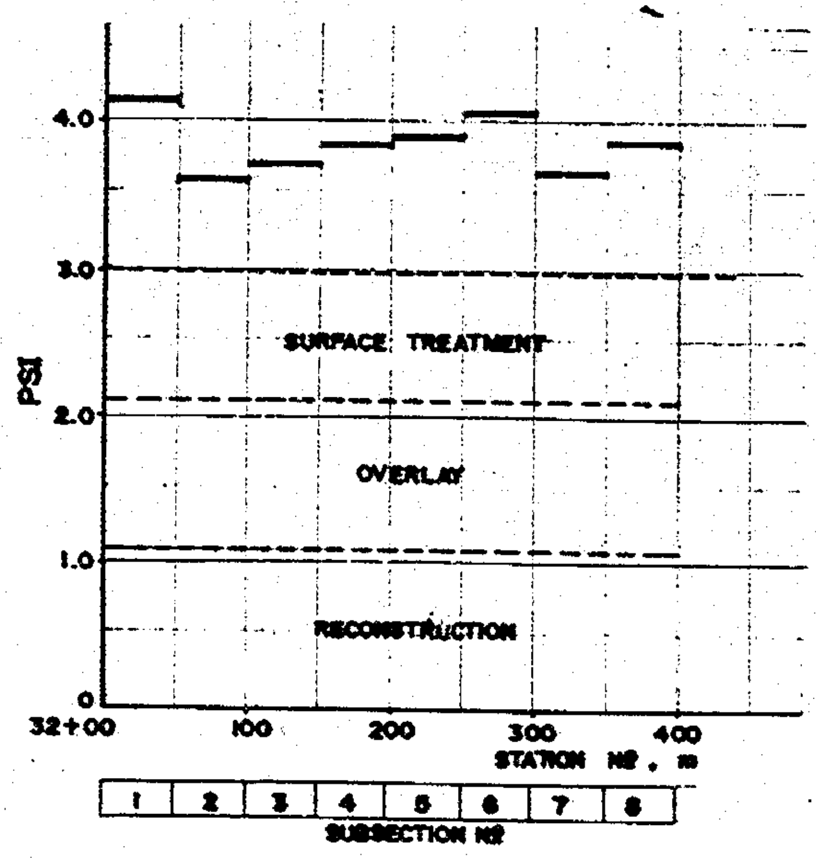

Fig. V. 4–4 PRESENT SERVICEABILITY INDEX (PSI) OF EACH SUBSECTION.

the surface condition as shown in Table V.4-4.

Table V.4-4 MAINTENANCE ALTERNATIVES FOR THE PSI.

PRESENT SERVICEABILITY INDEX (PSI)	COUNTER MEASURES FOR MAINTENANCE
3 ~ 2.1	Surface Treatment
2 ~ 1.1	Overlay
1 ~ 0	Reconstruction

(SOURCE) ROAD MAINTENANCE MANUAL, JAPAN ROAD ASSOCIATION (in Japanese)

V.5 TEMPERATURE MEASUREMENT

V.5.1 Temperature Distribution

Temperature distribution in the pavement structure, form the surface course to the bottom of base course, was measured in May, 1984. The measurements were performed from 7 a.m. to 5 p.m. Results of the measurements are shown in Fig. V.5-1. The surface temperature varies from 29°C to 55°C., although the air temperature showed much smaller variation from 27°C. to 39°C. At bottom of the surface, the temperature was the highest. Below this, the range of temperature variation was narrow. The distribution is best seen from subsections 4 and 5 from which several thermocouples were embedded in many levels.

For comparison of the temperature distribution at various period of the year, hourly temperature measurements was performed on subsection 4 in November, 1983, May, June and August, 1984. The results are shown in Fig. V.5-2. All the measurements showed similarities in the distribution. The temperature variation in November was the lowest. This was due to cool weather at that period.

V.5.2 Temperature VS. Time of the day

In general, the temperature increased with time since starting the measurement 7.00 a.m. until the peak was obtained at about 3.00 p.m. At the bottom of the surface, the temperature was the highest. Selected temperature variation in the day was shown in Fig. V.5-3.

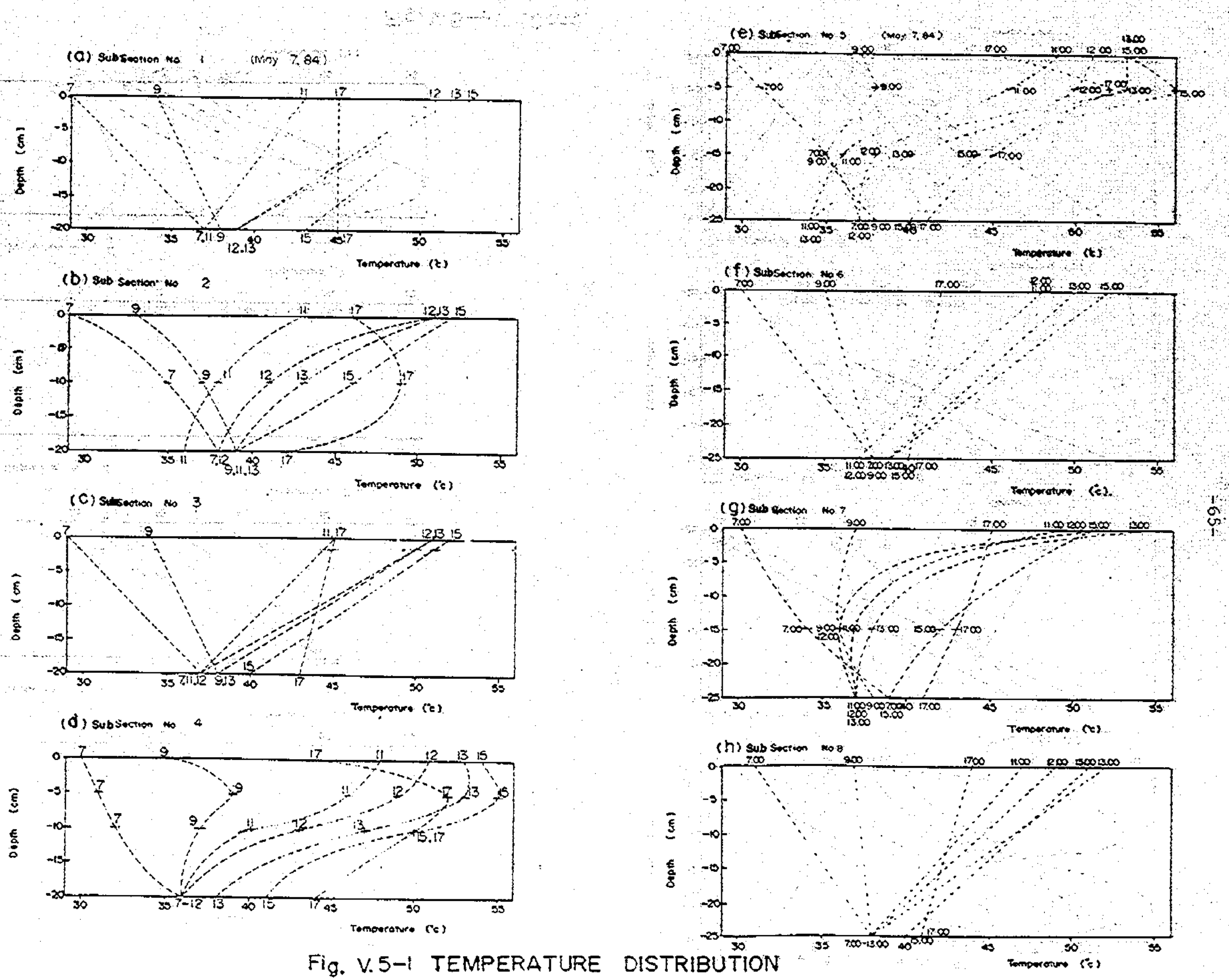

Fig. V.5-1 TEMPERATURE DISTRIBUTION

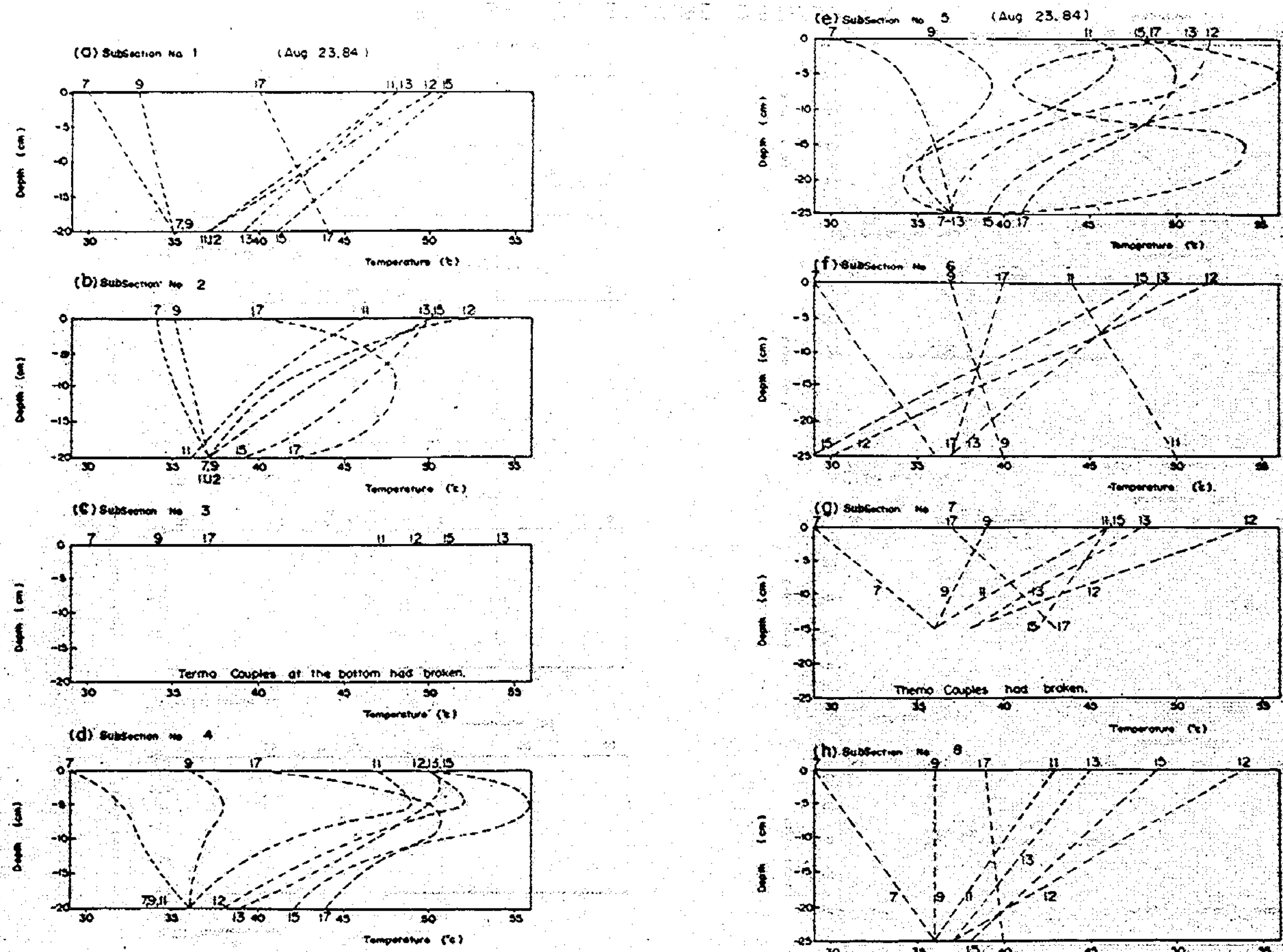
(a) SubSection No 1
(Aug 23.84)
Temperature (℃)
Depth (cm)
(b) SubSection No 2
(c) SubSection No 3
Termo Couples at the bottom had broken.
(d) SubSection No 4
(e) SubSection No 5
(Aug 23.84)
(f) SubSection No 6
(g) SubSection No 7
Thermo Couples had broken.
(h) SubSection No 8

Fig. V.5—I (Cont)

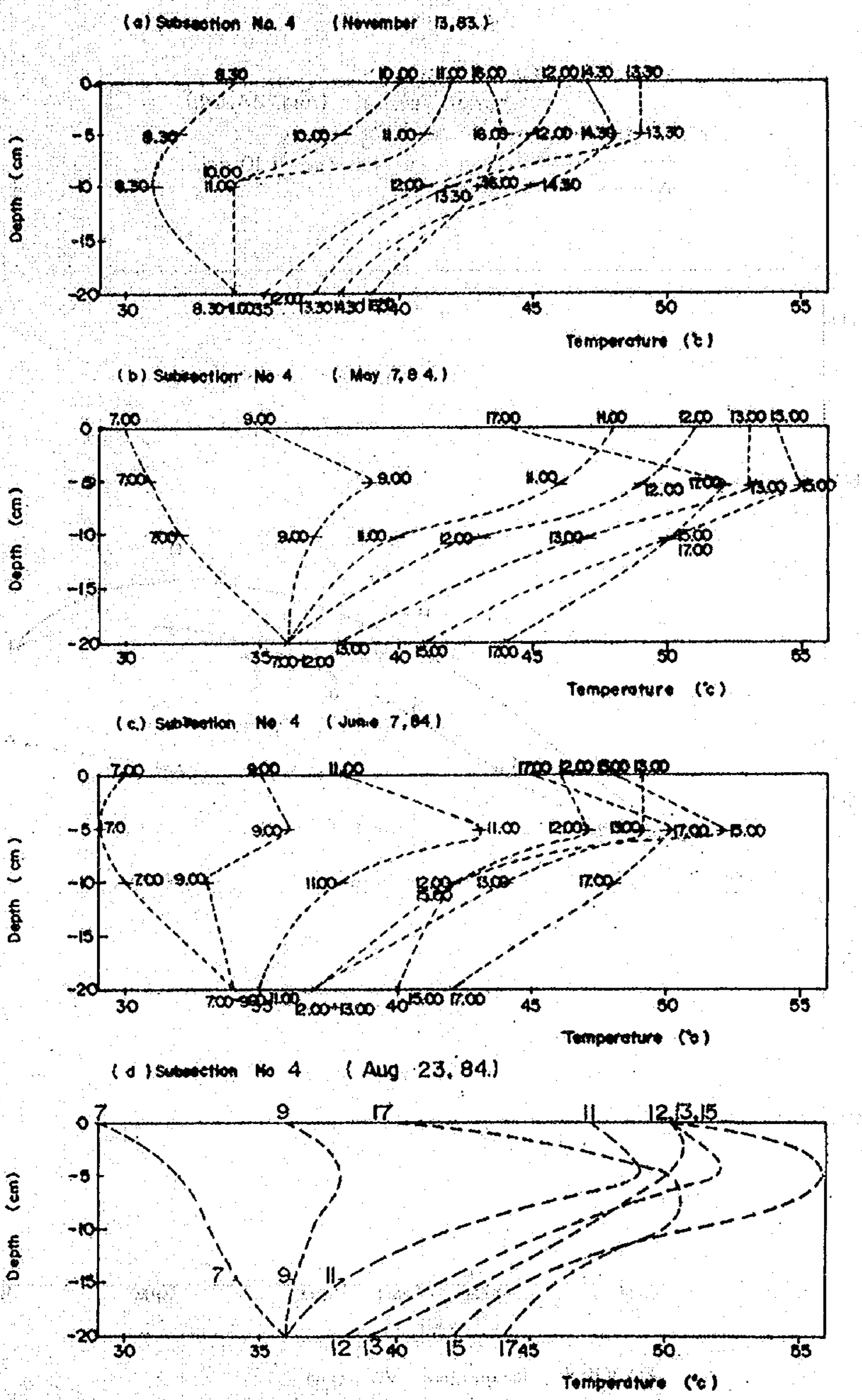

Fig. V. 5—2 TEMPERATURE DISTRIBUTION AT VARIOUS AGES

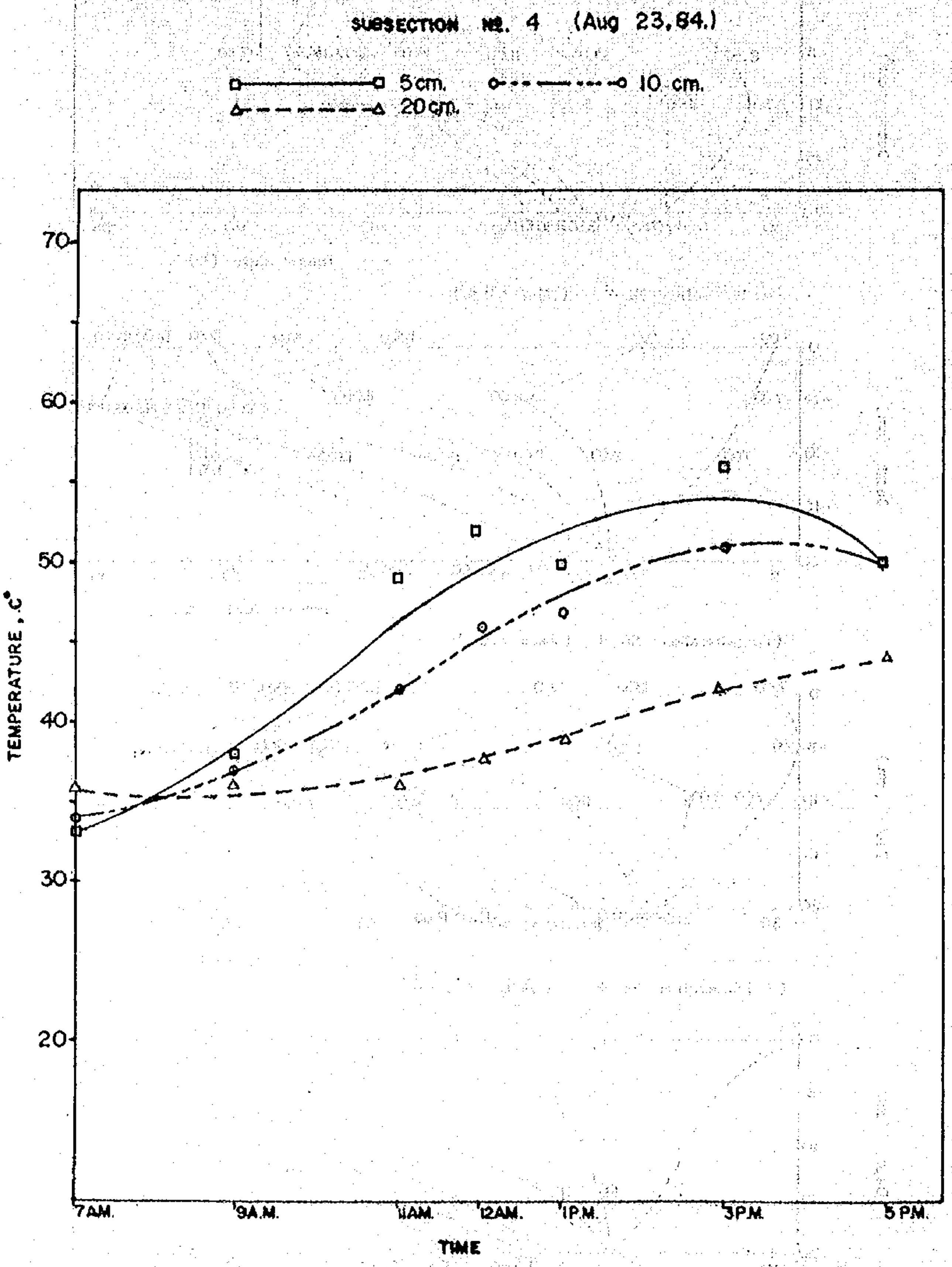

Fig. V.5-3 Temperature VS. Time

V.6 Static Vertical Stress

Pressure cells have been used to measure vertical stress. Cell no. 1,2,4 and 5 and 3 have been embedded at the bottom of Base and Subbase Courses, respectively.

V.6.1 Vertical Stress Vs.Age

Fig. V.6-1 has shown this relationship in subsection nos. 3,4,5 and 6. Stress range had varied from 0.5 to 8 KSC. Tendency of stress had been decreased upon the increasing age. Especially, after surface course construction, Vertical stresses have reduced about 2-3 times of the early age. Load condition A had been tested by Benkelman Beam Truck.

The relationship of vertical stress at the Bottom of Base Course VS. Age has shown in Fig. V.6-2. Vertical Stress in 15-cm. base thickness; for 4.3 % cement content had bigger stress than 7 % cement content. But in 20-cm. base thickness, before surface construction, Stress of 4.3 % cement content had smaller than the other type. Stresses in 15-cm. base thickness had bigger than those in the other thickness.

V.6.2 Load Dispersion Ratio VS. Age

Before surface course construction, there was big difference between vertical stress at the bottom of base and subbase. Fig. V.6-3 has shown the relationship of Load Dispersion Ratio and Age. This effect tended to reduce as the increasing age. The ratios were ranged from five to ten.

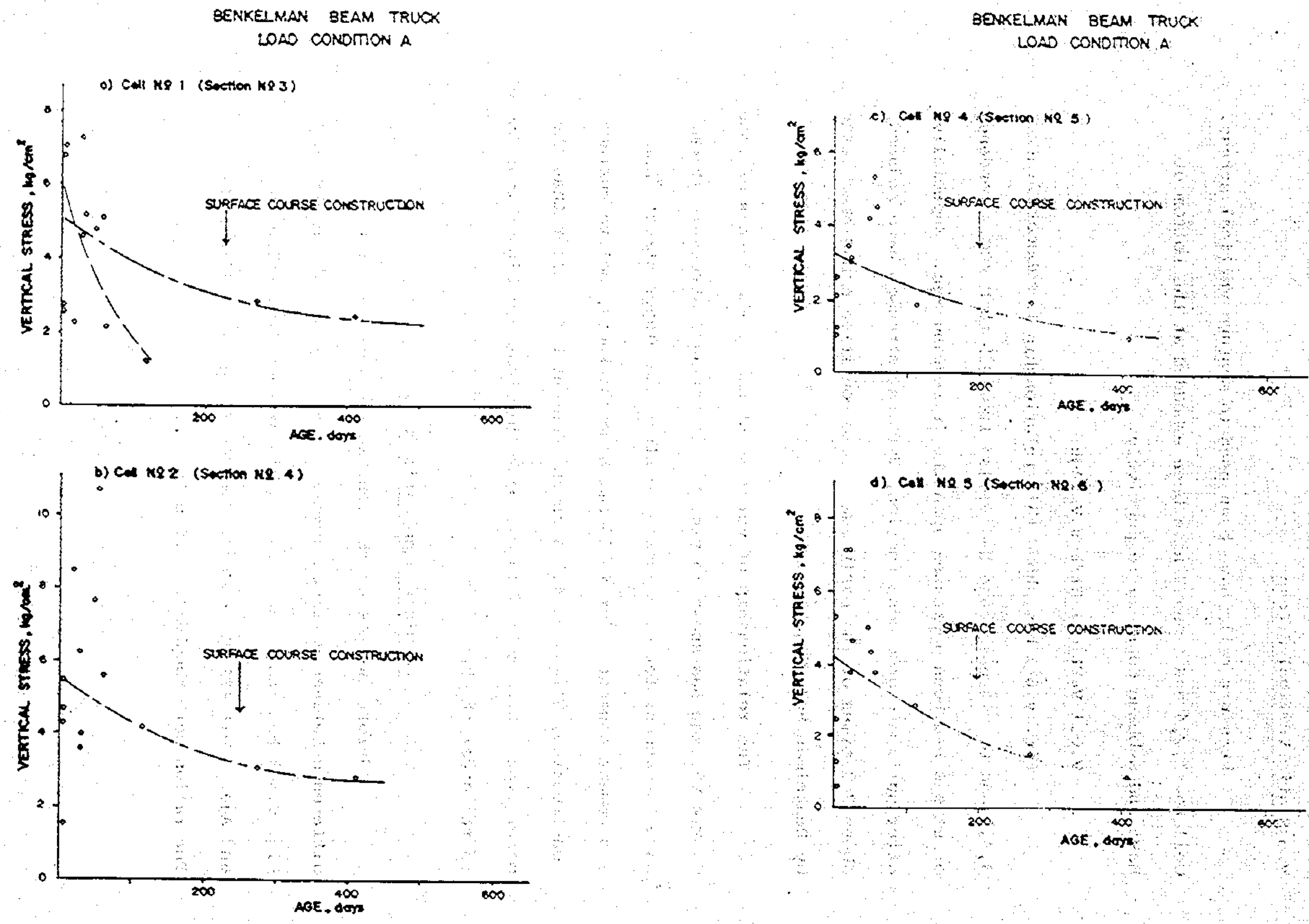

Fig. V. 6-1 Vertical Stress VS. Age

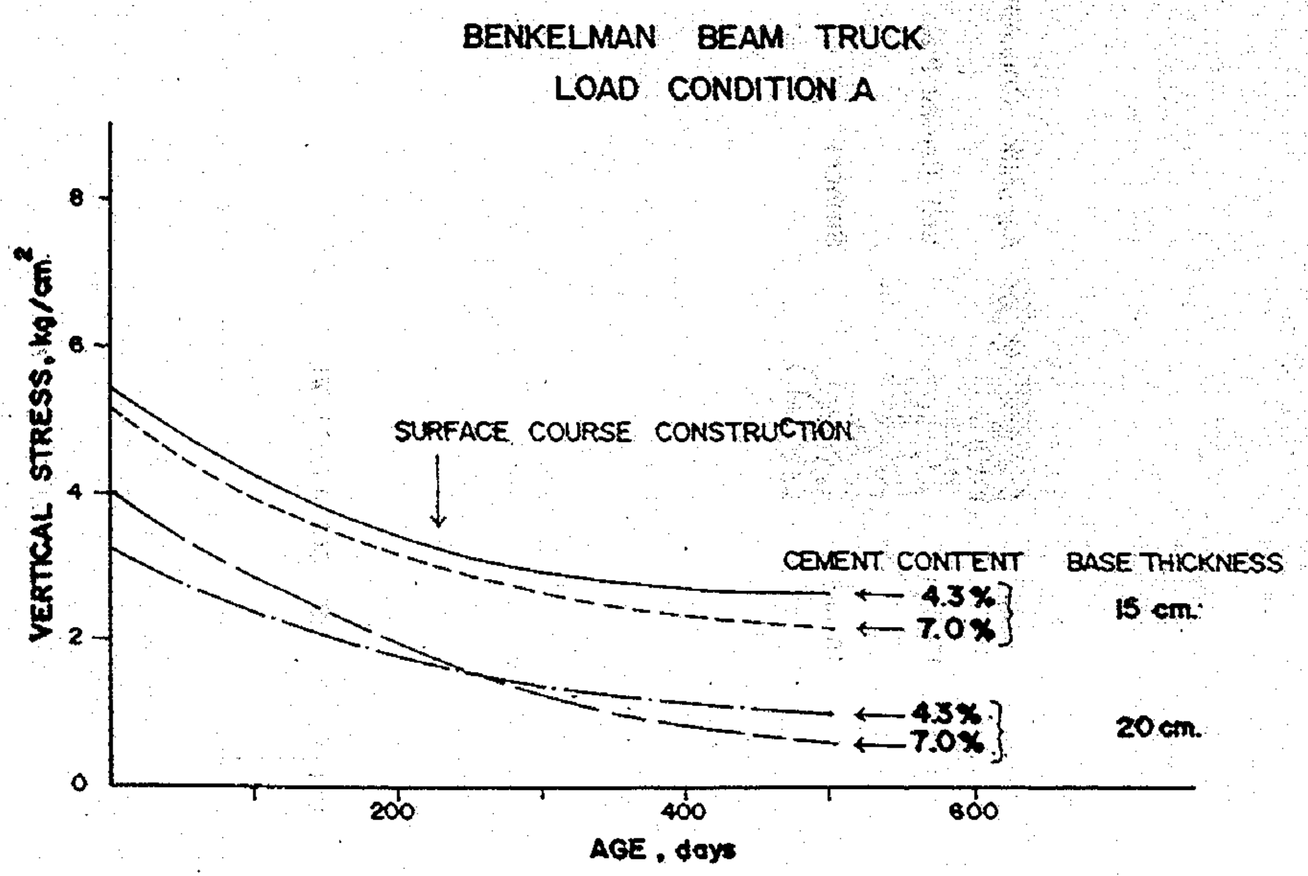

Fig.V.6-2 Vertical Stress at the Bottom of Base Course VS. Age.

BENKELMAN BEAM TRUCK
LOAD CONDITION A

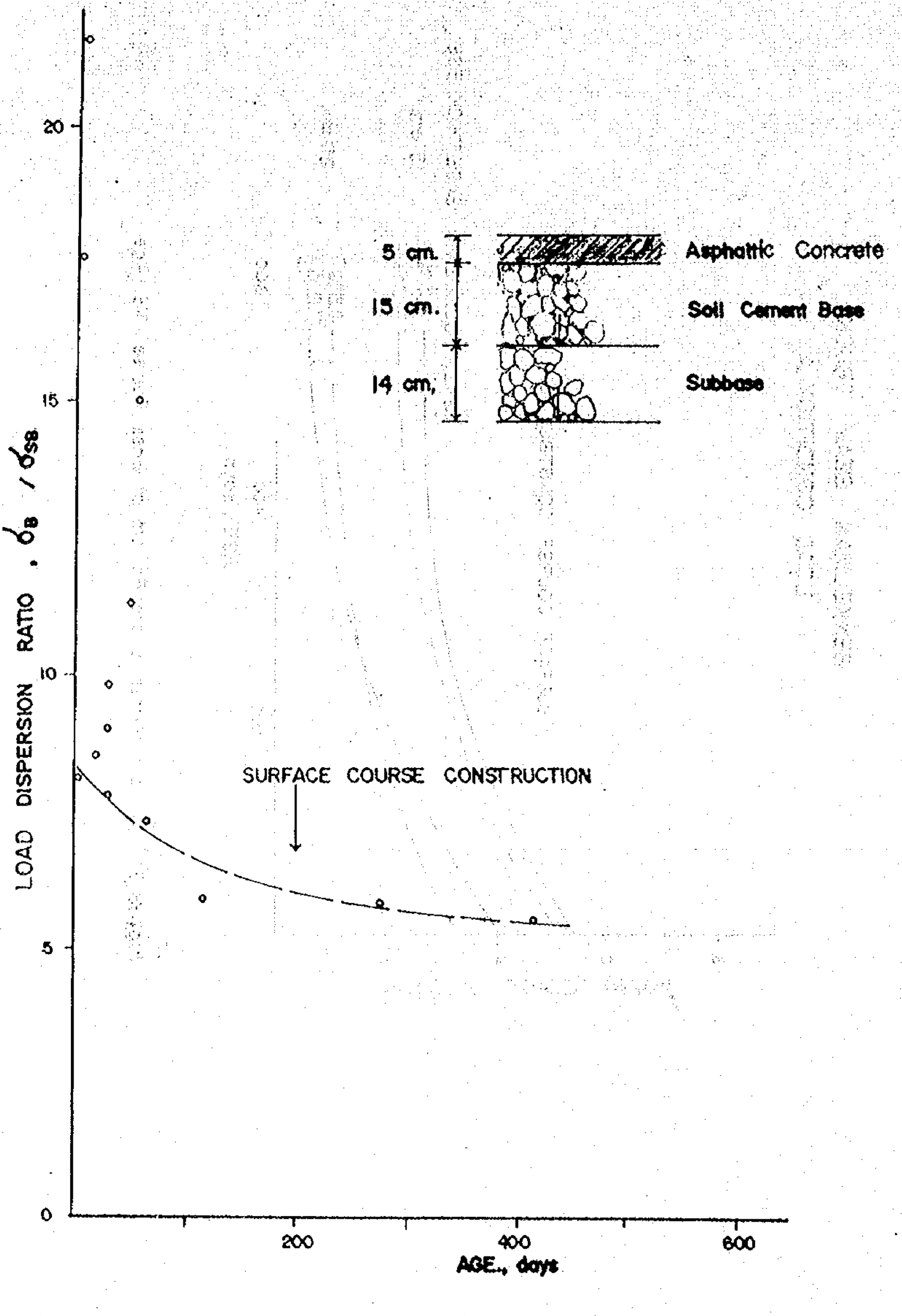

Fig. V. 6—3 Load Dispersion Ratio VS. Age.

V.7 Dynamic Vertical Stress

Four and one earth pressure cells were embedded at the bottom of soil-cement base course and subbase course, respectively. Cell No. 3 was at the bottom of subbase course. Various weights of Benkelman Beam Trucks had been used in the tests. Dynamic vertical strains were recorded by means of Dynamic Strain Meter and Amplifier.

V.7.1 Dynamic Vertical Stress VS. Speed

With various ages, these relationships had plotted in case of Load Condition A and B as shown in Fig. V.7-1 (a) to (c) and Fig. V.7-1 (d) to (f), respectively. Their trends were peaked within the range of 0-10 K.P.H., after surface construction. Both types of Load conditions, stresses of Cell No.3 were the smallest value,

V.7.2 Effect of Different Ages.

The stresses of each pressure cell, of both Load Condition, had shown some doubtful results. Their stresses ranged from 0.5 to 3.7 KSC. Cell No. 3 had shown small range of stress, but another did big range, as shown in Fig. V.7-2 (a) to (j).

V.7.3 Vertical Stress VS. Age

The relationship of verticle stress and age of Cell No.1,2,4 and 5 at speeds of 10, 20, 30 and 40 K.P.H. were used Fig. V.7-1 as references. Only Load Condition A has showed in Fig. V.7-3. Age has been counted after surface course construction. Vertical stresses of Cell No. 4 and 5 had decreased at 6 months age and they increased again, except Cell no.2. For Cell no.1, Vertical Stresses increased as the increased age.

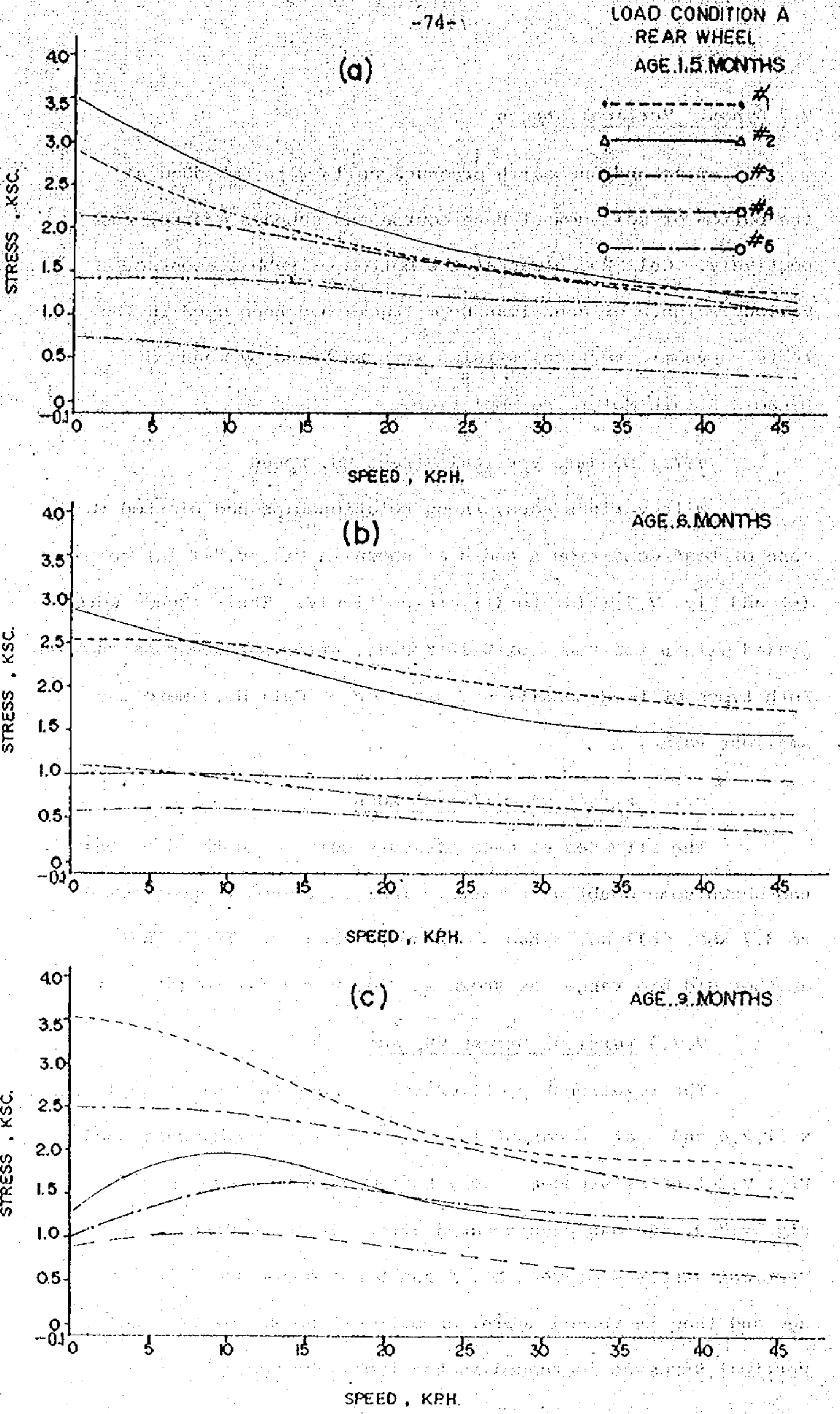

Fig.V.7-1 Vertical Stress vs. Speed

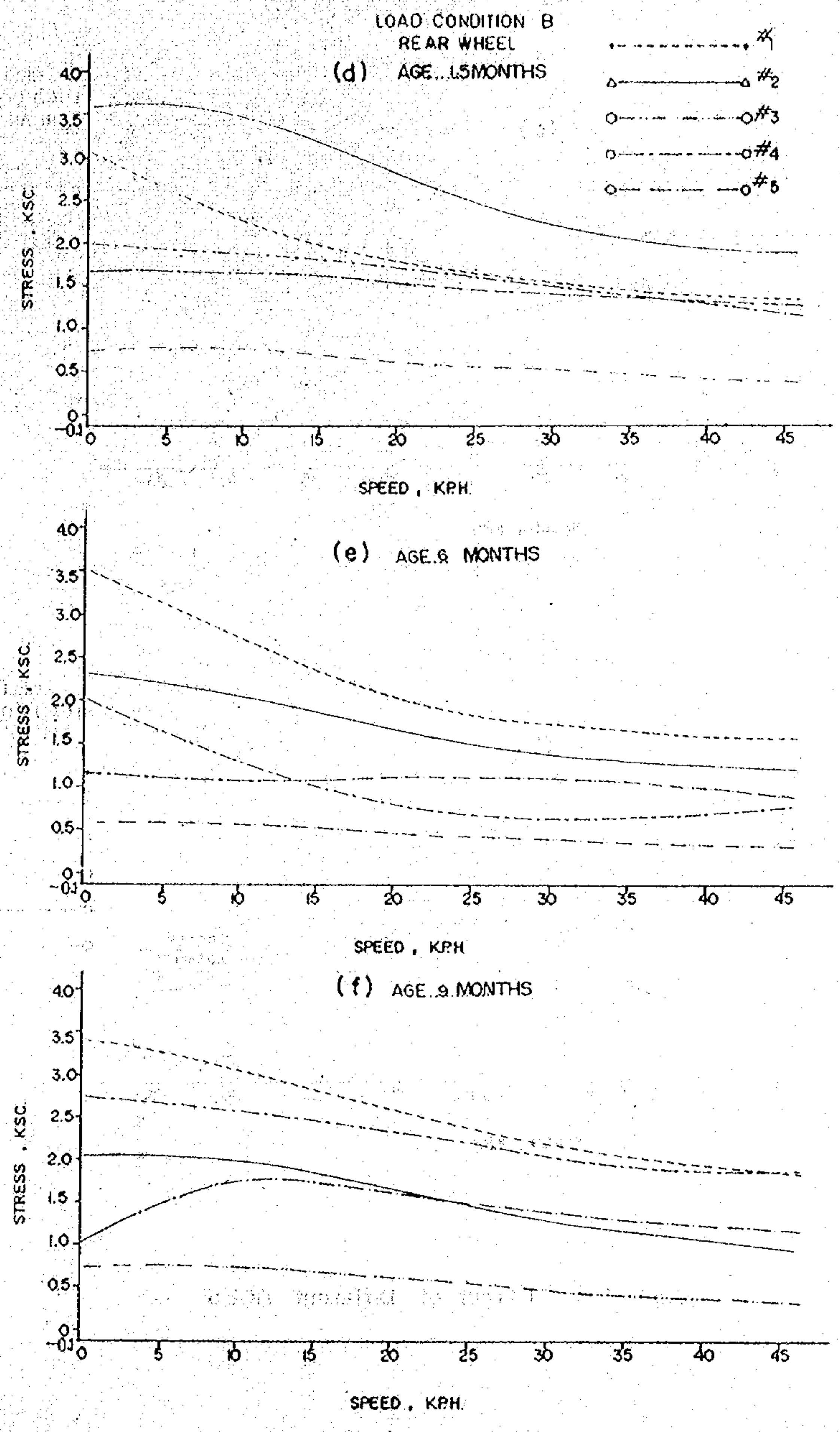

LOAD CONDITION B
REAR WHEEL
(d) AGE..1.5MONTHS
#1
#2
#3
#4
#5
STRESS , KSC.
4.0
3.5
3.0
2.5
2.0
1.5
1.0
0.5
0
-0.1
0 5 10 15 20 25 30 35 40 45
SPEED , KPH.
(e) AGE.6 MONTHS
STRESS , KSC.
SPEED , KPH
(f) AGE..9 MONTHS
STRESS , KSC.
SPEED , KPH.

Fig.V.7-1 (cont.)

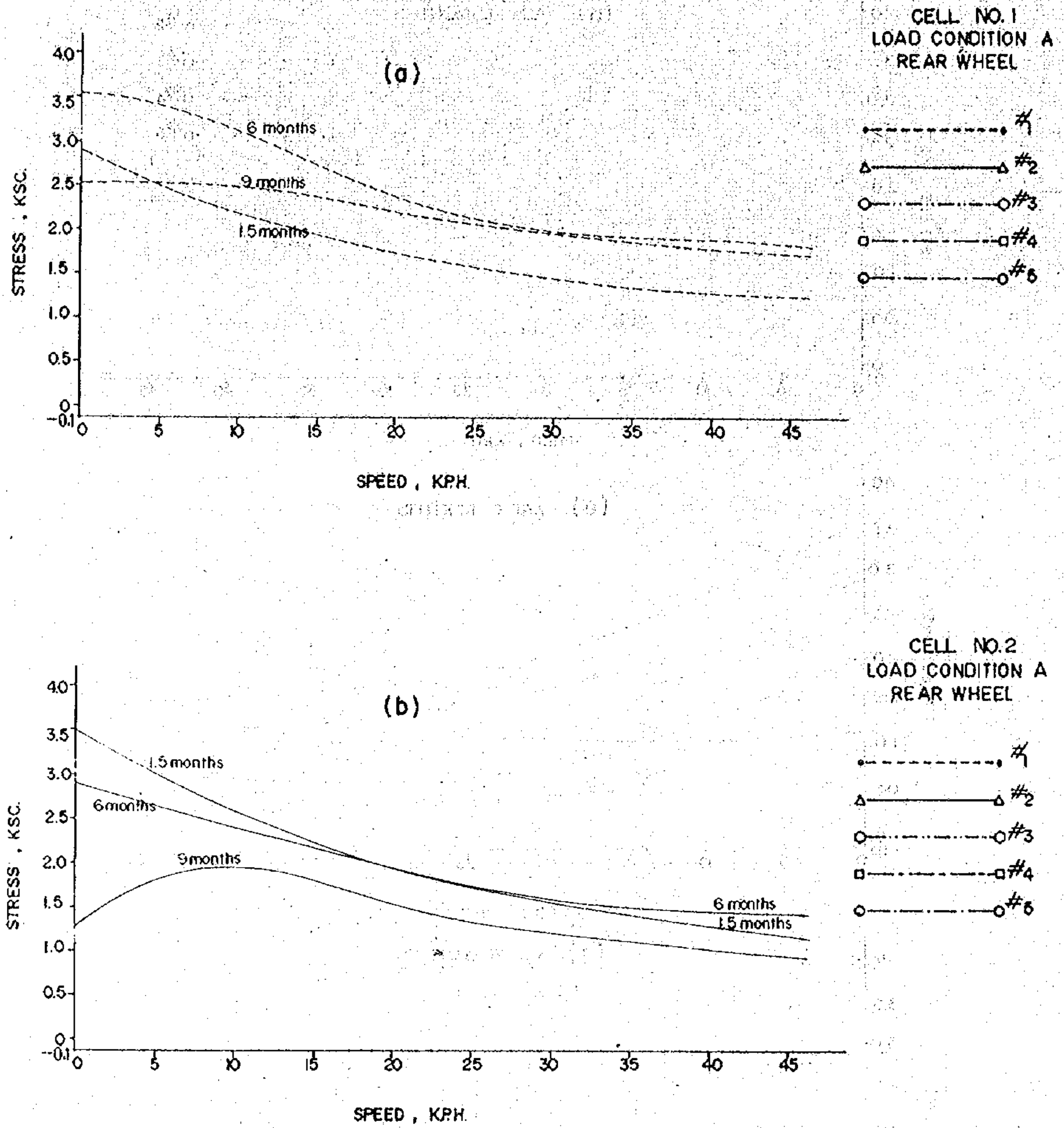

Fig. V.7-2 Effect of Different AGES

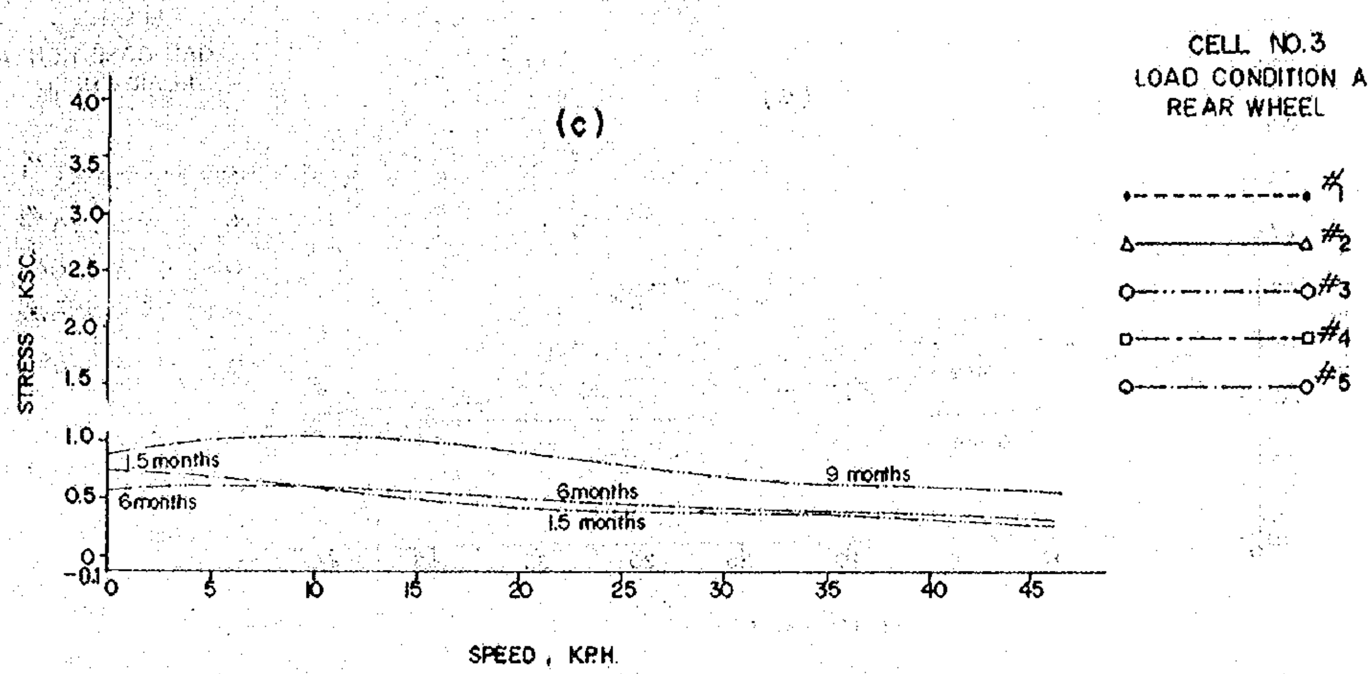

CELL NO.3
LOAD CONDITION A
REAR WHEEL
(c)
#1
#2
#3
#4
#5
STRESS , KSC.
4.0
3.5
3.0
2.5
2.0
1.5
1.0
0.5
0
-0.1
1.5 months
6months
9 months
6months
1.5 months
0
5
10
15
20
25
30
35
40
45
SPEED , KPH.

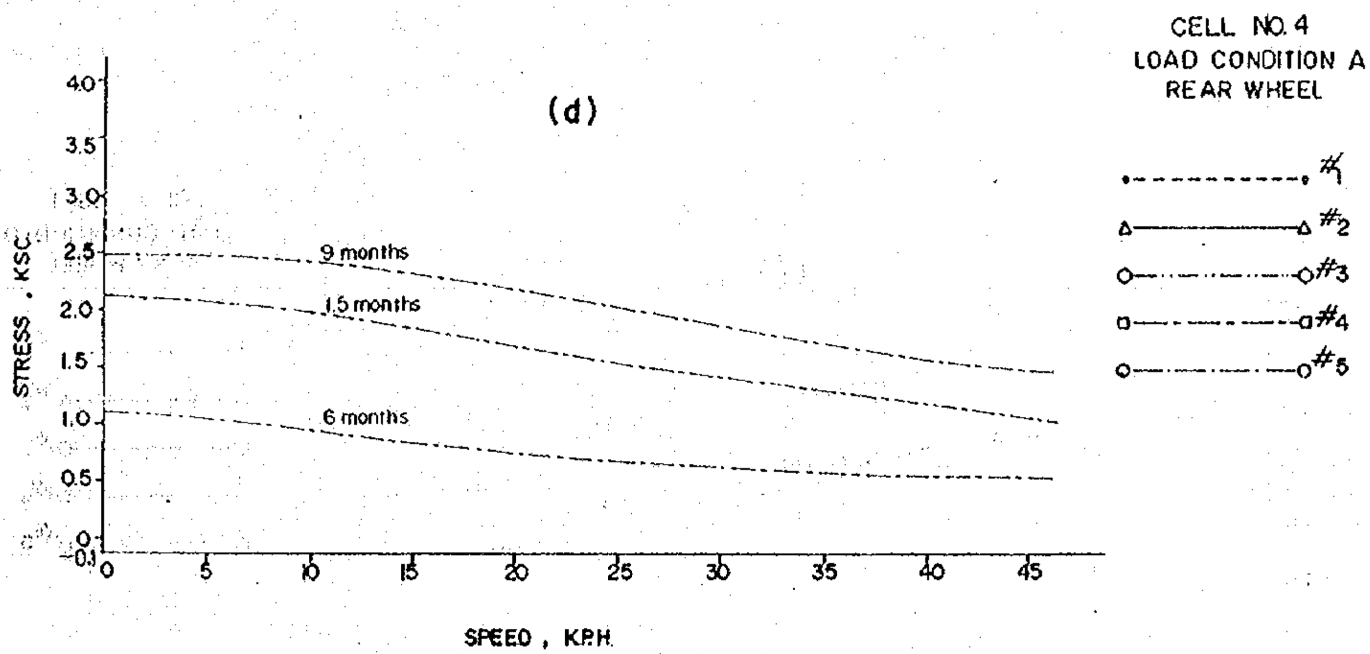

CELL NO.4
LOAD CONDITION A
REAR WHEEL
(d)
#1
#2
#3
#4
#5
STRESS , KSC
4.0
3.5
3.0
2.5
2.0
1.5
1.0
0.5
0
-0.1
9 months
1.5 months
6 months
0
5
10
15
20
25
30
35
40
45
SPEED , KPH.

Fig. V.7-2 (cont.)

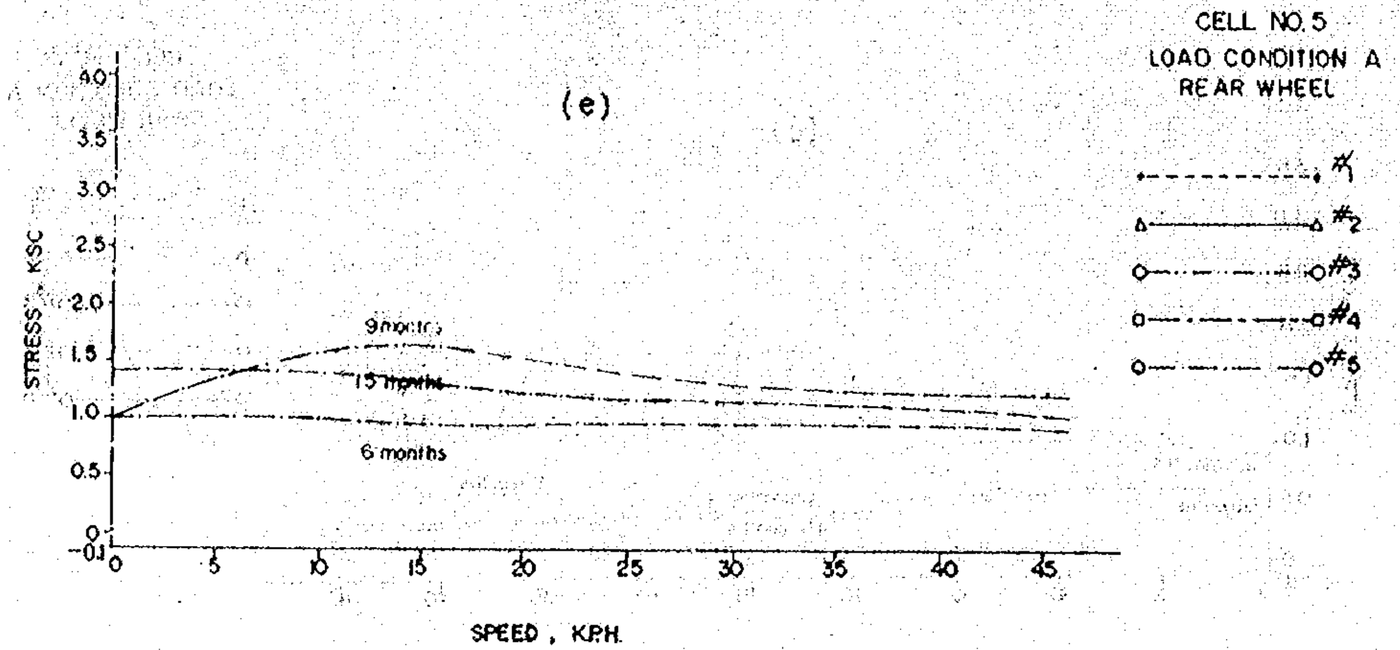
CELL NO. 5
LOAD CONDITION A
REAR WHEEL
(e)
#1
#2
#3
#4
#5
9 months
15 months
6 months
STRESS, KSC
SPEED, KPH
4.0
3.5
3.0
2.5
2.0
1.5
1.0
0.5
0
-0.1
0
5
10
15
20
25
30
35
40
45

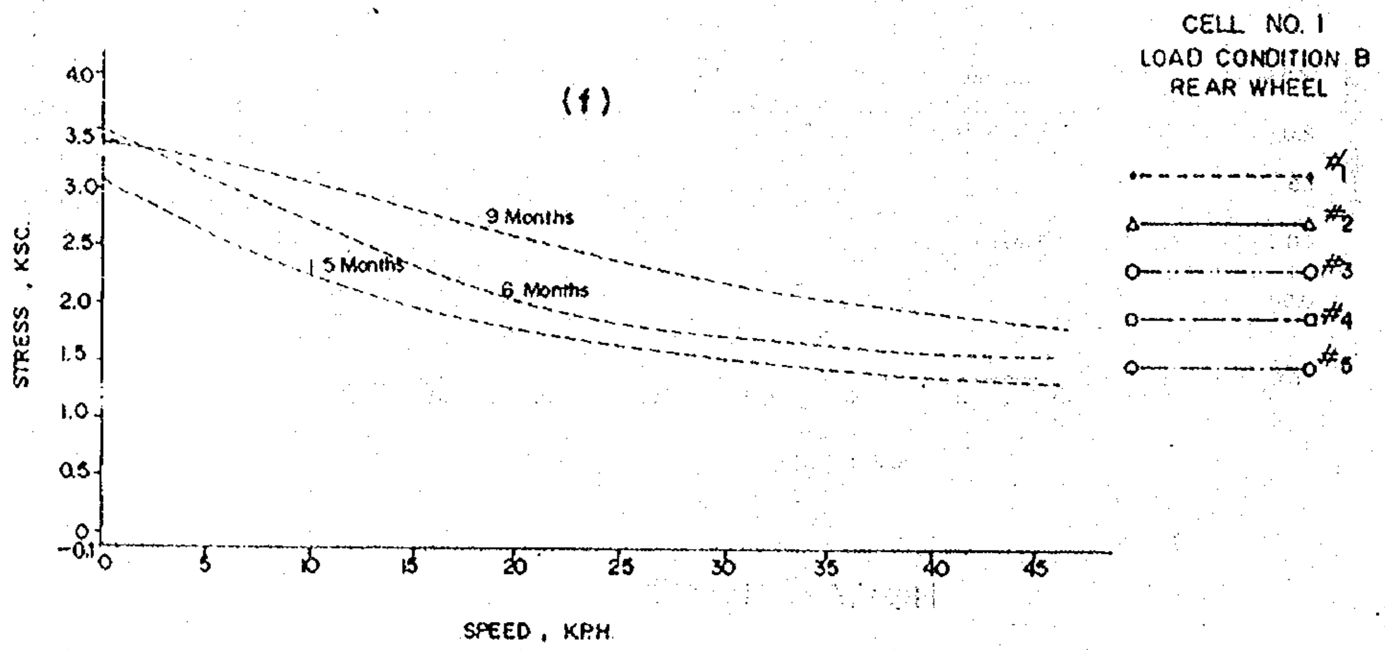
CELL NO. 1
LOAD CONDITION B
REAR WHEEL
(f)
#1
#2
#3
#4
#5
9 Months
15 Months
6 Months
STRESS, KSC.
SPEED, KPH
4.0
3.5
3.0
2.5
2.0
1.5
1.0
0.5
0
-0.1
0
5
10
15
20
25
30
35
40
45

Fig. V.7-2 (cont.)

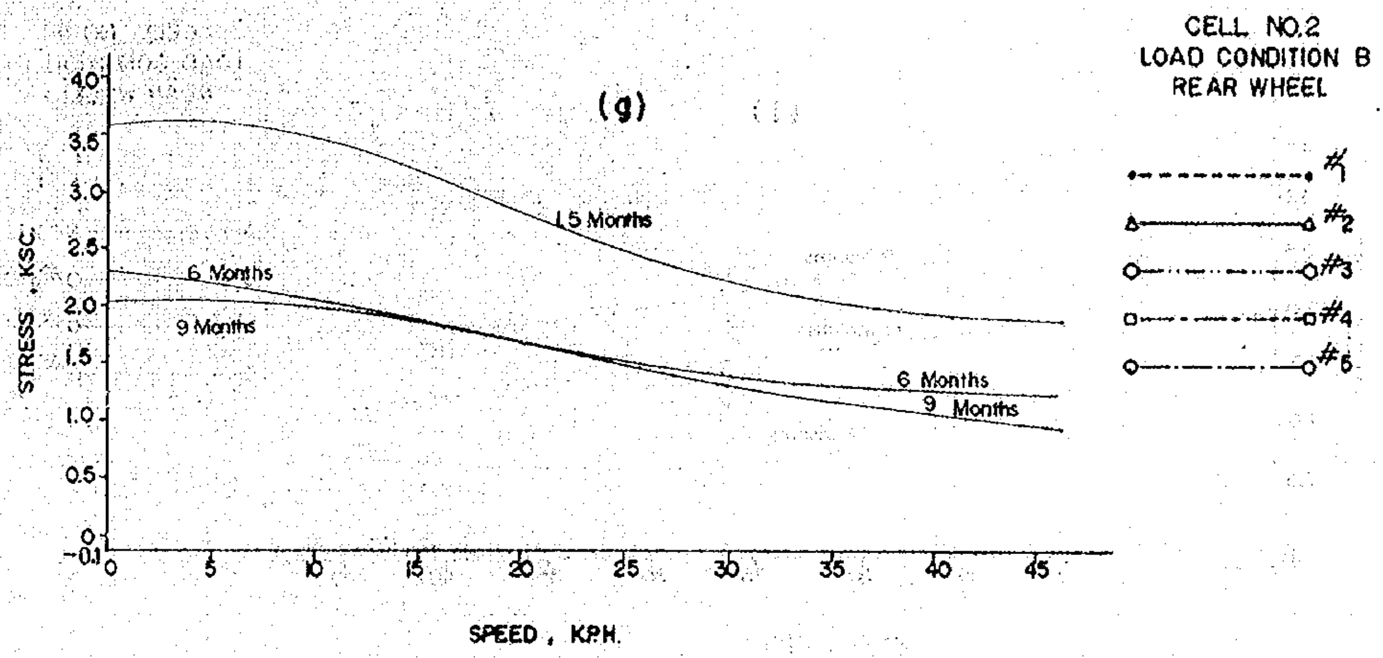

CELL NO.2
LOAD CONDITION B
REAR WHEEL
(g)
#1
#2
#3
#4
#5
STRESS , KSC.
SPEED , KPH.
1.5 Months
6 Months
9 Months
6 Months
9 Months

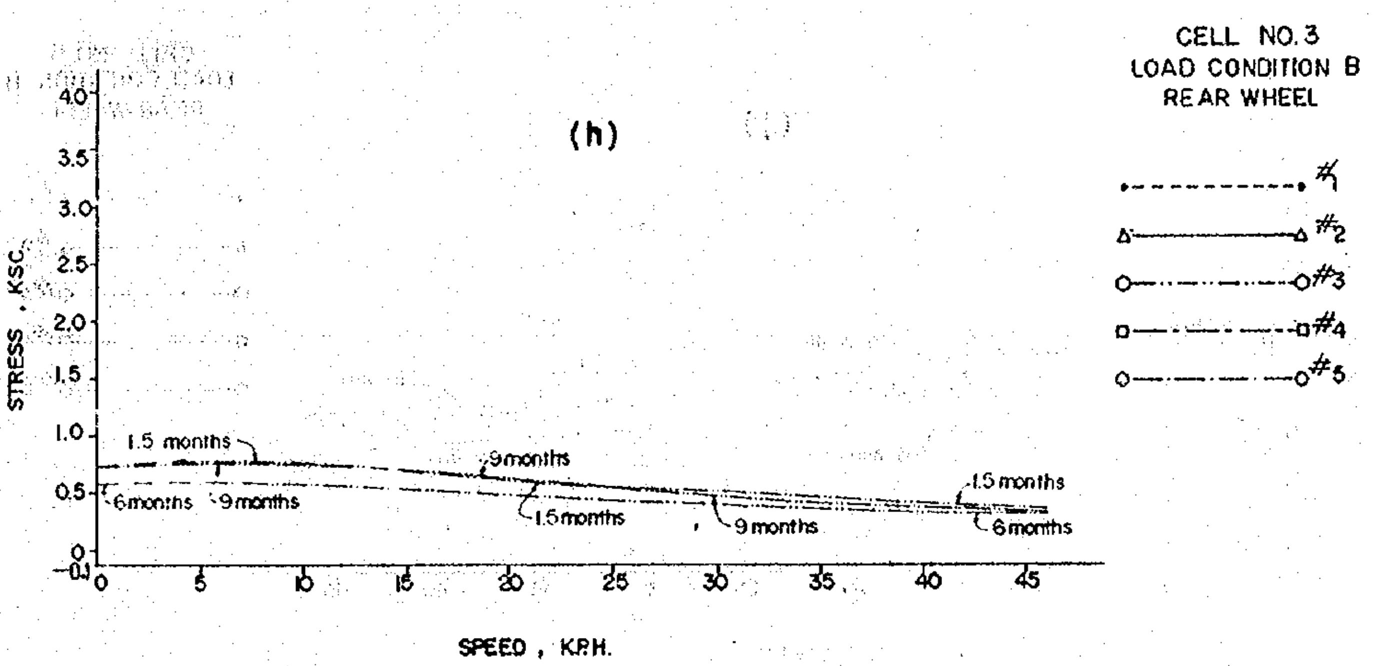

CELL NO.3
LOAD CONDITION B
REAR WHEEL
(h)
#1
#2
#3
#4
#5
STRESS , KSC.
SPEED , KPH.
1.5 months
9 months
6 months
9 months
1.5 months
9 months
1.5 months
6 months

Fig. V.7-2 (cont.)

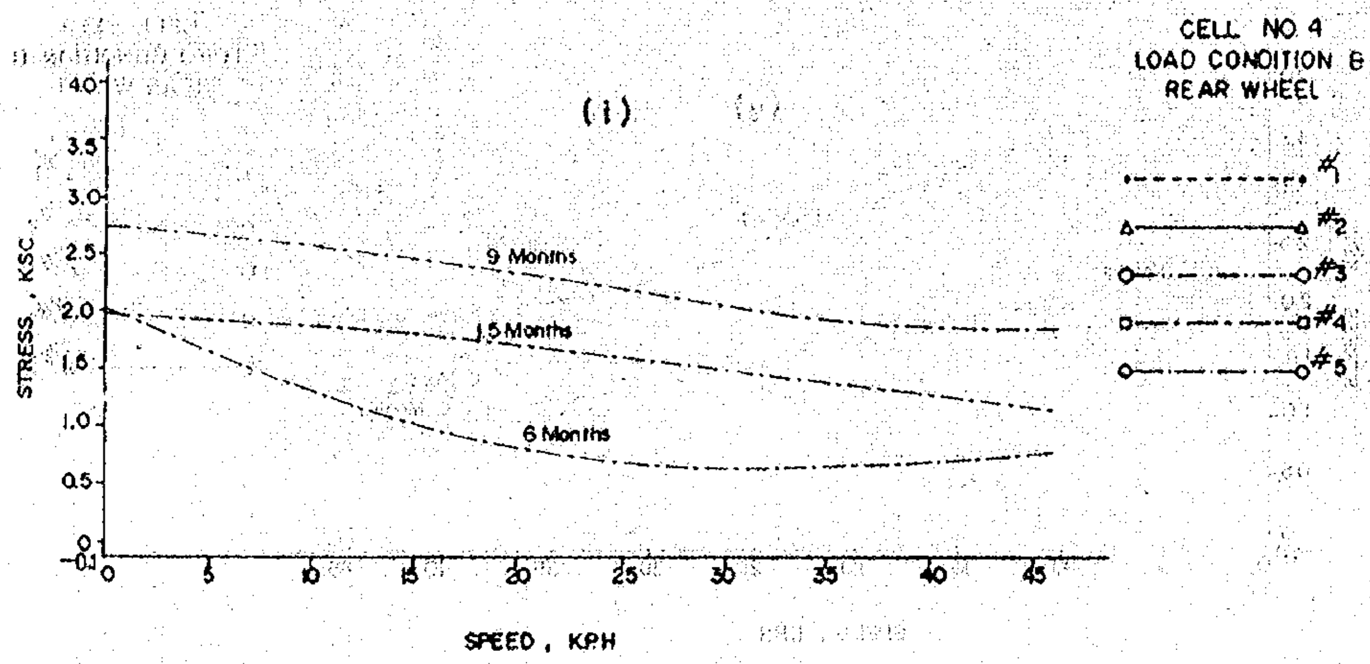
CELL NO. 4
LOAD CONDITION B
REAR WHEEL
(i)
#1
#2
#3
#4
#5
9 Months
1.5 Months
6 Months
STRESS , KSC
SPEED , KPH

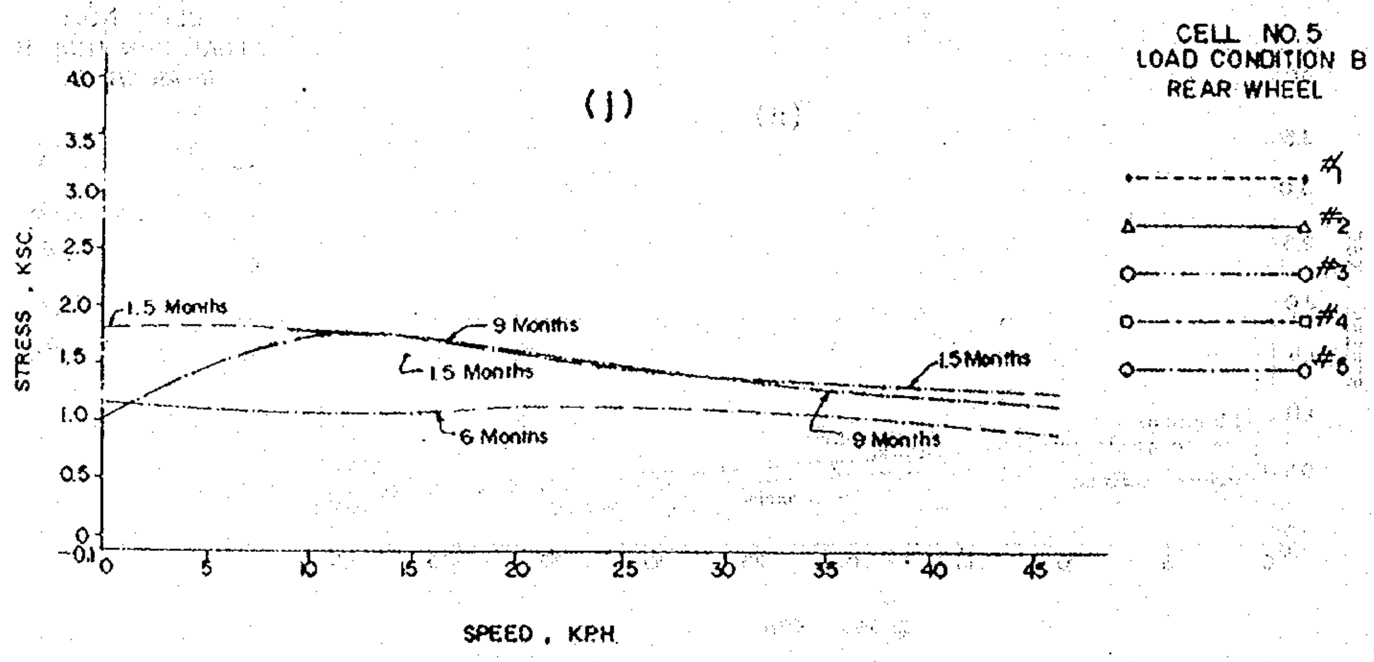
CELL NO. 5
LOAD CONDITION B
REAR WHEEL
(j)
#1
#2
#3
#4
#5
1.5 Months
9 Months
1.5 Months
6 Months
1.5 Months
9 Months
STRESS , KSC
SPEED , KPH

Fig. V.7-2 (cont.)

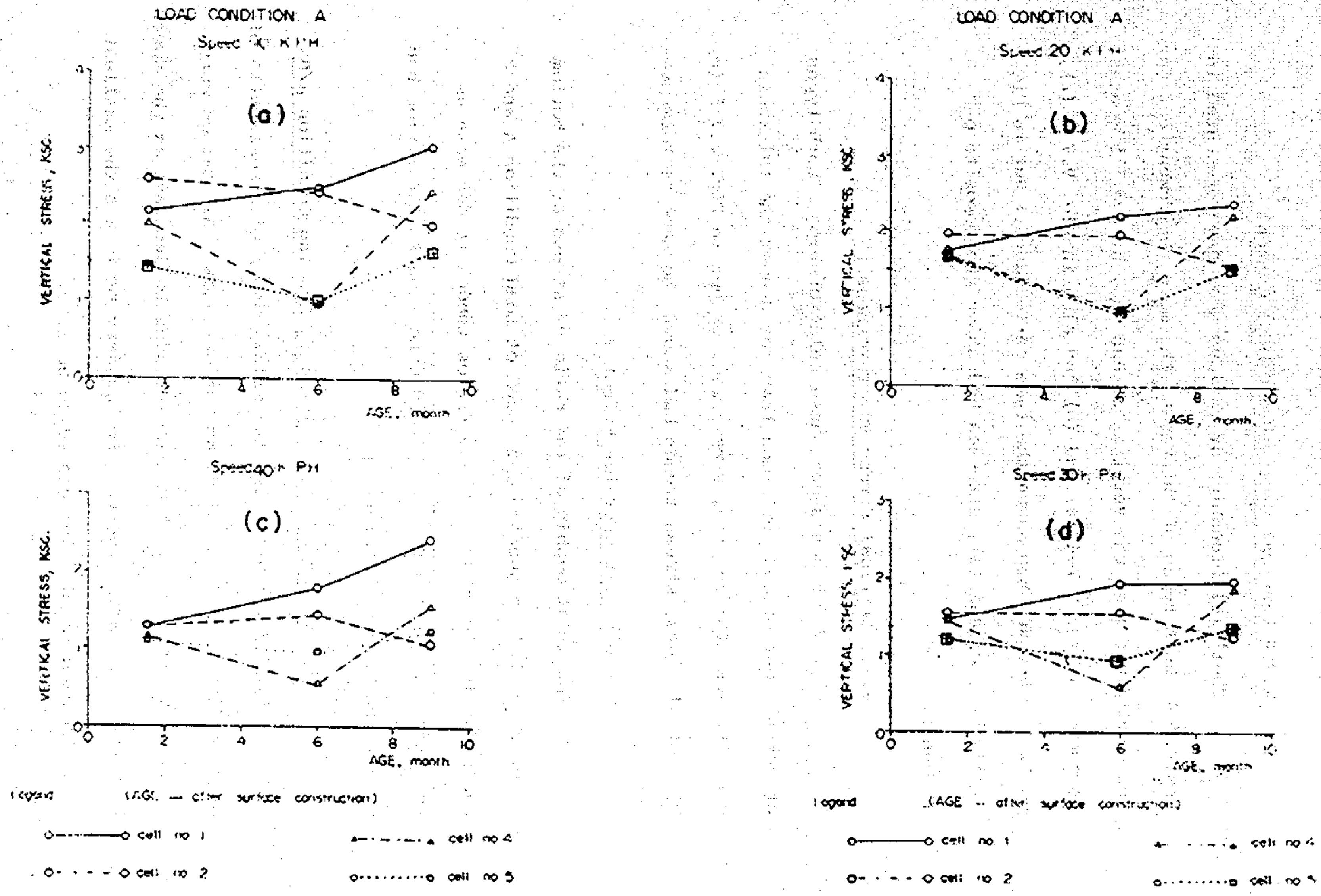

Fig. V.7—3 Vertical Stress VS. AGE

V.7.4 Vertical Stress VS. Cement Content

Their relationships at various ages have presented in Fig.V.7-4. Both types of thickness, the more the cement content increased, the less the vertical stress was, at age 1.5 months, as shown in Fig. V.7-4 (a) and (d). And also in Fig. V.7-4 (f), vertical stresses had shown the same performance. But in Fig. V.7-4 (b), (c) and (e), stresses had shown the opposite performance.

V.7.5 Vertical Stress VS. Thickness

Fig. V.7-5 has shown these relationships. Both types of cement content had performed that the deeper the thickness was, the less the vertical stress was, except in Fig. V.7-5 (c). Most of all ages, stress trends had shown the same performance.

V.7.6 Load Dispersion Effect

The relationship of the ratio of stress at the bottom of base to that at subbase and speed of Load Condition A and B had shown in Fig. V.7-6. These ratios tended to decrease as the increasing speed and age. Load Condition A, the ratios had bigger range than the other one.

V.7.7 Effect of Stress Ratio of Loading Condition A/B

Fig. V.7-7 has shown the relationship of stress ratio of Load Condition A/B and speed, at various ages. All ratios were positive values. Their boundaries tended to decrease as the speed increased. At age 9 months, the boundary ratio was the smallest one, and each ratio value closed to be 1.00.

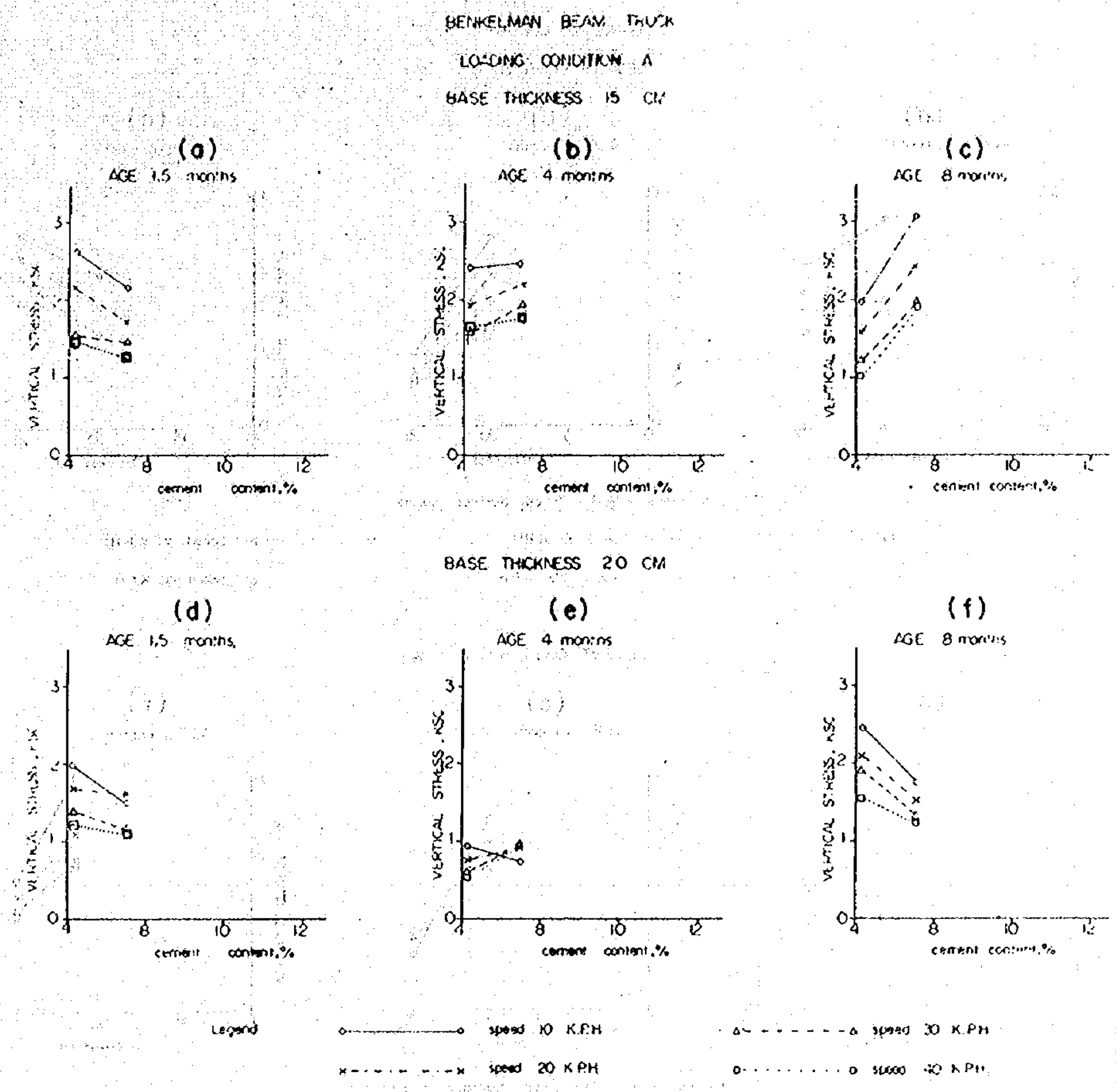

Fig. V.7-4 Vertical Stress VS. Cement Content

BENKELMAN BEAM TRUCK

LOADING CONDITION A

CEMENT CONTENT 4.5 %

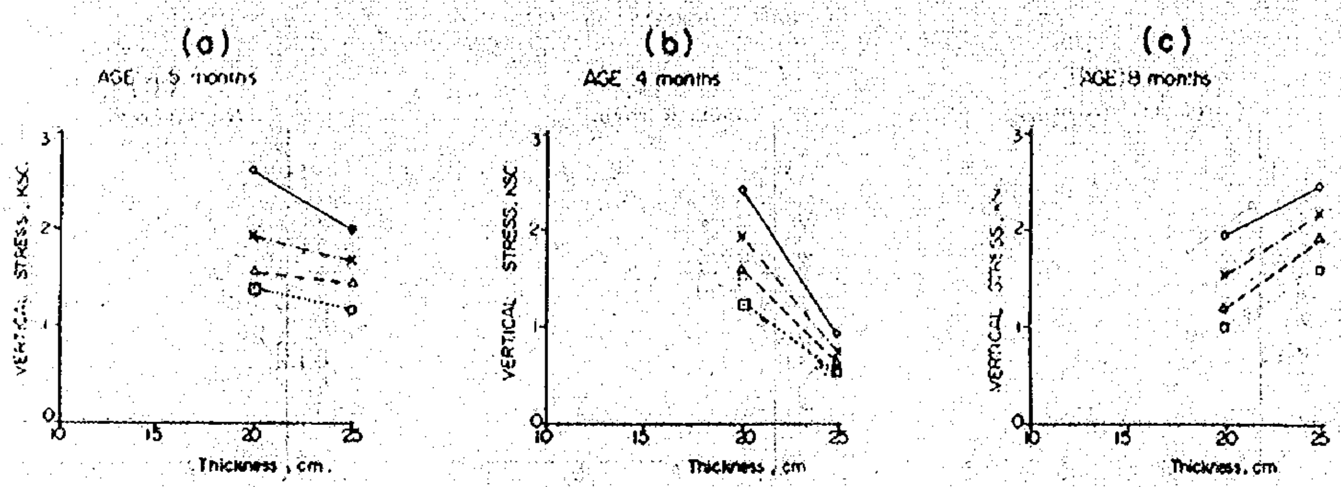

N.B. Thickness includes 5-cm. Surface course

Legend
o———o Speed 10 K.P.H.
x- - -x Speed 20 K.P.H.
△- - -△ Speed 30 K.P.H.
□ ····· □ Speed 40 K.P.H.

CEMENT CONTENT 7 %

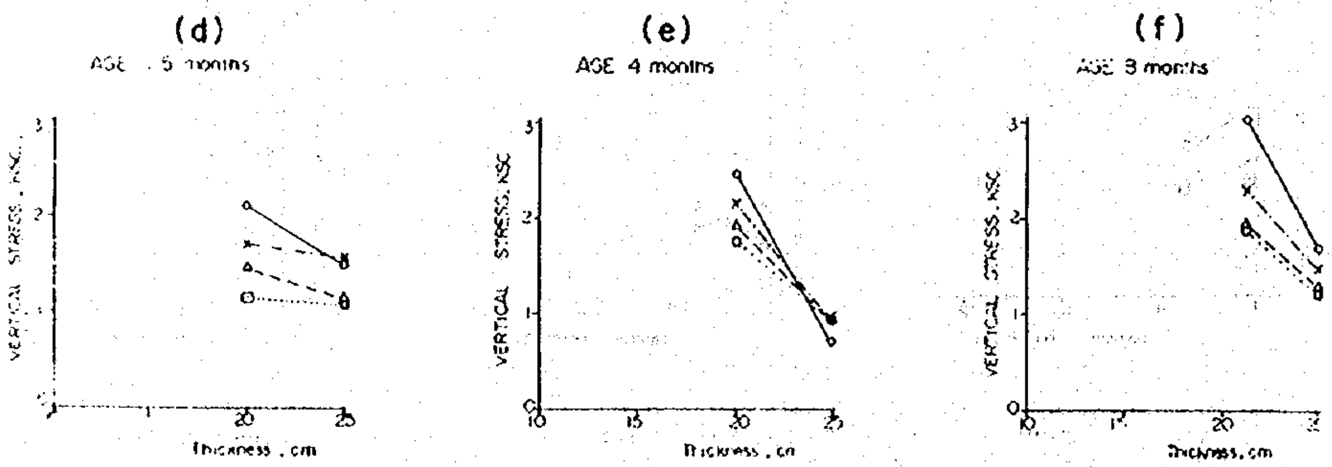

N.B. Thickness includes 5-cm. Surface course.

Legend
o———o Speed 10 K.P.H.
x- - -x Speed 20 K.P.H.
△- - -△ Speed 30 K.P.H.
□ ····· □ Speed 40 K.P.H.

Fig. V.7-5 Vertical Stress VS. Thickness

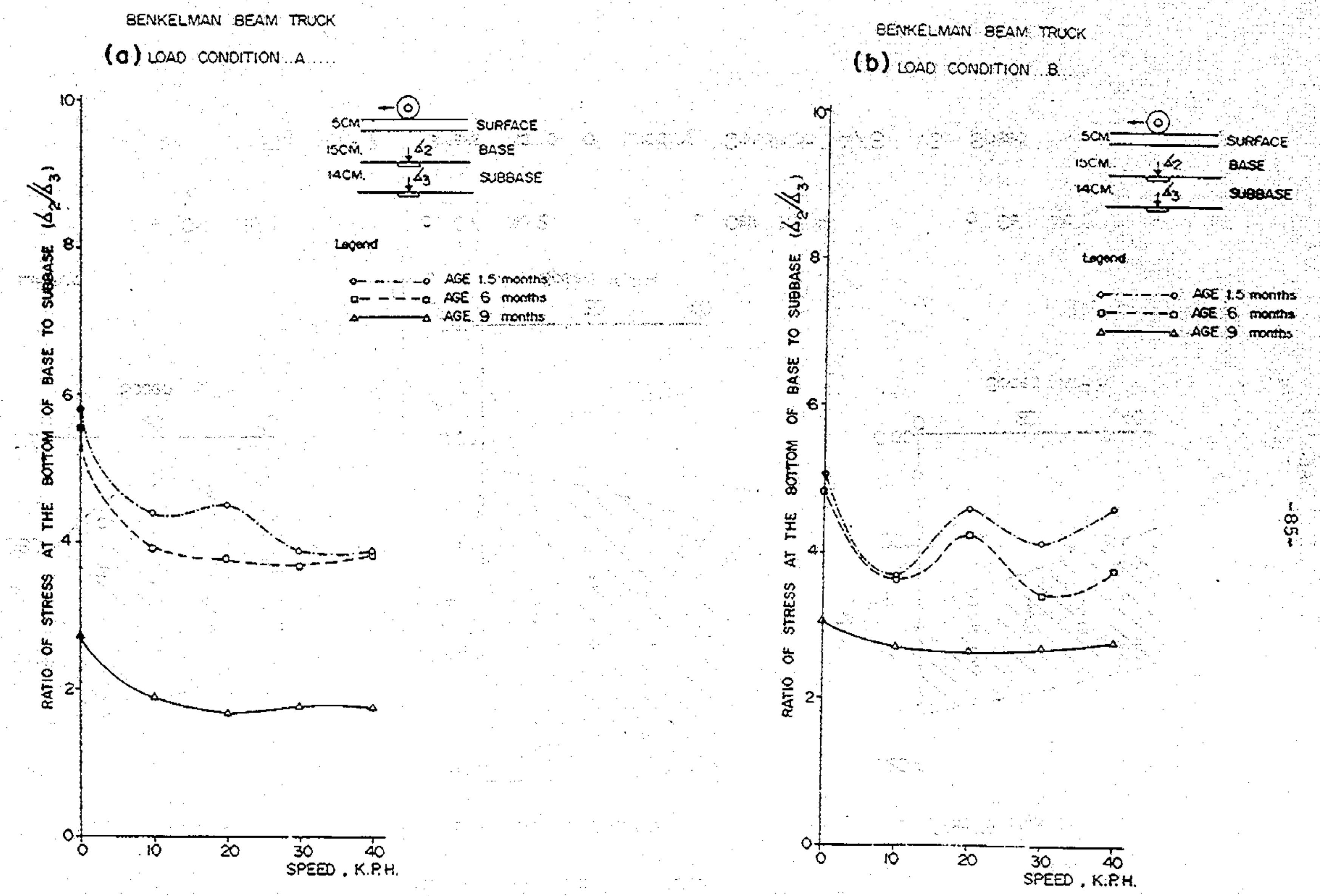

Fig.V.7-6 Load Dispersion Effect VS. Speed

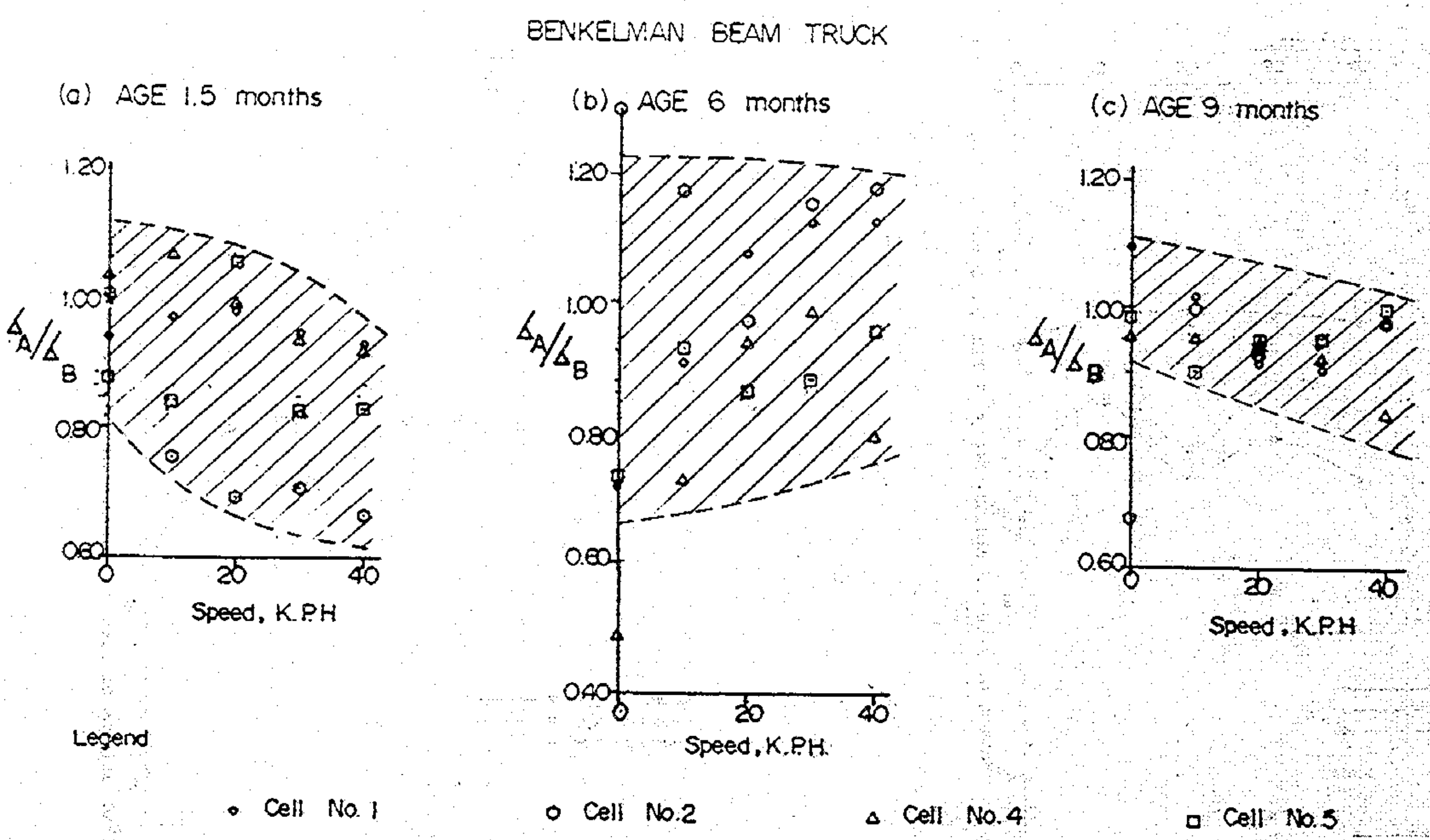

Fig. V.7-7 Stress Ratio of Loading Condition A/B VS. Speed

V.8 Accumulated Permanent Strain

V.8.1 Durability of Strain Gage in Soil Cement Base

The strain gages being used in this study, according to the manual, have tensile strain limit about 0.2 % (about 2,000 micron). From our experience, strain values up to -10,000 micron could be measured. In this report, the upper strain Limit is specified at -8,000 micron. The durability of a strain gage was then determined for three specified strain Limits = 2,000, over -4,000 and over -8,000 micron. The age at which a strain reading over the Limits was recorded and presented in Table V.8-1 from which the survival ratio at various time was determined. Survival ratio of gages was calculated from the equation below.

Survival Ratio of gages, %

$$= \frac{\text{Number of gages within Strain Reading Limit}}{\text{Total Number of Embedded Strain gages}} \times 100$$

Table V.8-1 shows the survival ratios for the specified strain limits. Fig. V.8-1 presents the survival ratio against age. The survival ratio at 50 % for strain limits of -8,000, -4,000 and ± 2,000 micron is obtained at 10, 7.5 and 4 months, respectively. Thus, all the strain measurement should be completed between 5-7 months after construction to have the survival ratio over 75 %.

V.8-2 Accumulated Permanent Strain in Soil Cement

Less than half of the embedded strain gages are survived. the measurement of the survived strain gages shows the general

Table V.8-1 Survival Ratio of Gage with Passed Months

	Age																	
	Months	0	1	2	3	4	5	6	7	8	9	10	11	12	13	14	15	16
	Days	0	30	60	90	120	150	180	210	240	270	300	330	360	390	420	450	480
Over ±2,000 μ	Number of Gage Over ± 2,000 μ	3	6	9	11	13	15	21	21	26	26	26	26	28	28	29	29	29
	Number of Gage Less than ±2,000 μ	27	24	21	19	17	15	9	9	4	4	4	4	2	2	1	1	1
	Survival Ratio of Gage (%)	90	80	70	63	57	50	30	30	13	13	13	13	7	7	3	3	3
Over -4,000 μ	Number of Gage Over -4,000 μ	1	1	3	4	4	7	11	12	18	18	22	22	24	24	25	25	25
	Number of Gage Less than -4,000 μ	29	29	27	26	26	23	19	18	12	12	8	8	6	6	5	5	5
	Survival Ratio of Gage (%)	97	97	90	87	87	77	63	60	40	40	27	27	20	20	17	17	17
Over -8,000 μ	Number of Gage Over -8,000 μ	1	1	3	3	4	5	7	7	13	13	15	15	17	19	21	22	22
	Number of Gage Less than -8,000 μ	29	29	27	27	26	25	23	23	17	17	15	15	13	11	9	8	8
	Survival Ratio of Gage (%)	97	97	90	90	87	83	77	77	57	57	50	50	43	37	30	27	27

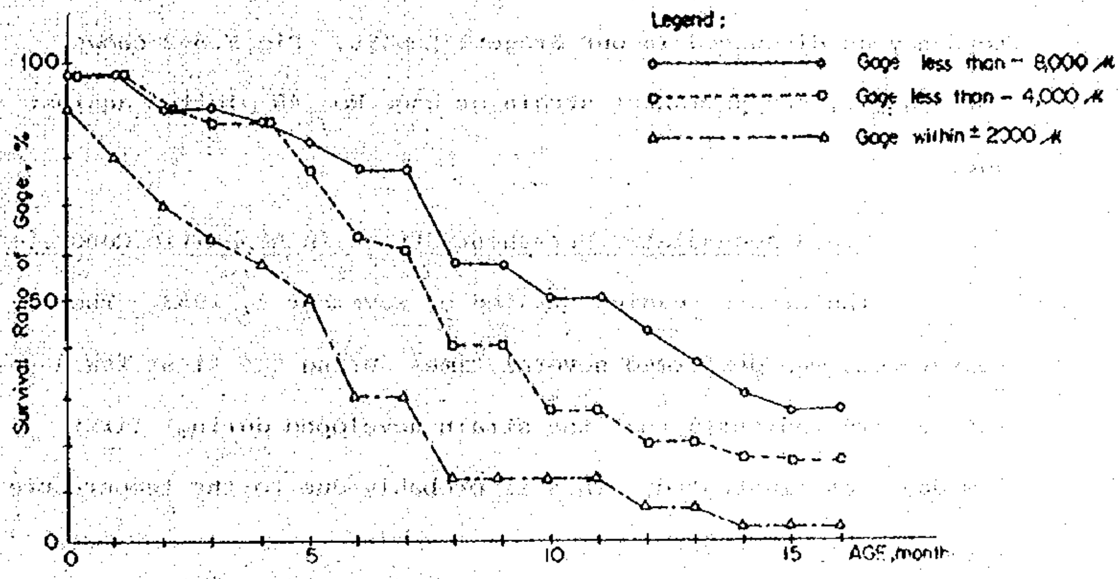

Fig. V.8-1 Survival Ratio of Gage vs AGE

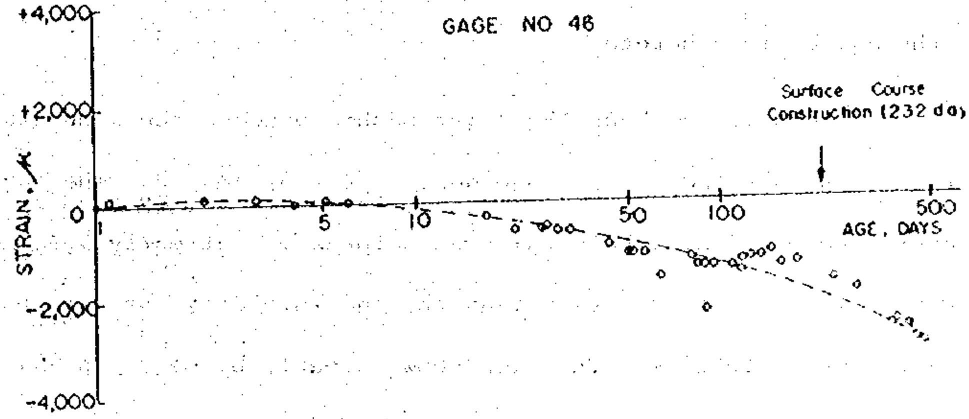

Fig V.8-2 Permanent Strain VS AGE

tendency as discussed in our Stage I Report. Fig.V.8-2 shows, for example, the permanent strain of gage No. 46 plotted against age.

V.8.3 Accumulated Permanent Strain in Asphaltic Concrete

The strain reading strated on November 9, 1983. The measurement was performed several times during the first few days. The results indicated that the strain developed during first few days was fluctuated. This is probably due to the temperature variation.

Strains of Gage Nos.51 and 52 are plotted against the temperature in Fig.V.8-3. There appears to be some linear relationship between these two parameters. Using linear regression analysis, the relationship between developed strain and temperature of Gage Nos. 41,42,51 and 52 are shown in Table V.8-2.

Since Gage No.41 shows poor correlation. The result has been discarded. It appeared that the temperature correction factor would be about 70/°C. This correction factor will be applied to determine the accumulated permanent strain developed in the asphaltic concrete.

Fig. V.8-4 shows the relationship between the accumulated permanent strain and age of Gage Nos.41, 42, 51 and 52. The adjusted temperature is 40°C. The strain was compressive at early ages. However, there is tendency that as the age is older, the strain will change to tensile. This is shown clearly by Gage Nos. 51 and 52.

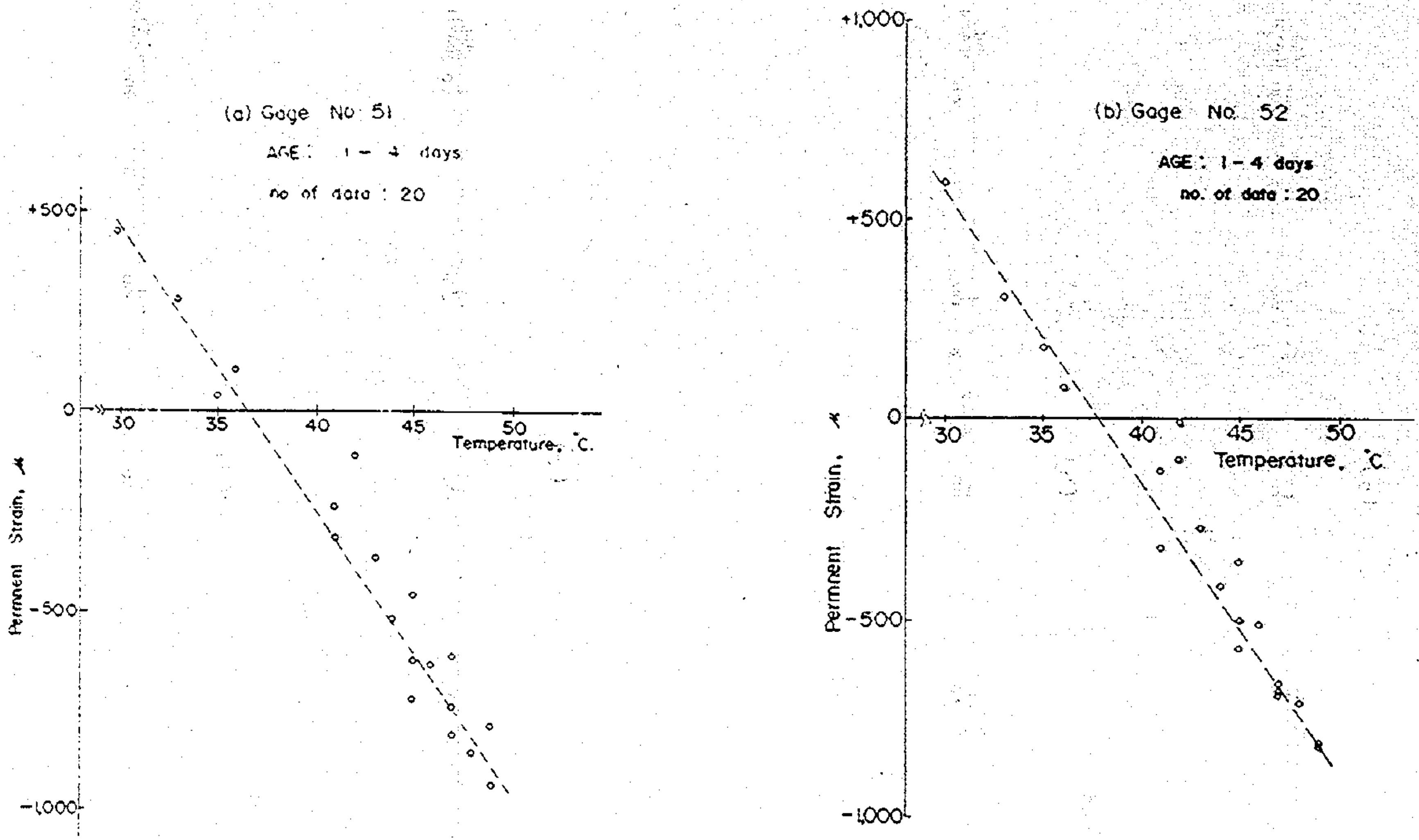

Fig. V.8—3 Permanent Strain VS. Temperature

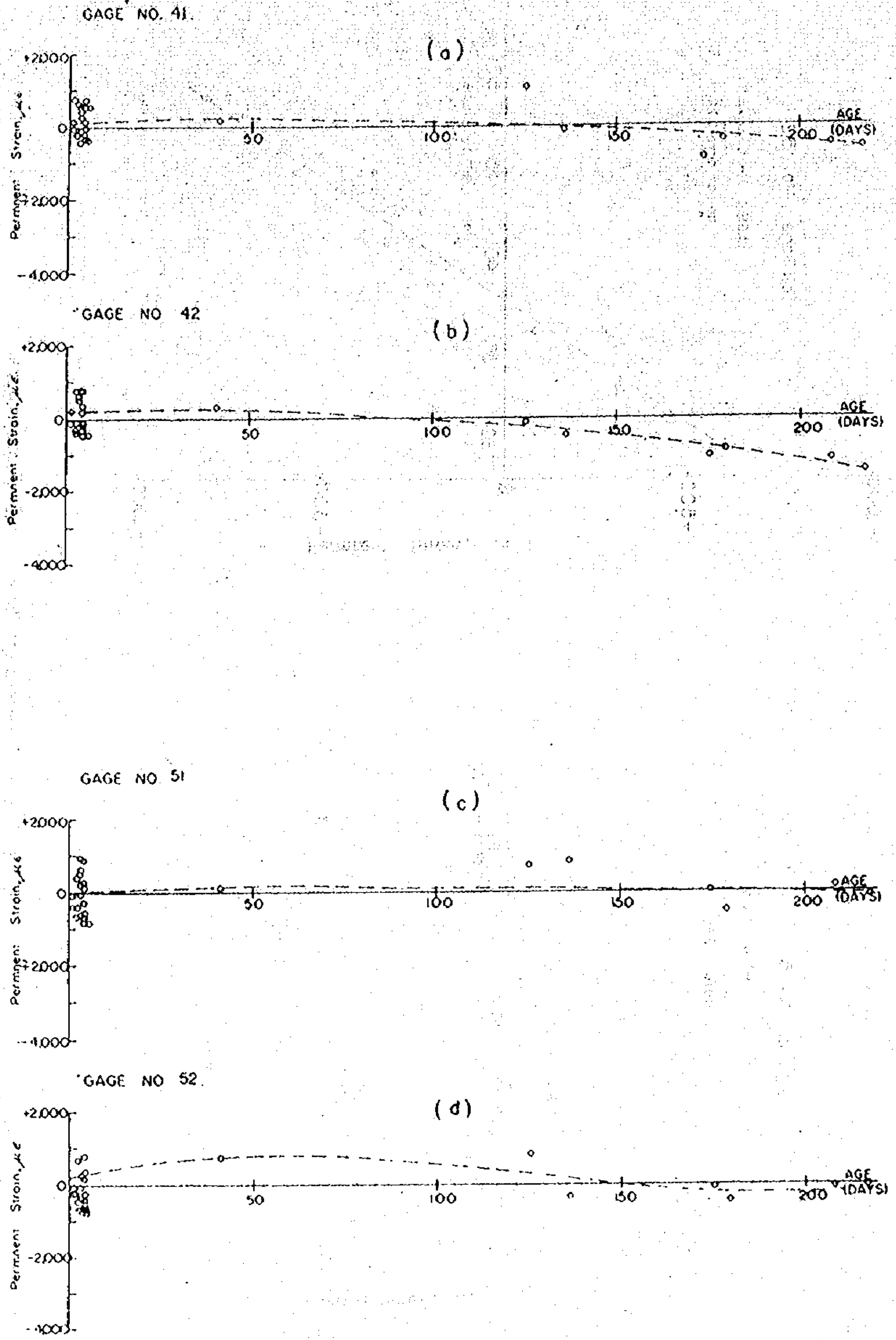

Fig. V. 8-4 Permanent Strain in Asphaltic Concrete VS. Age

TABLE V.8-2. Relationship Between Strain and Temperature.

GAGE NO.	RELATIONSHIP	CORRELATION
41	$Y = -33.3\,X + 1661$	−0.4643
42	$Y = -66.6\,X + 2895$	−0.9133
51	$Y = -71.2\,X + 2651$	−0.9542
52	$Y = -70.9\,X + 2712$	−0.9694

NOTE.: Y = Strain.

X = Temperature

V.9 Static Horizontal Strain

As mentioned before, there are three types of loading conditions. Those are Load Condition A,B and C. And also, Longitudinal and Transverse Gage have been embedded in the test sections. Benkelman Beam trucks have been used in the tests.

V.9.1 Static Strain VS. Age

Only the sample of Load Condition A and embedded strain gages on the top of soil-cement base course had shown in Fig. V.9-1. The tensile strain of Longitudinal Gages increased as the age increased. And Transverse Gage's strains reduced as the increasing age.

V.9.2 Distribution of Static Strain

Because of small number of survival strain gages in all sections, only Longitudinal Gages in subsection No.5 and 7 could show strain distribution in the pavement. Fig. V.9-2 has presented the distribution of static strain with various ages and load conditions. Generally, the strains at the top of base course have tended to be greater than those at the bottom of base course. Most cases, tensile strains had increased at the upper gages and compressive strain had increased at the lower gages as the increasing age, except in case of Load Condition A&B of strain gages in subsection No.1. (picking up Transverse Gage No.12 and 14).

V.9.3 Strain Ratio or Stress Ratio at the Bottom To at the Top of Base Course

It could say the strain ratio or stress ratio because the Young's Modulus of Eleaticity (E) of all strain gages have

BENKELMAN BEAM TRUCK

LOAD CONDITION A

(a) Longitudinal Gage

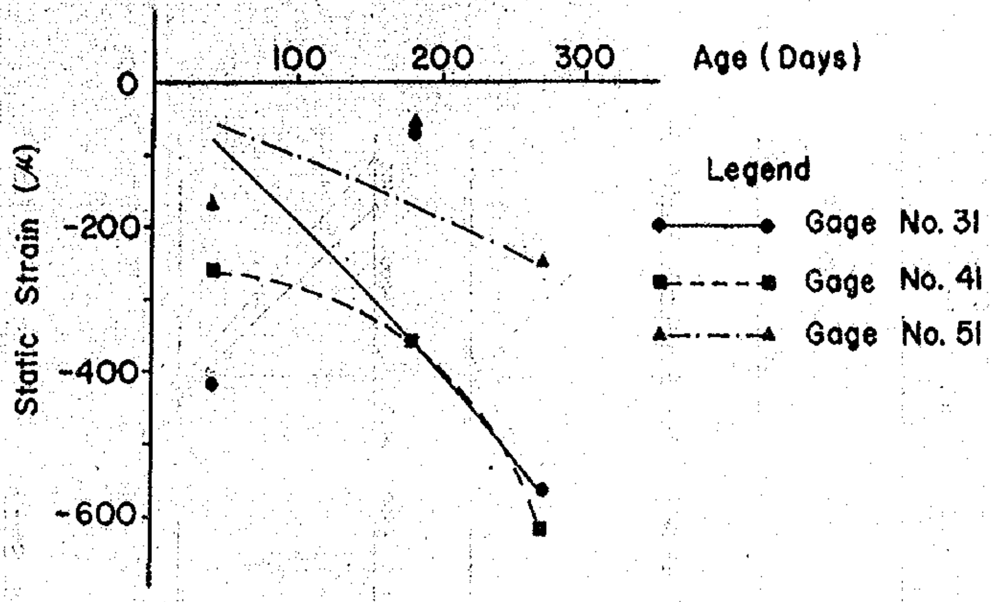

(b) Transverse Gage

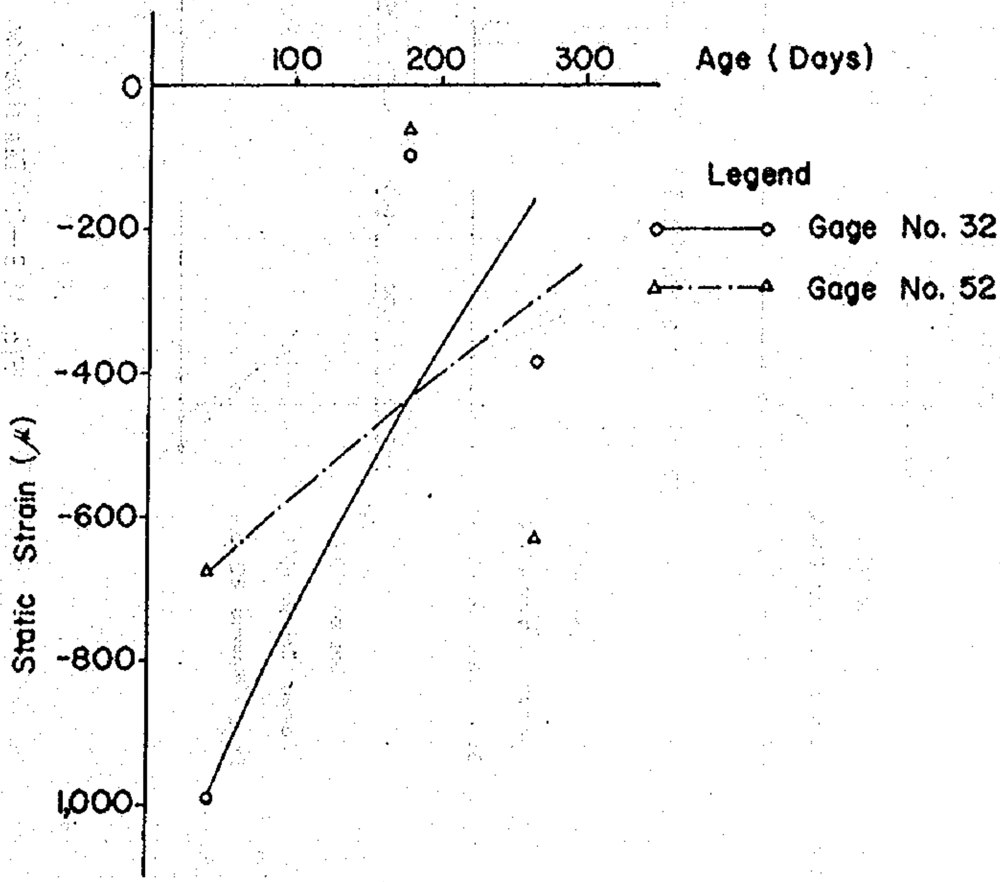

Fig. V. 9—1 Static Strain VS. Age

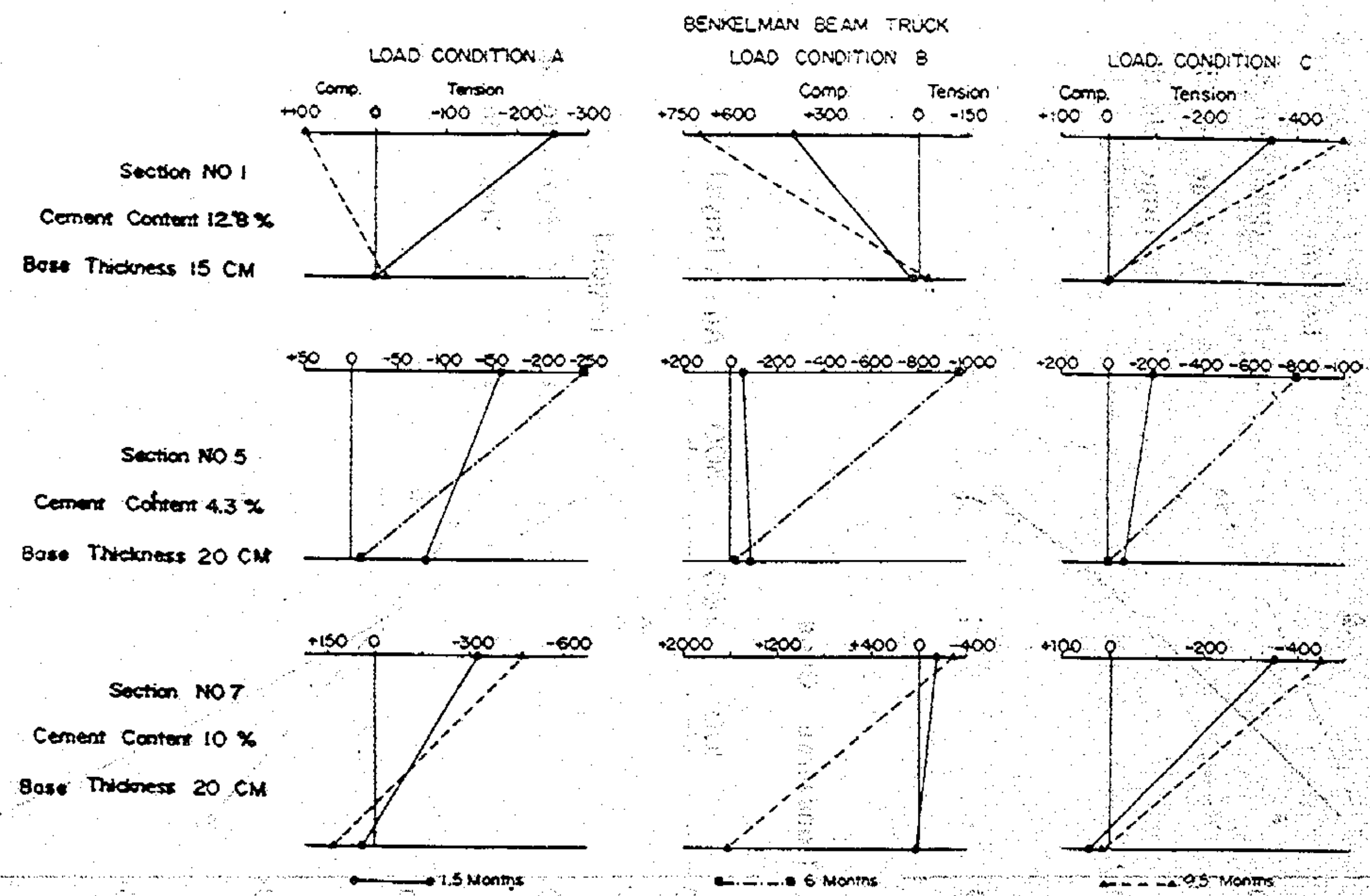

Fig. V. 9—2 Distribution of Static Strain the same value (E=28,000 KSC.). These stress ratios and cement content relationship has presented in Fig. V.9-3. Only three types of cement contents (4,3,10 and 12.8 %) could be figured out the stress ratios in subsection No.5,7 and 1, respectively. Subsection No.5 and 7 had calculated from Longitudinal Gage No. 51 & 55 and 71 & 75, respectively. Only Transverse Gage No.12 & 14 could be represented the results of subsection No.1. Fig. V.9-3 has shown the comparison of Unload and three kinds of Load Conditions, with ages 1.5 and 9.5 months after surface course construction. The ratios in cases of 4.3 and 10 % cement content were less or equal to one at age 1.5 months. And older age, the ratios of 4.3 and 7% cement content had been constant and bigger results, respectively. But 12.8 % cement content, stress ratios had been big and small range in the early and elder ages, respectively.

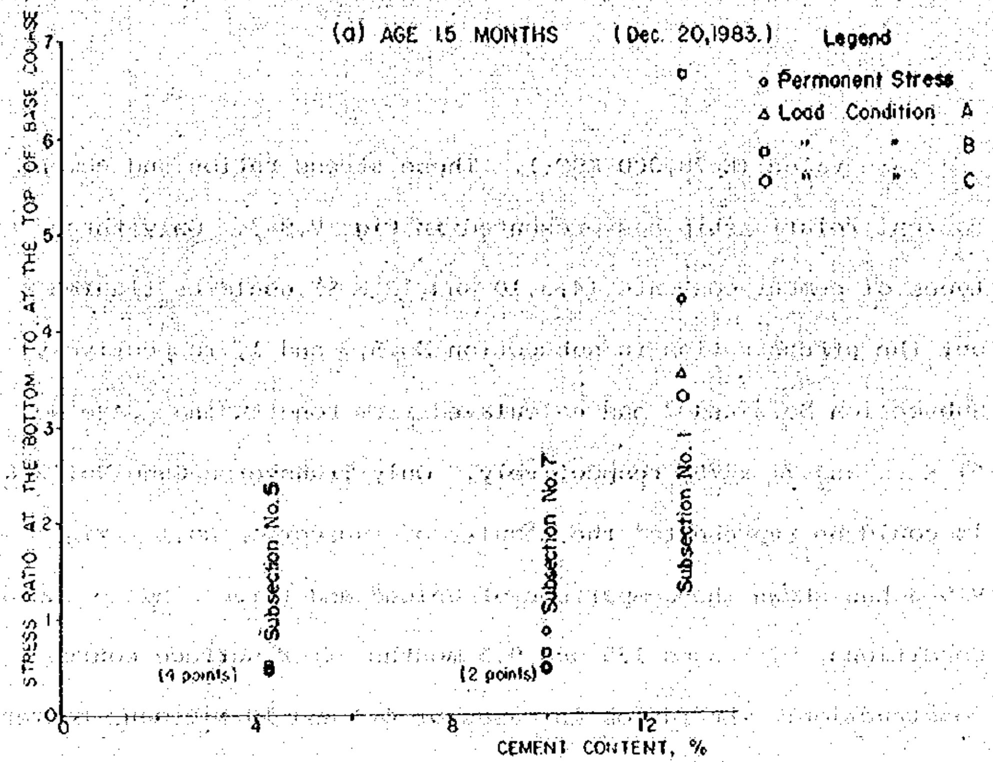

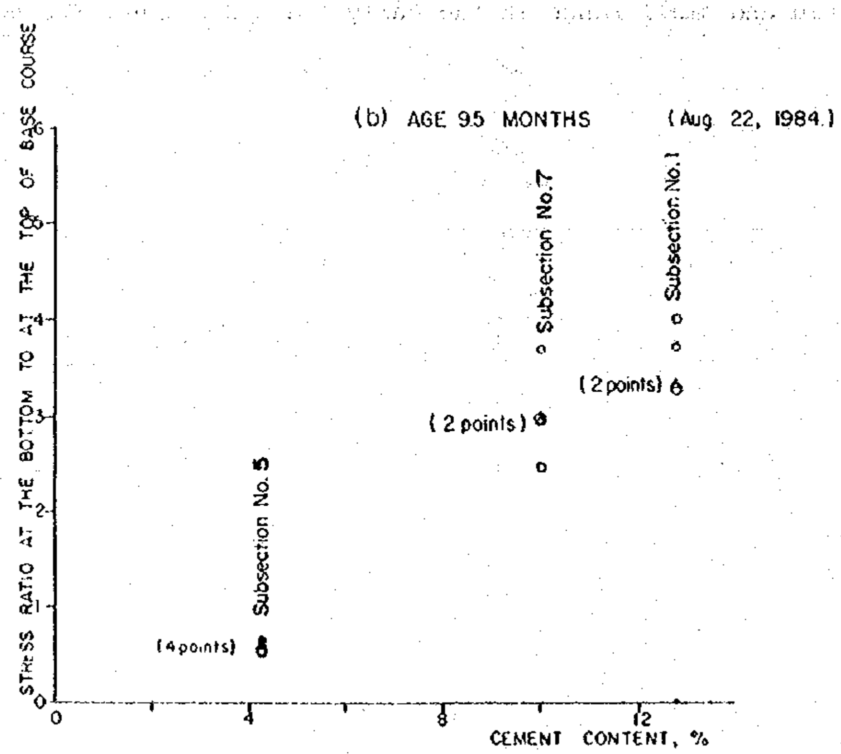

Fig. V. 9-3 Stress Ratio at the Bottom to at the Top of Base Course

V.10 Dynamic Horizontal Stress

After surface course construction, subsection No.3,4 and 5 were selected only the results of strain gages at the bottom of asphaltic concrete surface course. Those Longitudinal and Transverse strain gages are Gage No.31,41 & 5, and 32, 42 &52, respectively. Both Load Conditions were shown the results with various ages. The sign convention : tensile and compressive stresses are negative and positive, respectively.

V.10.1 Horizontal Stress VS. Speed

Fig.V.10-1 (a) to (c) and (d) to (f) were represented these results in case of Load Condition A and B, Respectively. Most of their relationship were tensile stresses, except Gage No. 41 and age 1.5 months. Most of the stresses had small ranges of stresses. Only static stresses (atO.K.P.H.) had wide ranges of stresses. Their peak's trends were within speed's range of 10 to 20 K.P.H., except age 6 months of both load conditions.

V.10.2 Effect of Different Ages

Comparison of the relationship of the Horizontal Stress and Speed at various ages of each strain gage had shown fluctuation results. The more speed increased, the less the tensile stresses were. There were no big stress difference at various age. Gage No.42 had been broken since July 11, 1984., as shown in Fig. V.10-2.

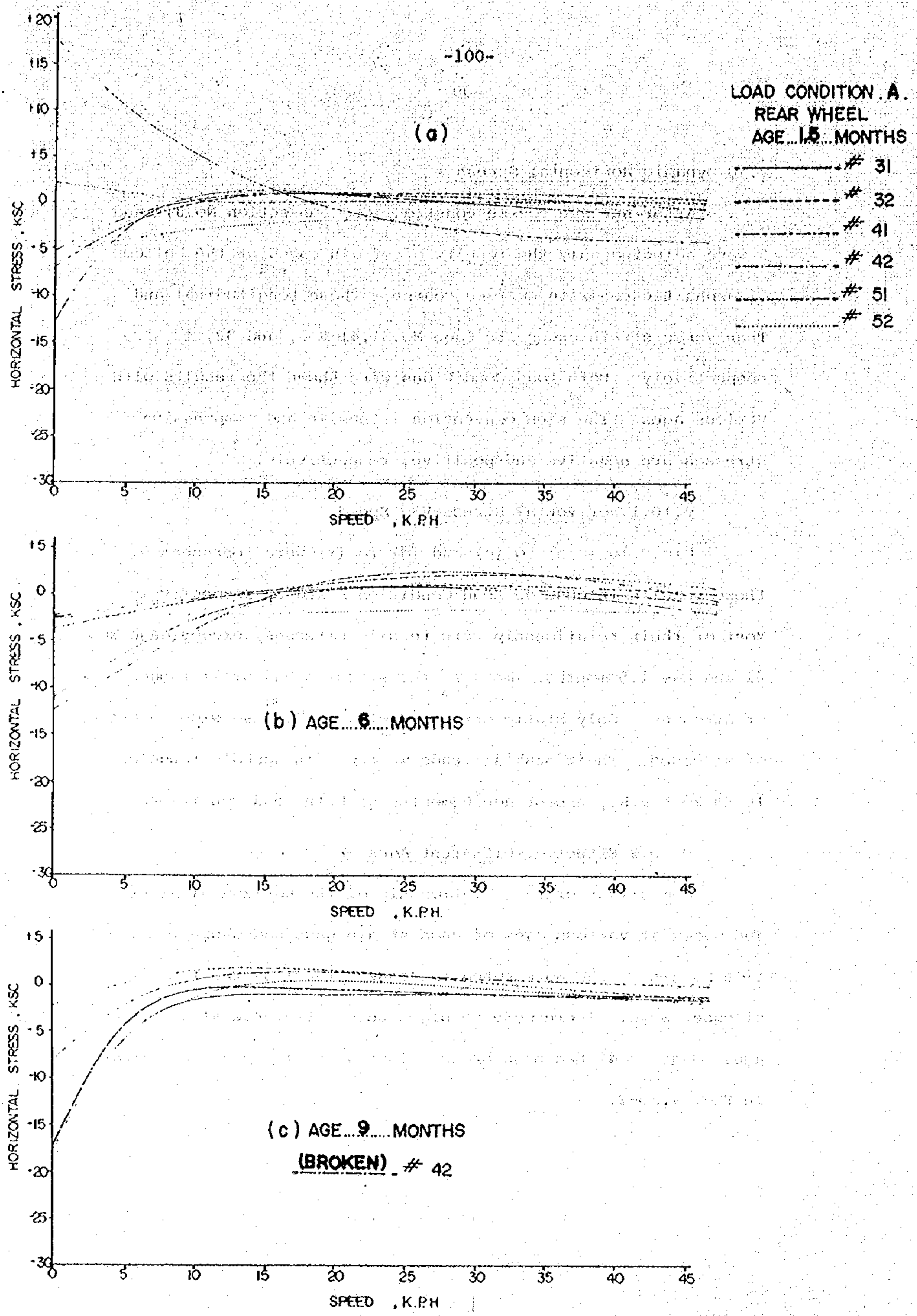

Fig. V. 10—1 Horizontal Stress VS. Speed

LOAD CONDITION . B .
REAR WHEEL

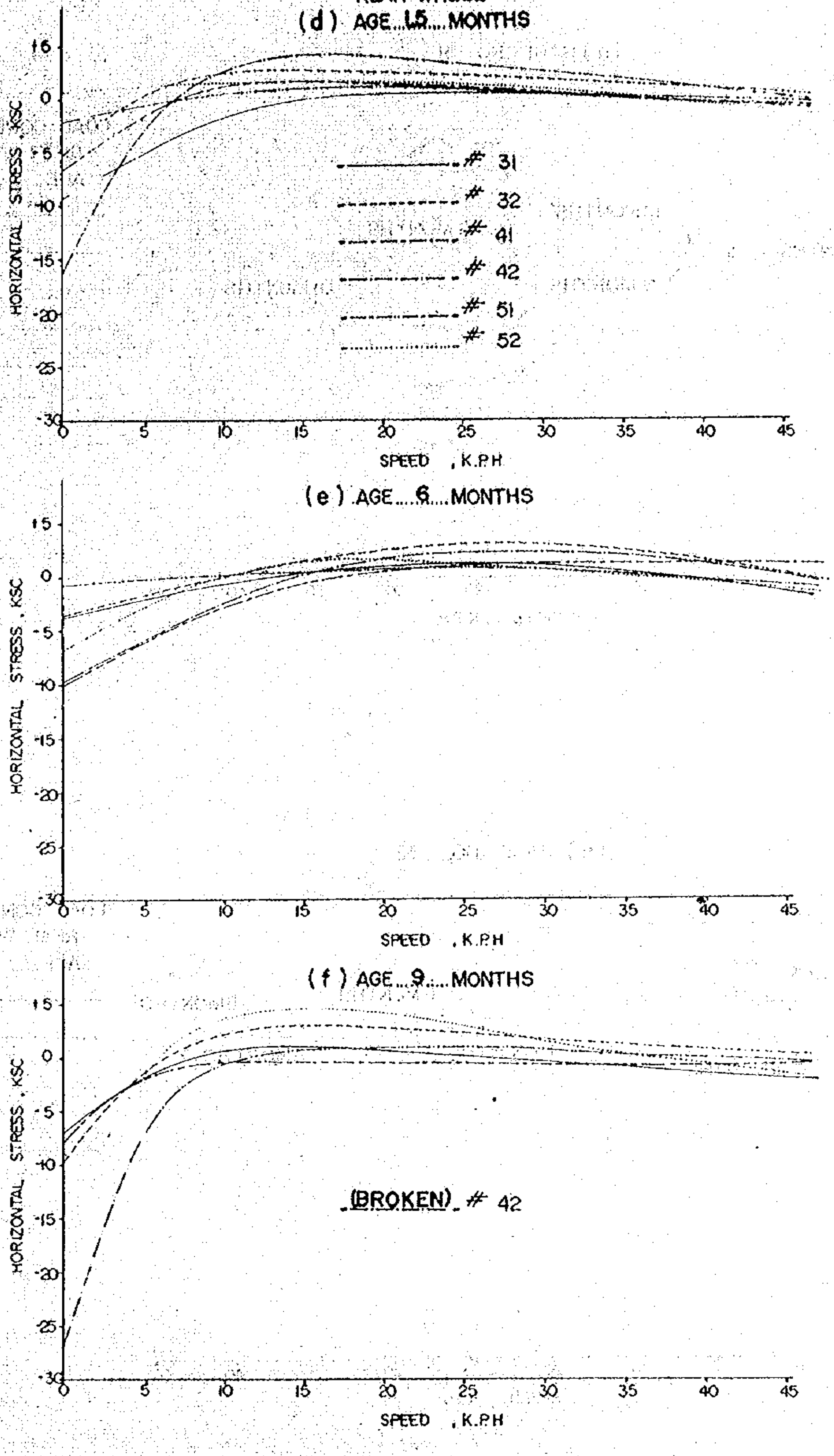

Fig. V.10—I (Cont.)

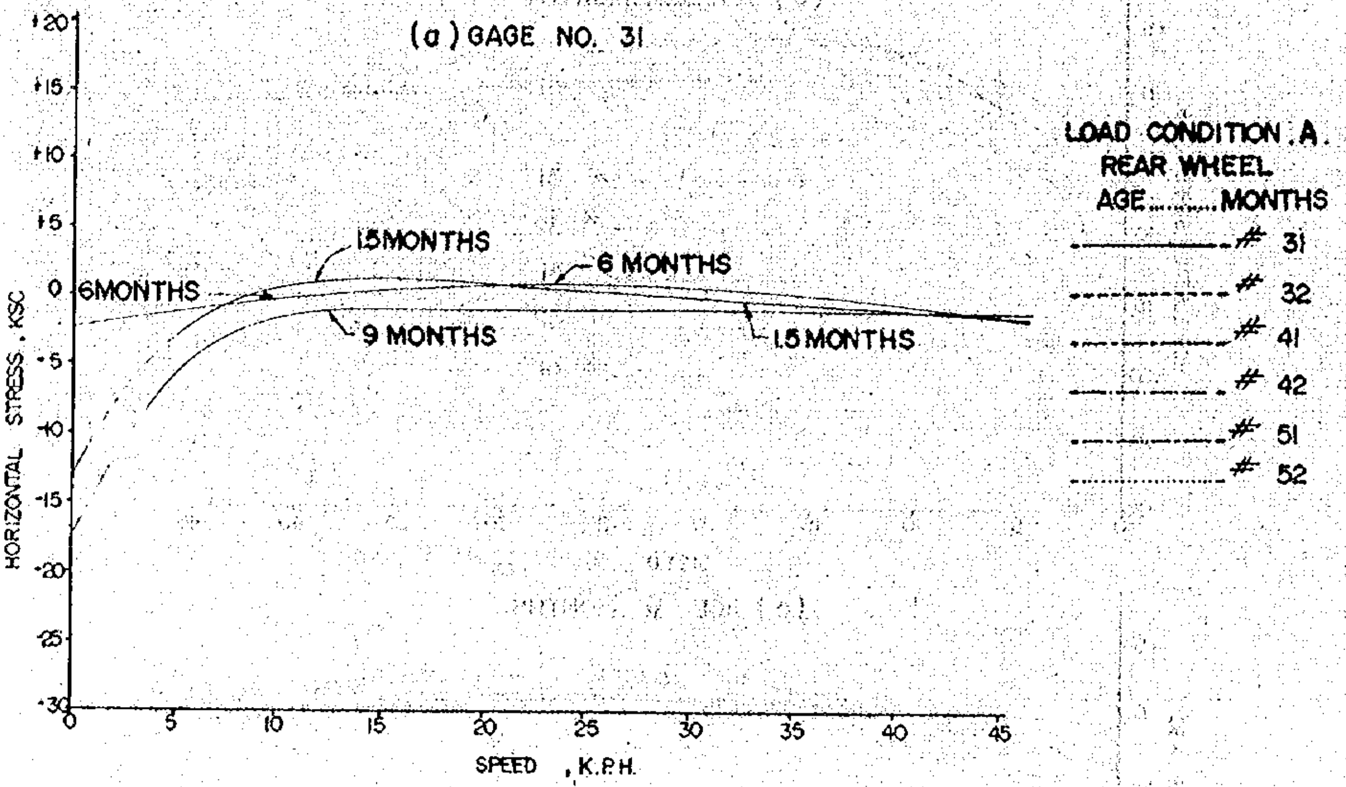

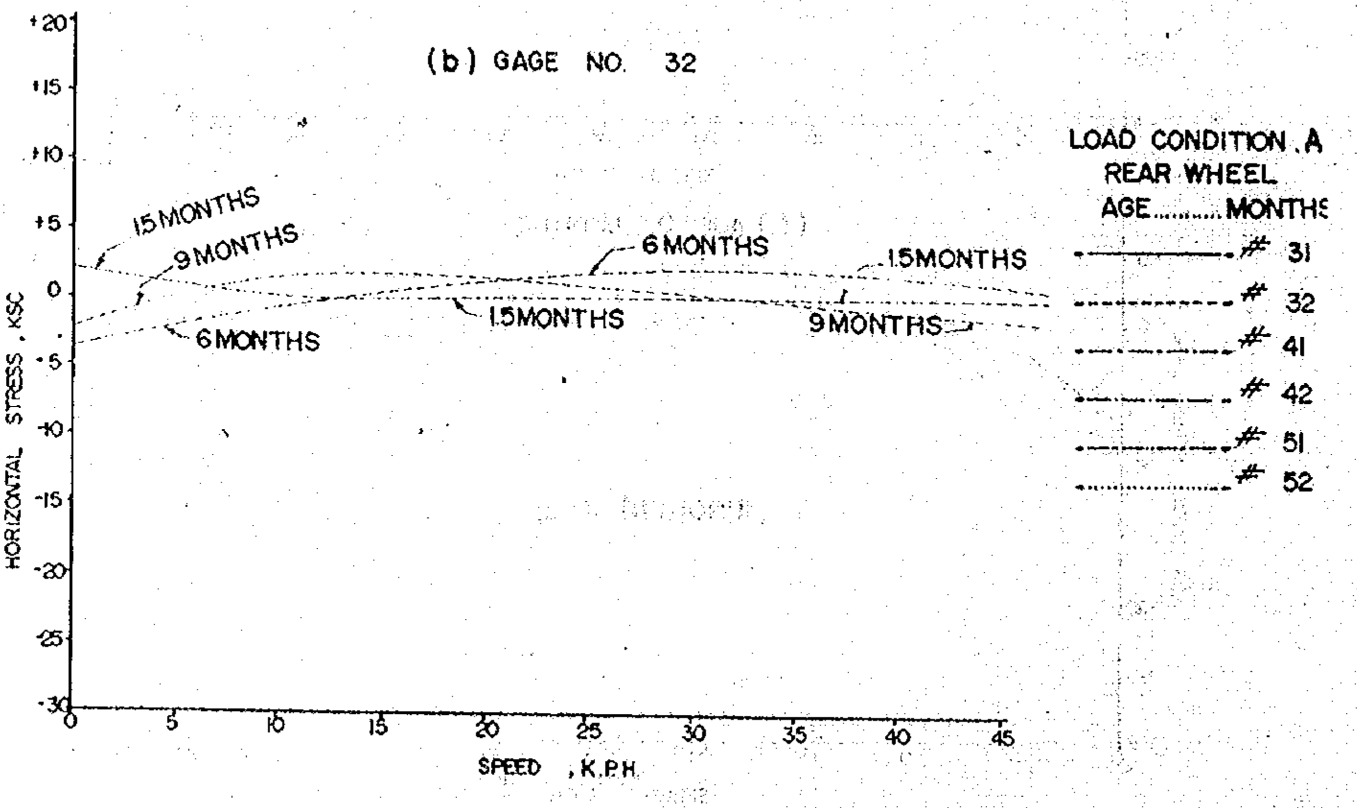

Fig, V.10—2 Effect Of Different Ages

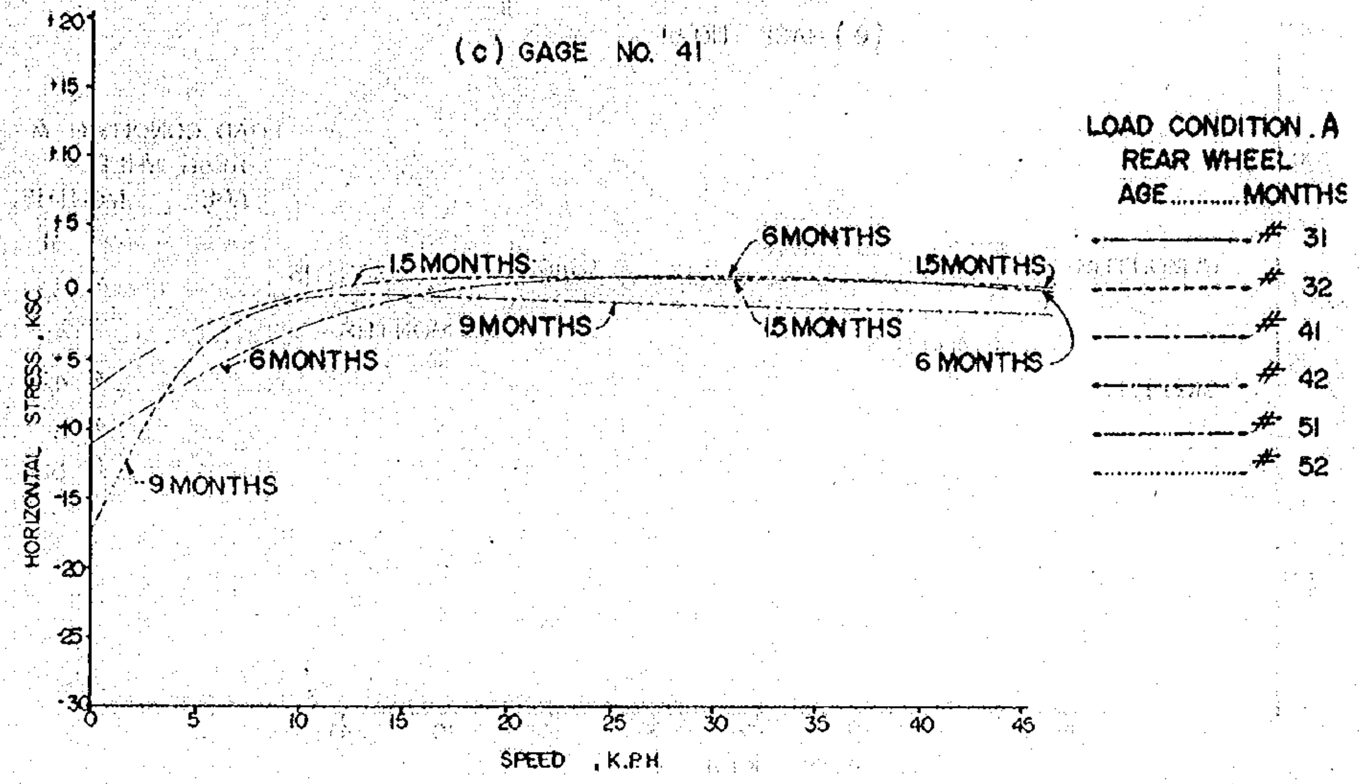

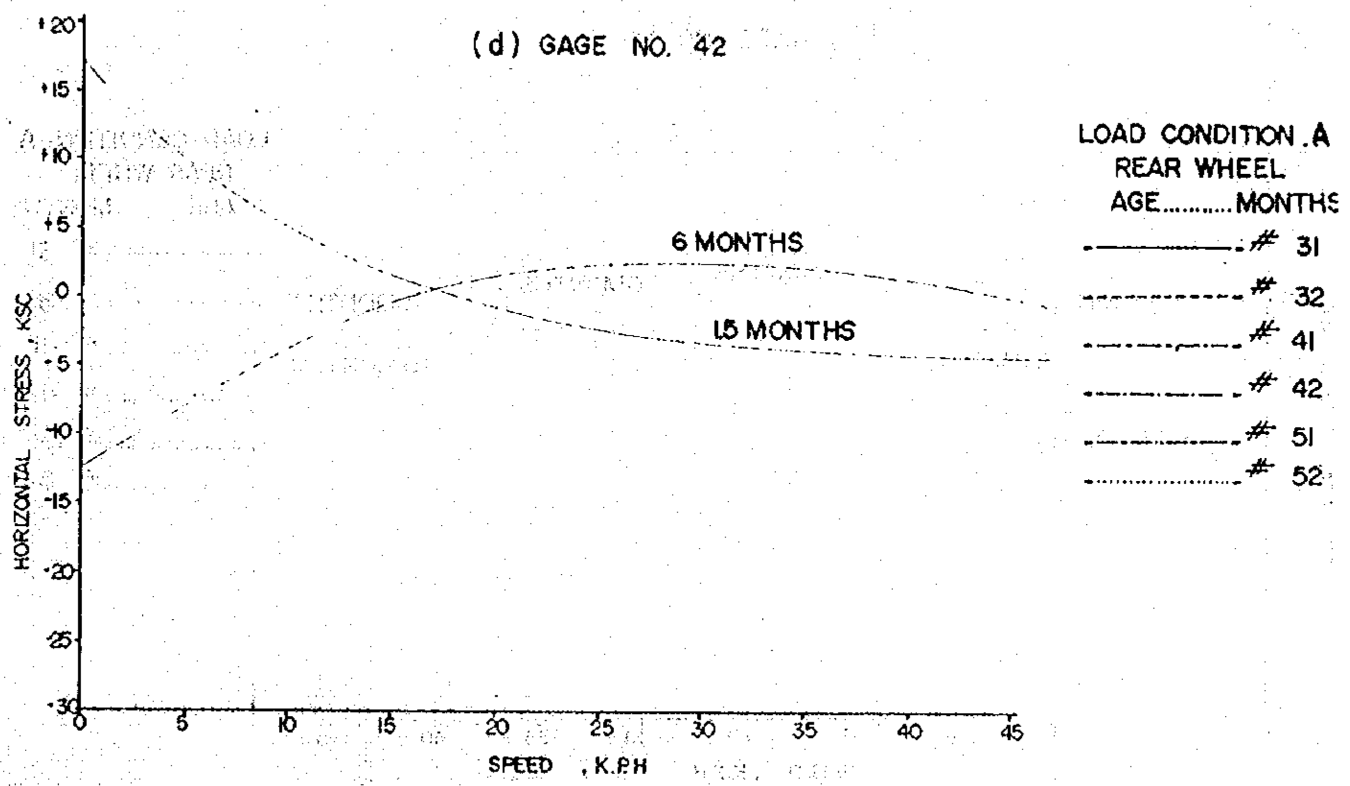

Fig. V. 10—2 (Cont.)

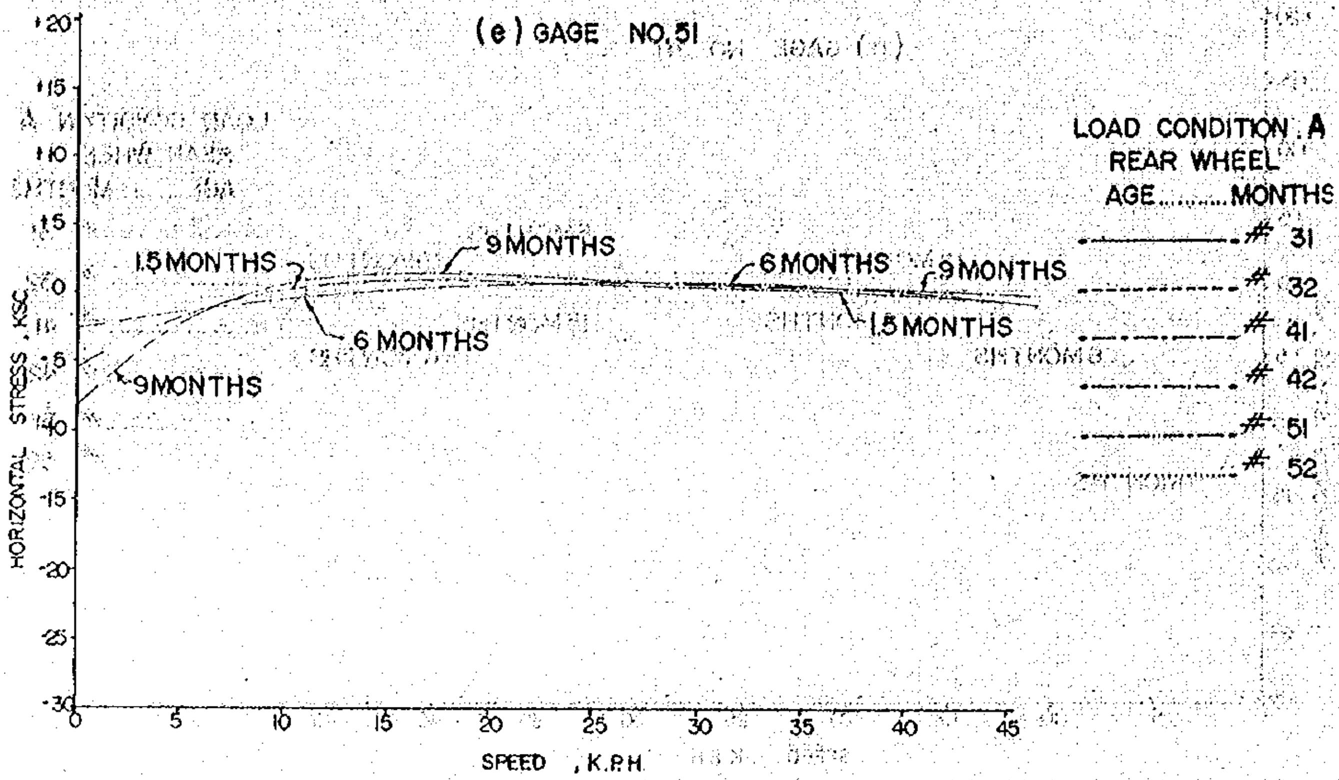

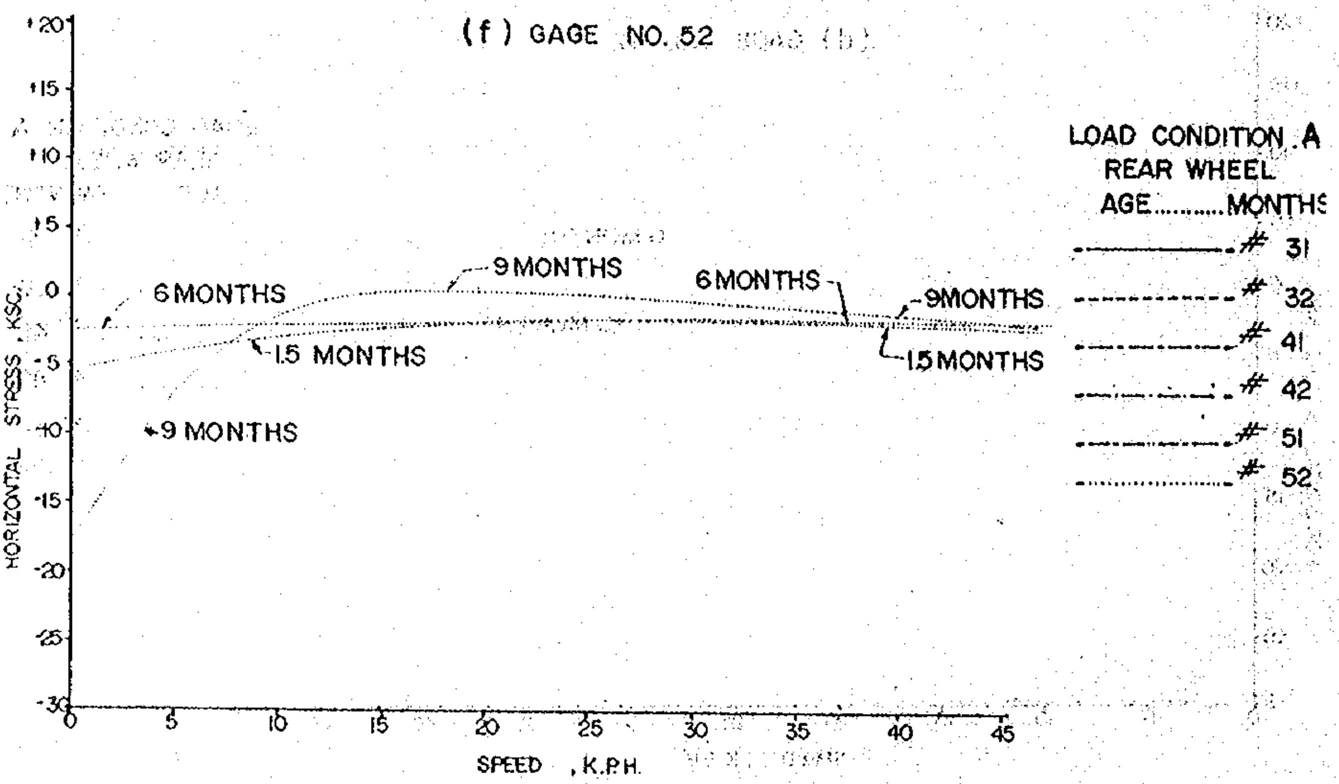

Fig. V. 10—2 (Cont.)

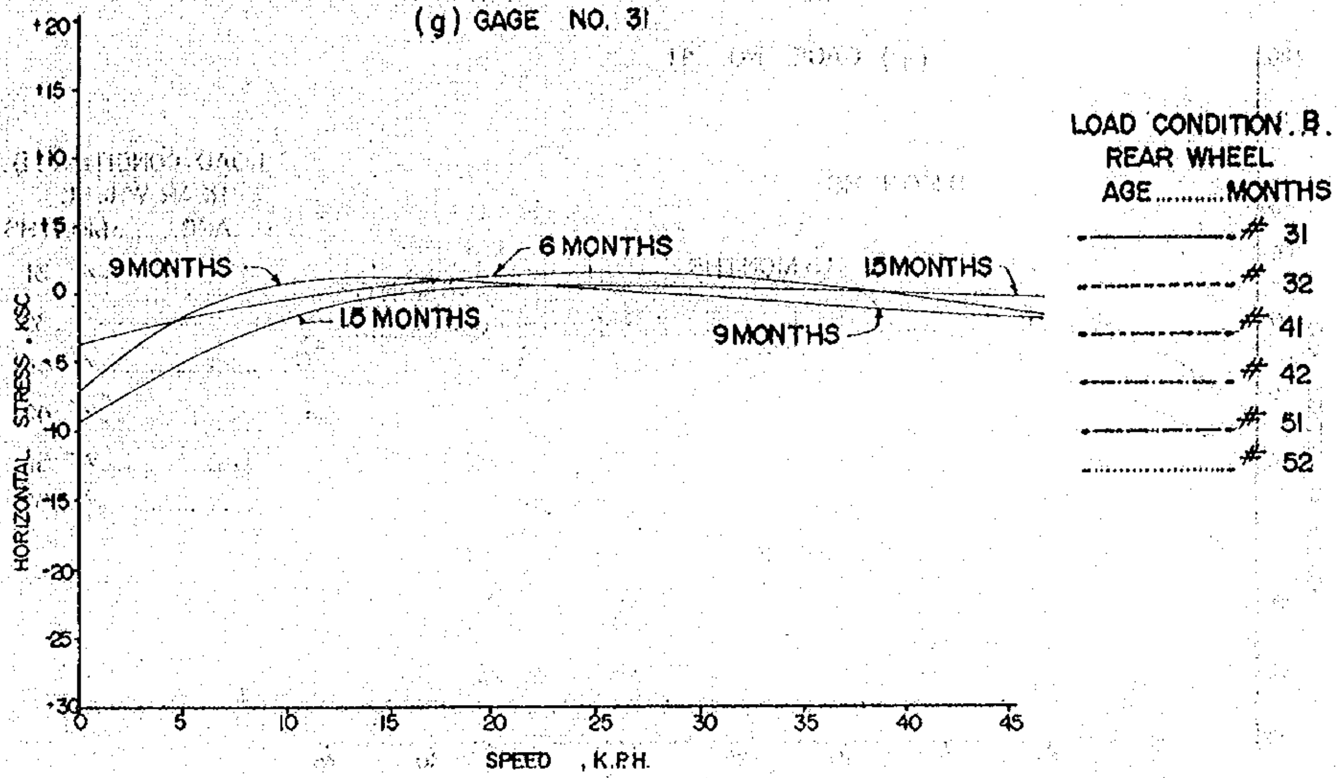

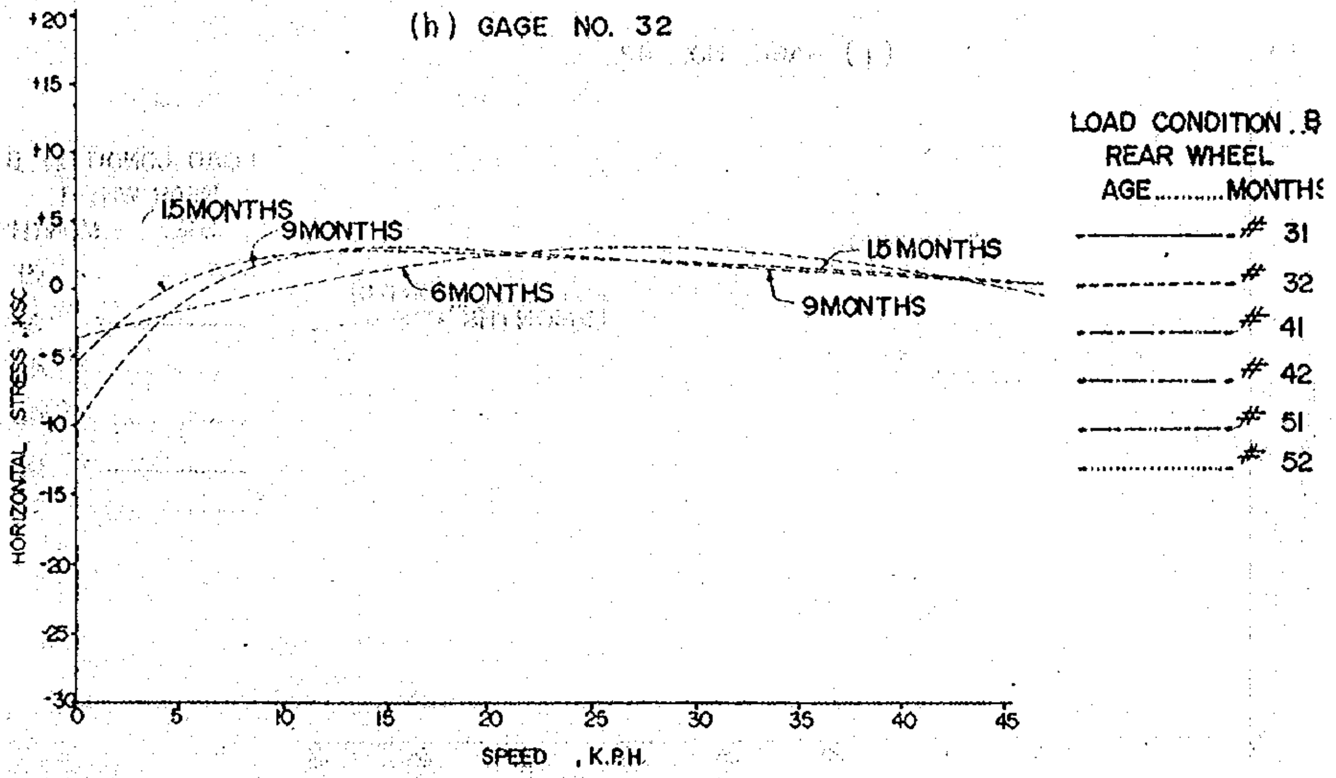

Fig. V. 10—2 (Cont.)

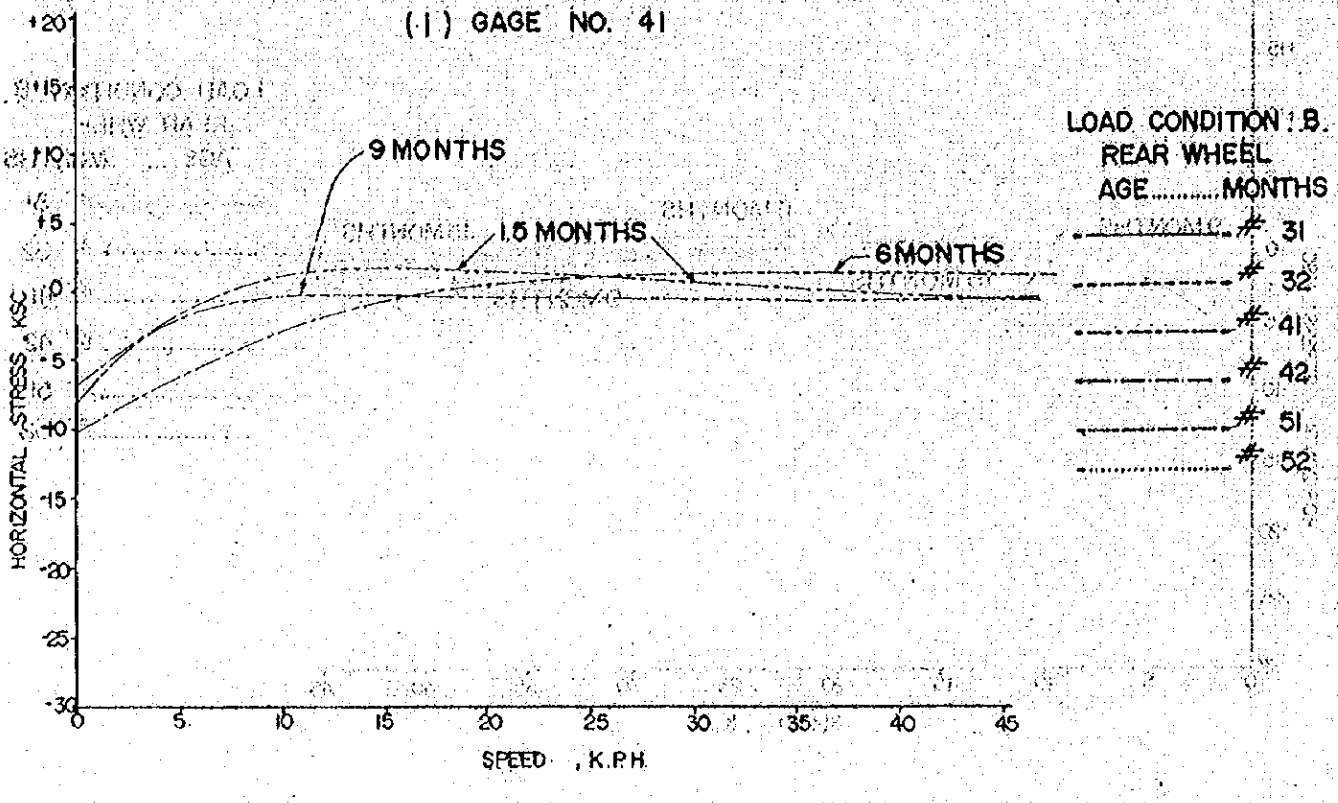

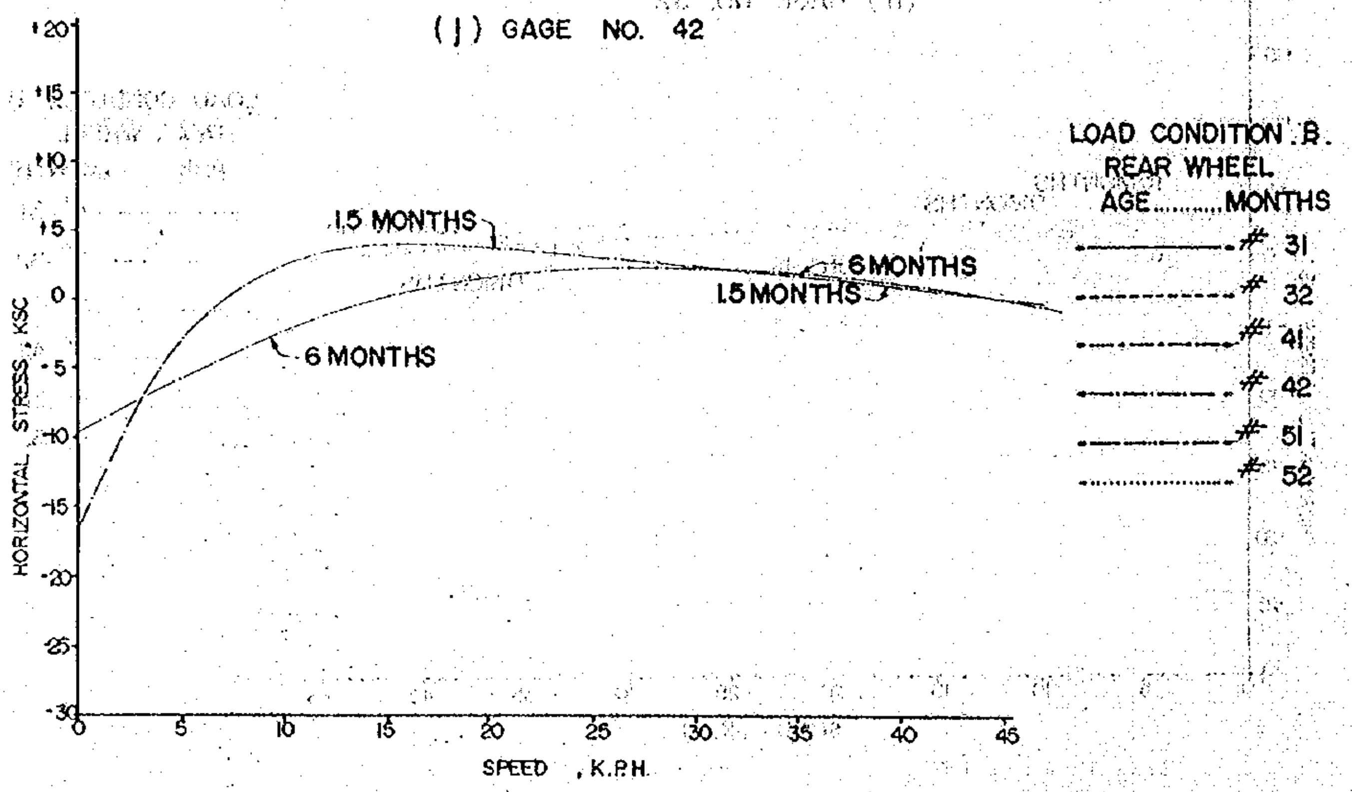

Fig. V.10—2 (Cont.)

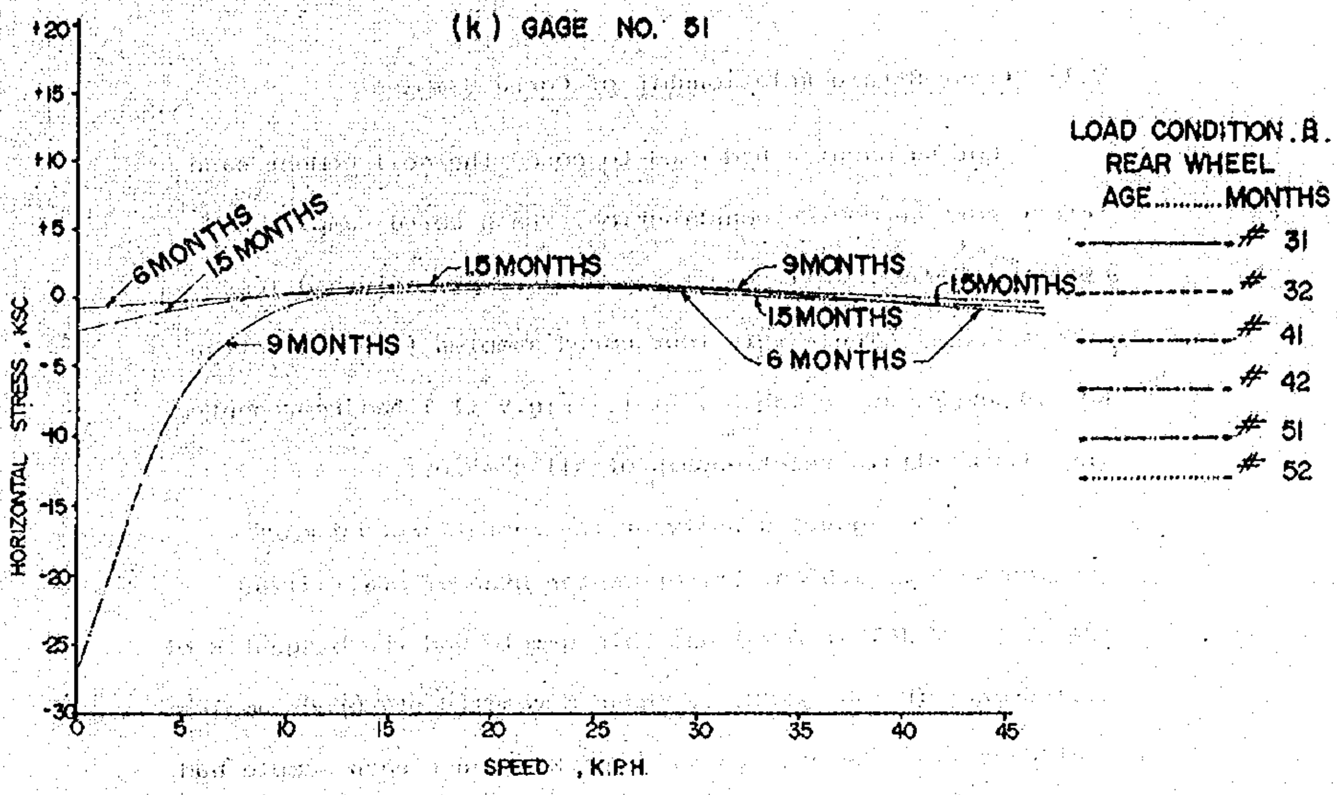

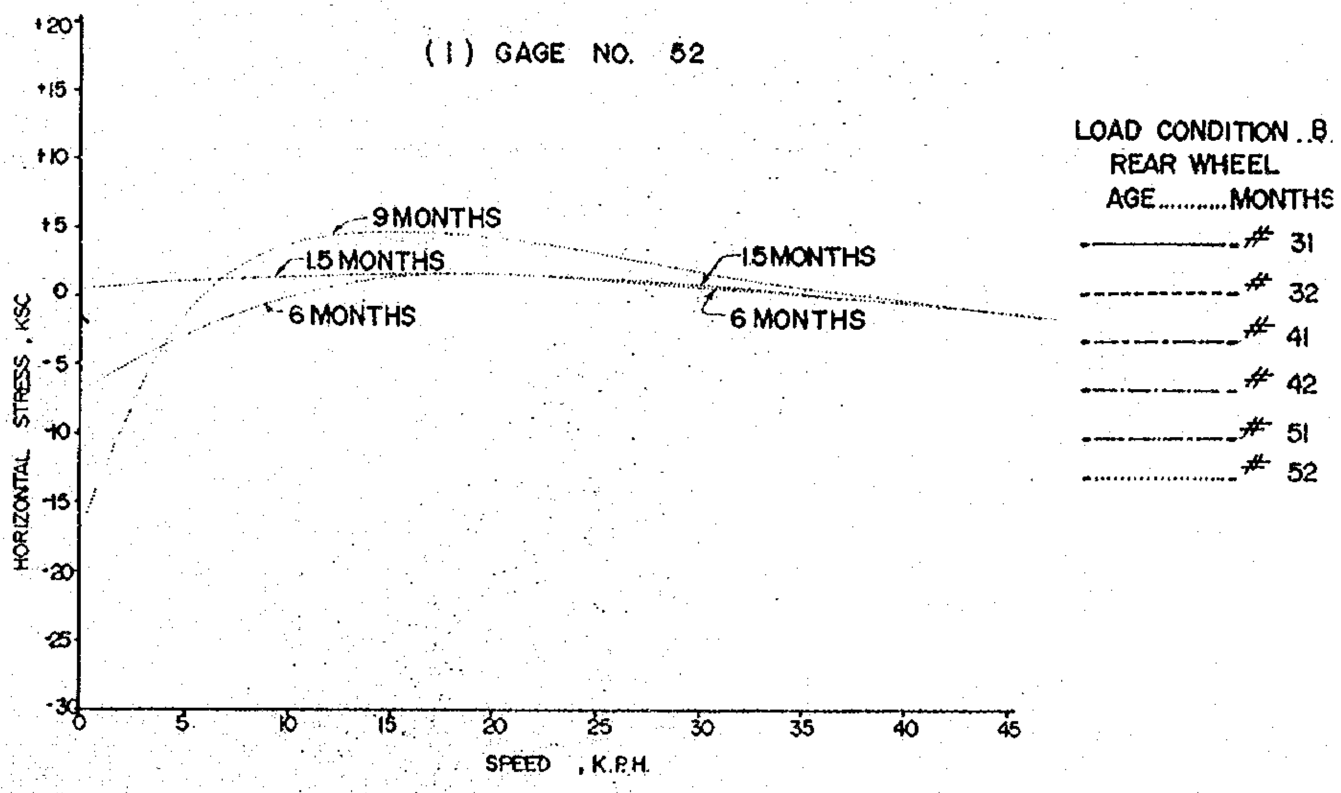

Fig. V.10-2 (Cont.)

V.11 Stress-Strain Relationship of Cored Samples

Coring Machine had used to cored the soil-cement base before surface course construction. Less cored samples had obtained because soil-cement base course probably had less homogeneous There were four cored samples from subsection No.2,4 and 6, as in Table V.11-1. Fig.V.11-1 had represented the stress-strain relationship of all samples.

The biggest density of the sample was from sub-section No.6 at 3.50 m. Lt. of Center Line of Sta. 32+268 (density = 2.363 gm./cc.) and this sample had the biggest E of soil-cement (E = 4663 KSC.). Those E results of cored samples could not find the average value of E because each sample had different cement content.

TABLE V. II-1 RESULT OF UNCONFINED COMPRESSIVE STRENGTH TEST OF CORED SAMPLE

Sample No.	1	2	3	4
Section No.	2	4	6	6
Date of Soil Cement Construction	Mar. 19, 1983	Mar. 20, 1983	Mar. 23, 1983	Mar. 23, 1983
Location of Sampling	1.30 M. Lt. of ℄ Sta. 32+071	2.50 M. Lt. of ℄ Sta. 32+183	4.00 M. Lt. of ℄ Sta. 32+282	3.50 M. Lt. of ℄ Sta. 32+268
Date of Unconfined Compressive Strength Test	Feb. 20, 1984.			
Unit Weight (gm./cm^3)	2.102	1.977	2.109	2.363
Strenght (kg./cm^2)	32.5	31.0	31.5	45.5
Elastic Modulus (kg./cm^2)	3250	3300	2700	4663

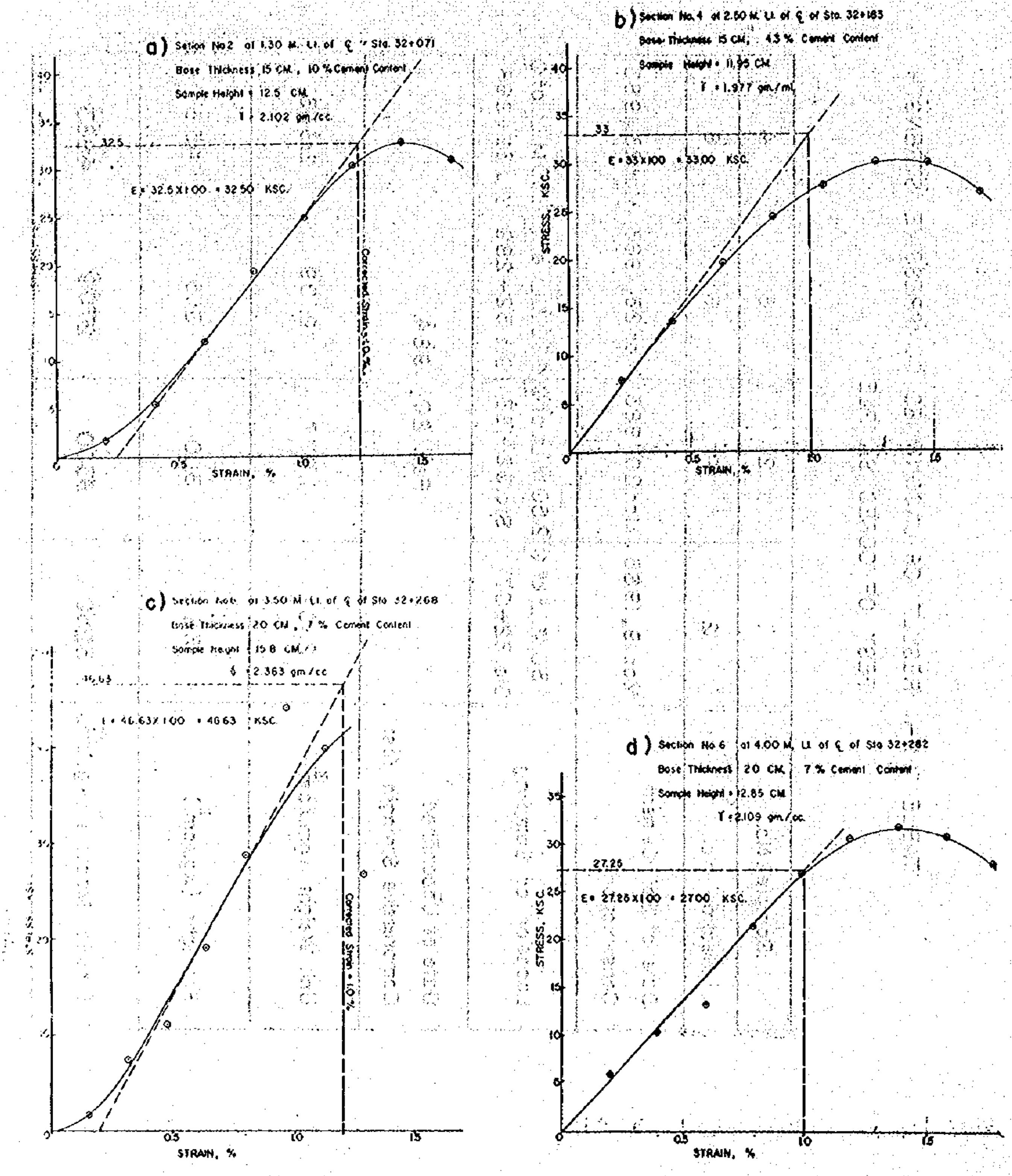

Fig VII-1 Results of Stress - Strain Relationship of Core Samples.

VI. CONCLUSION

The study in Stage II started from the completion of the surface. Most of the data collection in this study were within 10 months after the surface construction.

1. Asphaltic concrete surface of the test section was constructed 7 months after the completion of soil-cement base. The asphaltic concrete was designed following the Marshall method.

2. Results of material testing after construction indicated that the surface construction was satisfactory. Properties of the mix were in general conformed with the design.

3. Benkelman beam deflection of surface course with soil-cement base was lower than that with crushed rock base, verying from 0.01 to 0.04 cm. The variation of the deflection of the surface course with 15-cm. base was high. On the other hand, the deflection of the surface course with 20-cm. base showed tendency that it decreased with % cement content.

4. Roughness of the surface course was measured using 3-m. profilometer. Roughness deviation and roughness index were then determined. The results indicated that the surface course was in very good condition.

5. Cross sections along the test section were surveyed by levelling method. The crossfall was deviated from the designed crossfall of 2.5 %. The deviation of the crossfall from the design along the surveyed line varied from 3.6 to 18.9 mm.

The rut depth was also measured varying from 0 to 3 mm.

6. The crack ratio in every subsection was less than 7 %

and tended to increase as the cement content increased. However, as the cement content over 10 %, the crack ratio tended to decrease.

7. The crack ratio and roughness deviation were plotted together to determine surface condition. It was shown that all subsections were in good condition.

The crack ratio was also used with the roughness deviation and rut depth to determine PSI (Present Serviceability Index) of the test section. The calculated PSI varied from 3.50 to 4.14 which was relatively high.

8. Temperature measurement within the pavement throughout the day showed that the surface Temperature varied from 23°C. to 55° C. and was peaked at about 3 p.m. At the bottom of the surface, the Temperature was the highest.

9. The vertical stress at the bottom of the base was much reduced than the stress developed at the early age. This was due to the addition of surface layer and the increasing in age of soil-cement.

The stress at the bottom of base with 4.3% was smaller than that of 7.0 %, in both thickness.

10. The vertical stress under dynamic load showed tendency as without the surface course, except that the magnitude of the stress was reduced. The stress was peaked within the range of 0-10 km./hr. and decreased and flattened as the speed increased.

11. Less that half of the embedment strain gages in the soil-cement base were survived. The strain developed in similar fashion as without the surface course.

Five strain gages were installed beneath the surface. The results of measurements showed that the strain was compressive at early age and change to tensile as the age increased.

12. For static Horizontal Strain; only the sample of Load Condition A, as the increasing age the tensile strain increased and reduced on Longitudinal and Transverse Gages, respectively. Generally, distribution of strains showed that tensile strains had increased at the upper gages and compressive strains had increased at the lower gages.

Strain Ratio at the Bottom to at the Top of Base Course could figure out from the gages in subsection nos. 5,7 and 1 with 4.3, 10 and 12.8 % cement content, respectively. At early age the ratios of 4.3 and 7 % cement content had been constant and bigger results, respectively.

13. Dynamic Horizontal Strain showed only the strains at the bottom of asphaltic concrete surface course of strain gages in subsection nos. 3,4 and 5. The relationship of stress and speed, their peak's trends were within speed's range of 10-20 K.P.H., for Load Condition A and B. These relationships at various ages of each strain gage had shown fluctuation results. The more speed increased, the less the tensile stresses decreased.

14. Less cored samples of soil-cement base could be done only in subsection nos. 2,4 and 6 before surface course construction. Stress-Strain Relationship of Cored Samples had been done to find the Young's Modulus,E, of each sample. The densities of samples were 1.977 to 2.363 gm./c.c. (123.36-147.45 lb./ft^3.) and E values were 2700-4663 kg./cm.^{2}(38,400-66,300psi).The average of E value could not find because each sample had different cement content.

REFERENCES

1. "Study Report on Lateritic Soil for Road Construction, Technical Report, Stage I", Department of Highways, Ministry of Communications, Thailand, Ministry of Construction, International Engineering Consultants Association, Japan, March, 1983.

2. "Manaul of Profilometer KKY-3T", Tokyo Tanifuji Co.Ltd., Tokyo, Japan.

3. TAI, "Methods for Asphaltic Concrete and other Hot Mix Types, MS-2", Third Edition, The Asphalt Institute, College Park, Maryland, U.S.A., October, 1969.

4. Thum-Umnauysuk, Suthi, "Asphaltic Concrete-Design Principles and Construction", Pavement & Soil Stabilization DOH Technical Group, Department of Highways, Bangkok, Thailand, March, 1982.

5. Nagumo, Seto, Yamashita, Satori, "Doora kensetsu koozo 12 (Highway Construction Series 12)" Dooro Hosoo ni Kansuru Shikenhoo (Testing Method on Highway Pavement), (in Japanese) August, 1975.

6. Japan Road Association, "Manual for Design and Construction of Asphlat Pavement," December, 1980.

7. Highway Research Board, "The AASHO Road Test," Highway Research Beard Special Report 61-E, 1962.

8. Japan Road Association, "Road Maintenance Manual", (in Japanese) July, 1978.

9. Ruenkrairergsa, Teeracharti, "Proposed Specifications for Soil-Cement Base Construction in Thailand," Report No. 82, Materials & Research Division, Department of Highways, Ministry of Communications, Thailand, December, 1982.

APPENDIX A

Table A-1 Specification of Earth Pressure Cell

Item	Description
1. Model	BE-5kA
2. Capacity	5 kg/cm^2 (71 psi)
3. Diameter of Pressure Sensitive Surface	Ø 88 mm
4. Disc Thickness	20 mm (0.8in.)
5. Disc Diameter	Ø 100 mm (4 in.)
6. Length of Cable	10 m (33 ft.)
7. Manufacturer	Kyowa Electronic Instrument Co., Ltd. Japan

Table A-2 Specification of Strain Gage.

Item	Description
1. Model	KM - 120 - HZ - 11, L100 - 3
2. Resistance	120 ± 1 %
3. Dimensions	120 x 15 x 4.5 (mm)
4. Modulus of Elasticity	28,000 kg / cm^2 (4×10^5 psi.)
5. Length of Cord	10 m. (32.8 ft)
6. Manufacturer	Kyowa Electronic Instrument Co, Ltd. Japan

APPENDIX B

B.1 Measuring Instrument and Method

B.1.1 Permanent Strain

B.1.1.1 Instrument

1. Bridge Box
2. Static Strain Indicator (Type SM-60D, Kyowa)

B.1.1.2 Connection (see Fig.B-1)

1. First connect terminal of strain gage embedded with Bridge Box.
2. Second, connect the bridge box cable with Static Strain Indicator.

B.1.1.3 Method

Permanent Strain is measured under no loading condition above the strain gage.

B.1.2 Static Strain and Vertical Static Stress

B.1.2.1 Instrument

The same as B.1.1.1. In case of vertical static stress, only Static Strain Indicator.

B.1.2.2 Connection

The same as B.1.1.2. In case of vertical static stress, connect earth pressure cell cable with Static Strain Indicator directly.

B.1.2.3 Method

Static strain and vertical static stress are measured with various weights of Benkelman Beam Truck as shown in Table V.1-1 and under 3 different loading condition as shown in Fig.B-2

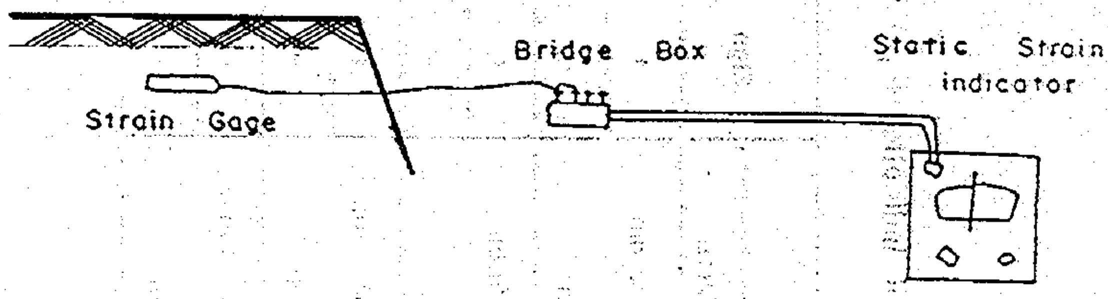

Fig. B-1. Static Strain Measurement Method

Table. B-I Meaning of Indication + , - for Strain Reading.

Connection		Sign	Meaning
Sensor	Meter		
Strain Gage	Static Strain Indicator	+	Compression
		-	Tension
Pressure Cell	Static Strain Indicator	+	Tension
		-	Compression
Strain Gage	Dynamic Strain Indicator	+	Tension
		-	Compression
Pressure Cell	Dynamic Strain Indicator	+	Compression
		-	Tension

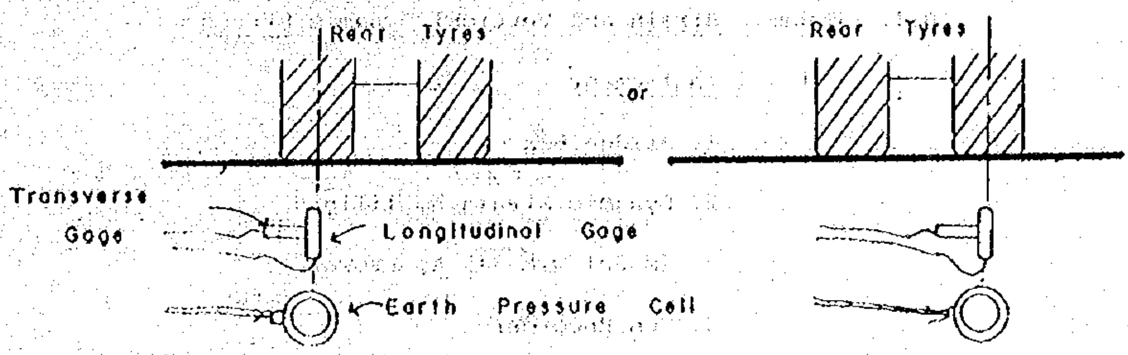

(a) Condition A (under the Rear Tyres)

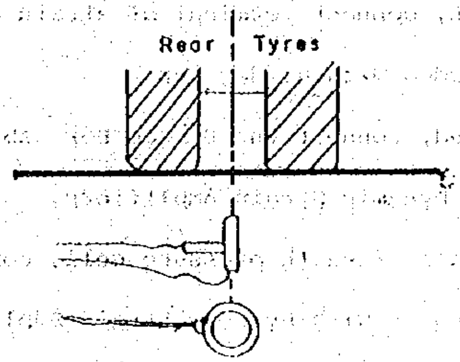

(b) Condition B (between the Rear Tyres)

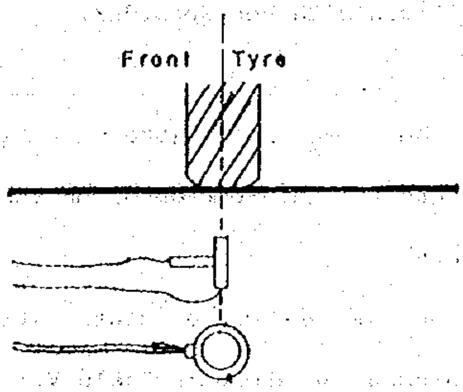

(c) Condition C (under the Front Tyre)

Fig. **8-2** Three - kind of Loading Conditions

B.1.3 Dynamic Strain and Vertical Dynamic Stress

B.1.3.1 Instrument

1. Bridge Box
2. Dynamic Strain Amplifiers
   (Model DPM-311 A, Kyowa)
3. Pen Recorder
   (Model Multicorder, MC-6620, Watanabe)

B.1.3.2 Connection (See Fig. B-3)

1. First, connect terminal of strain gage enbedded with Bridge Box.
2. Second, connect the Bridge Box cable with Dynamic Strain Amplifiers.
3. In case of earth pressure cell, connect the cable with Dynamic Strain Amplifiers directly.
4. Connect each channel of Dynamic Strain Amplifiers with Pen Recorder.

B.1.3.3 Method

1. Mark the survey point (the place where gage and cell are embedded) on the pavement surface.
2. Use the same vehicle as static strain measurement as shown in Table V.1-1.
3. Measure the weight of front and rear axle.
4. Prepare the measuring instruments and connect them.
5. Make the vehicle run as if the center of rear tires passes right on the survey

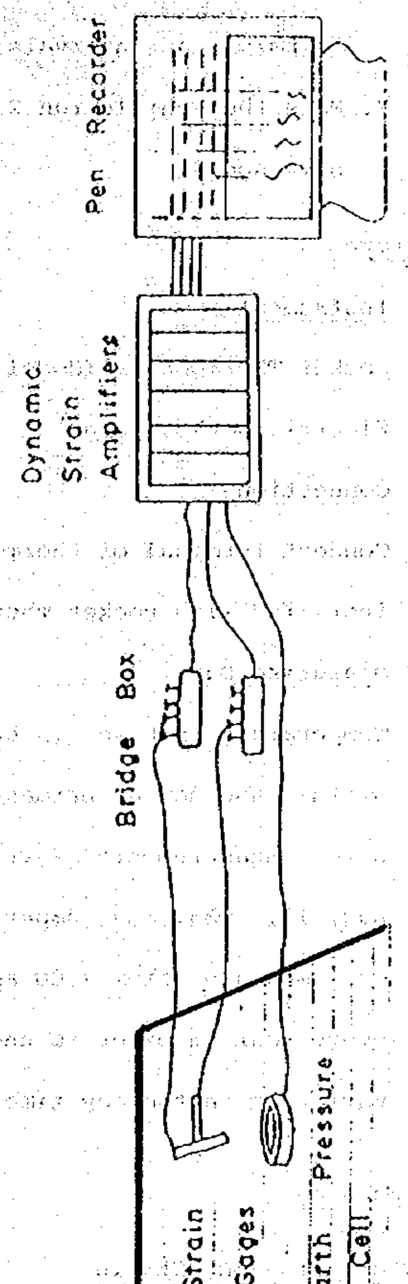

Fig. B-3. Dynamic Strain Measurement Method point. The loading condition is the same as condition B. in Fig. B-2.

6. Change vehicle speed from 5 km/hr. to 50 km/hr. at intervals of 5 km/hr.
7. Make the vehicle run 2 times under the same speed.

B.1.3 Temperature

B.1.3.1 Instrument

Pocket Thermometer (Model 2542 Tokogawa Electric Works, Japan)

B.1.3.2 Connection

Connect terminal of thermo-couple installed with Pocket Thermometer.

B.1.3.3 Measuring Date

Temperature in base has been measured at the same day as permanent and static strain measurement. Particularly on Aug, 13, 1983, the temperature in base were measured from 7.00 am to 5.00 pm. every hour in order to understand the variation in the day time.

B.2 Interpretation of Reading

B.2.1 Reading of permanent Strain

B.2.1.1 Definition of Curing Time

The soil-cement base construction in every sub-section was finished in the evening. In the end of the construction, strain gage, earth pressure cell, thermo-couple were installed. Initial reading (Initial Measured Value) was measured at about 9 a.m. in the day after the construction day. Therefore, curing time is defined to start from the day after the construction day as the initial day (0 day curing time)

B.2.1.2 Permanent Strain

Permanent strain is calculated as follows

$$\varepsilon_p = \varepsilon_m - \varepsilon_i \qquad \text{..........(1)}$$

where ε_P = permanent strain

ε_m = measured value concerned

ε_i = initial value on 0 day curing time

Permanent strain value expresses the comparison (difference) with initial value.

B.2.2 Reading of Static Strain

Static strain is calculated as follow.

$$\varepsilon_s = \varepsilon_m - \varepsilon_0 \qquad \text{..........(2)}$$

where ε_s = static strain

ε_m = measured strain under the loading condition

ε_o = measured strain under no loading condition

Static strain value expresses the strain amount caused by some load.

B.2.3 Reading of Dynamic Strain (See Fig.B-4)

Dynamic strain is calculated as follows.

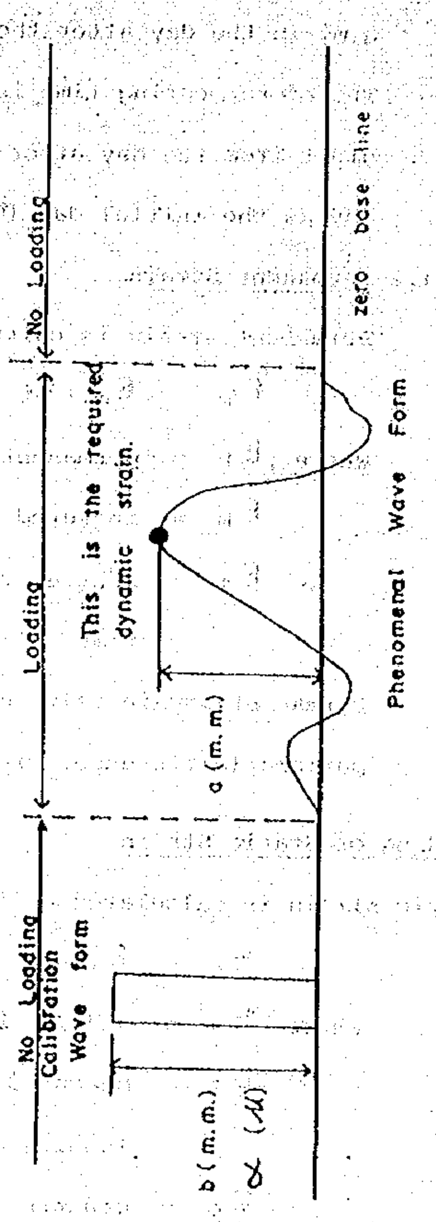

Fig. B-4 Example of the Recorded Dynamic Strain wave form

$$\varepsilon_d = \frac{a}{b} \times \alpha \quad \ldots\ldots\ldots\ldots\ldots(3)$$

Where ε_d = dynamic strain

a = measured length of the required dynamic strain on the chart paper (mm)

b = length of calibration on the chart paper (mm)

α = calibration strain value

If one wants to know more detail, refer to "Operation Manual, DPM-300 Series, Dynamic Strain Amplifiers".

B.2.4 Reading of Perssure Cell

B.2.4.1 Static Stress

Static stress is calculated as follows.

$$P_s = C_c \times (\varepsilon_m - \varepsilon_o) \quad \ldots\ldots\ldots(4)$$

where P_s = static stress (kg/cm.^{2})

C_c = calibration constant (kg/cm.^{2})

ε_m = measured strain under the loading condition.

ε_o = measured strain under no loading condition.

B.2.4.2 Dynamic Stress

Dynamic stress is calculated as follows

$$P_o = C_c \times \frac{a}{b} \times \alpha \quad \ldots\ldots\ldots\ldots(5)$$

where P_o = dynamic stress (kg/cm.^{2})

C_c = calibration constant (kg/cm.^{2})

a = measured length of the required dynamic stress on the chart paper (mm)

b = length of calibration on the chart paper (mm)

α = strain value of calibration

(see Fig. B-5)

B.2.5 Reading of Vehicle Speed

When we make the vehicle run above the earth pressure cell installed in the dynamic load test, we receive the recording as shown in Fig. B-6 (a)

Vehicle speed is calculated as follows.

$$V = \frac{c \times d}{e} \qquad \ldots\ldots\ldots\ldots (6)$$

where V = vehicle speed (cm/sec)

c = chart paper speed (cm/sec)

d = distance between the front wheel and the rear wheel of the vehicle (cm) (See Fig. B-6 (b))

e = distance between the front wheel phenomenon and the rear wheel phenomenon on the chart paper (cm)

B.2.6 Meaning of Indication + and - in Instrument

Owing to the instrument characteristics, that is, kind and connection of instruments, the meaning of

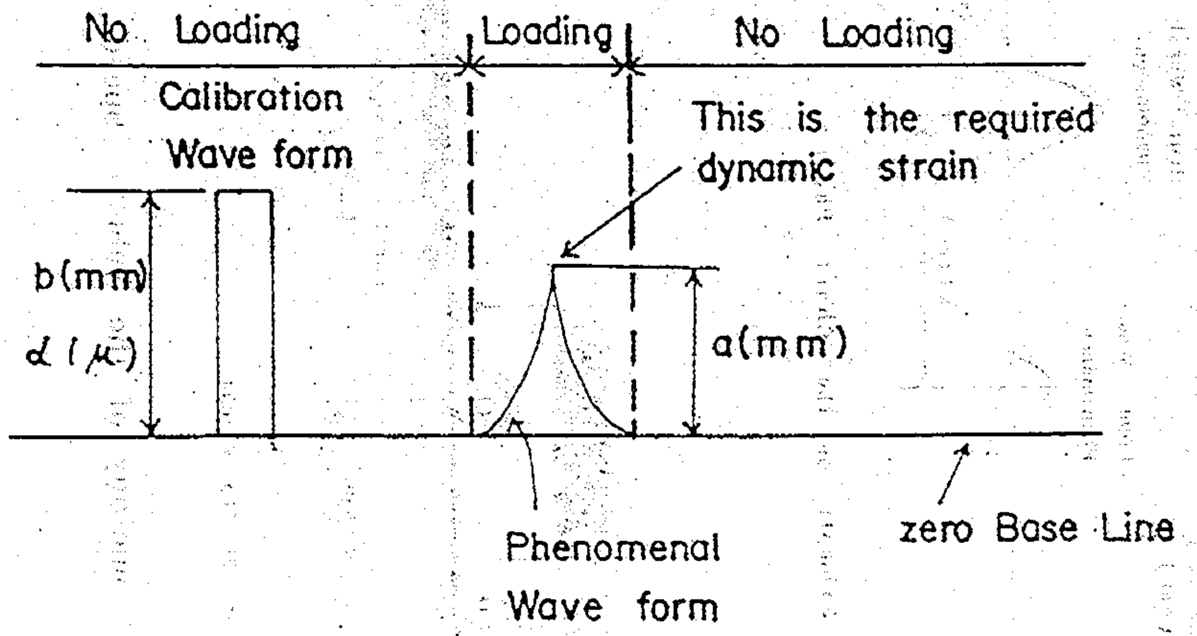

Fig B-5 Recording Example

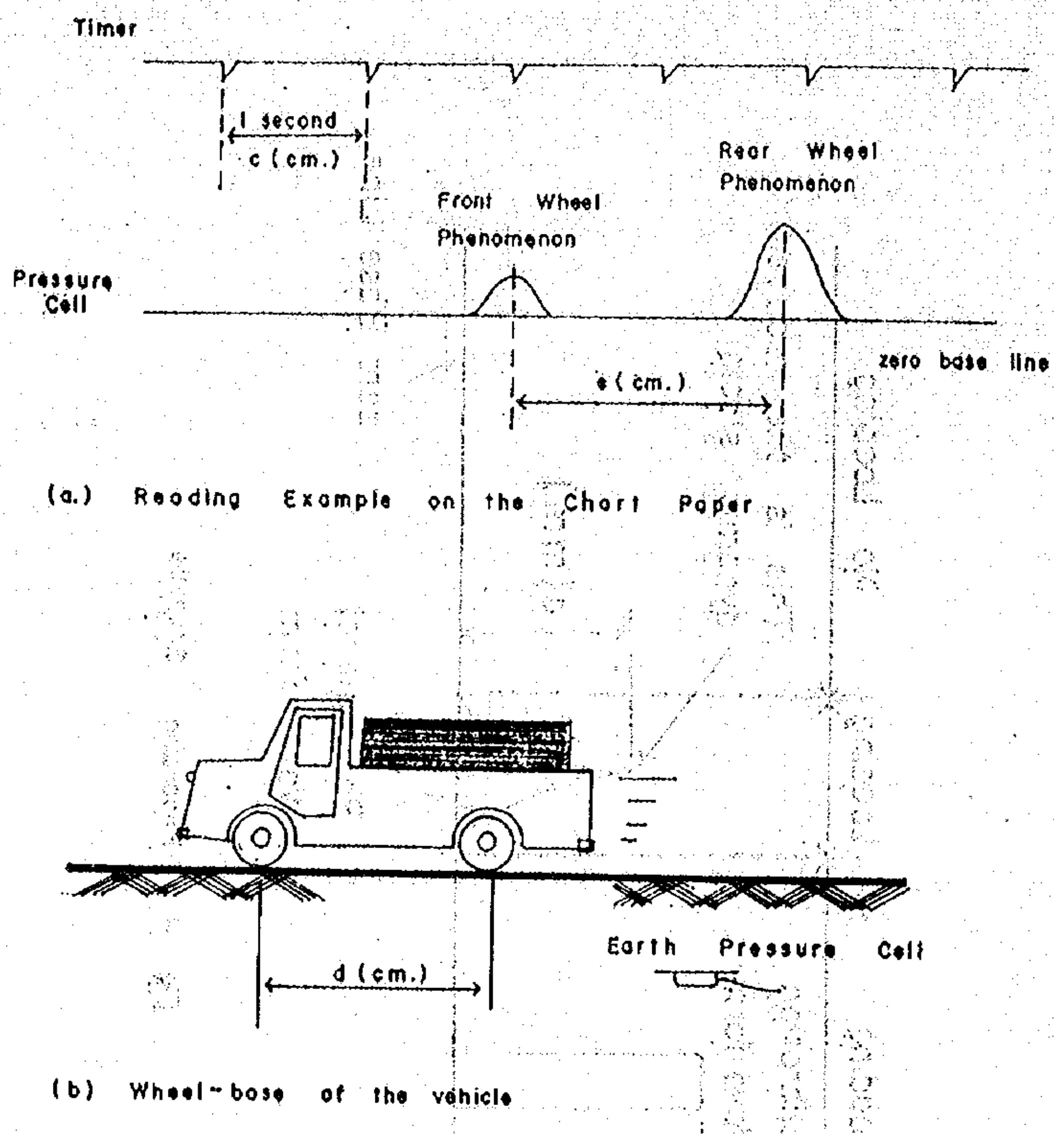

Fig. B-6 Analogy of the Vehicle Speed.

indication + and - changes.

Table B-1 shows the meaning of indication + and -.

B.3 Discussion of Stress and Strain Measurement

B.3.1 Stress Measurement

Pressure cell is used to detect strain through a minute change in the pressure-sensitive surface and converts it to an out put voltage proportional to the soil pressure.

In the structure, as shown in Fig.B-7(a), each 2 strain gages are set at 4 places in the outer ring and strain gage has a strain under the external force.

Calculation curve is made using oil pressure as shown in Fig. B-7(b)

Non-linearity is 2 % of Full Scale, 5 kg/cm.^{2} (71 psi.)

Therefore, we consider that we measure approximately correct pressure with this cell.

B.3.2 Strain Measurement

Strain gage is used for measurement of internal stress of mortar or concrete and embedded into these test materials for its application.

A special surface treatment is provided to secure good bonding with mortar, and due considerations are given for the water proofing property and

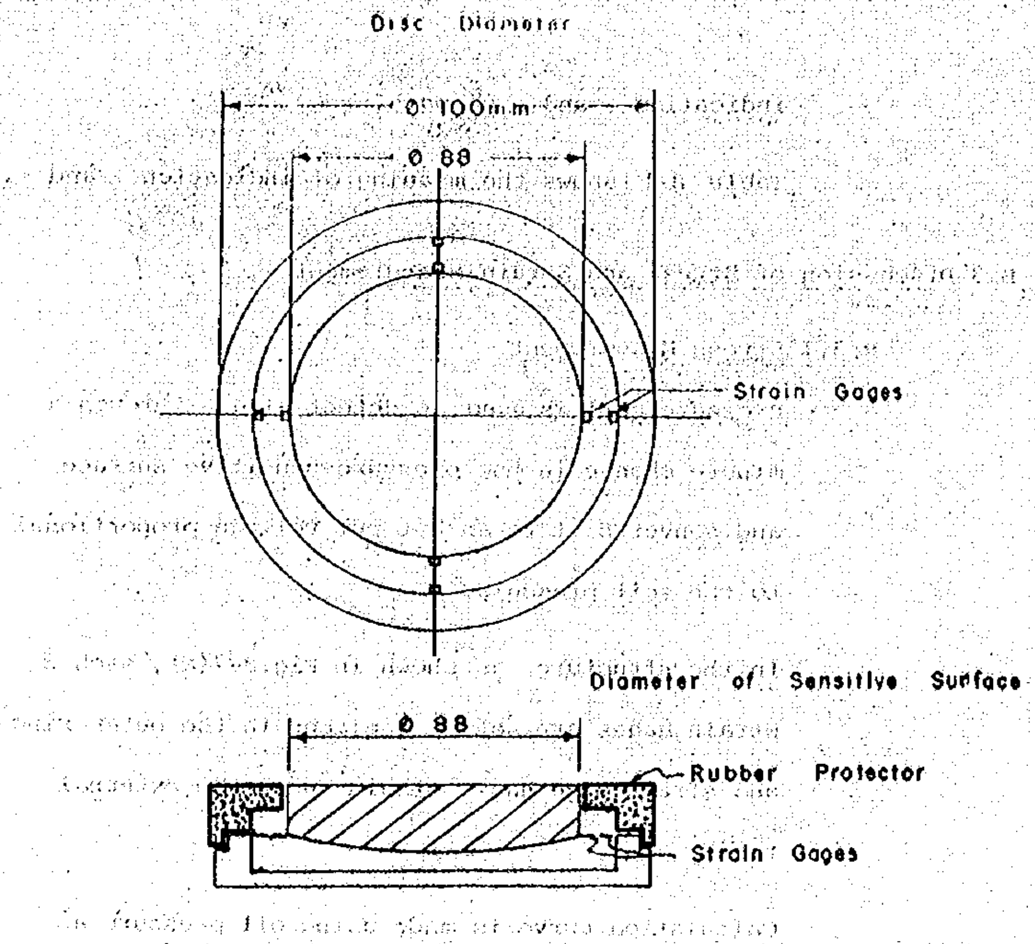

(a) Structure

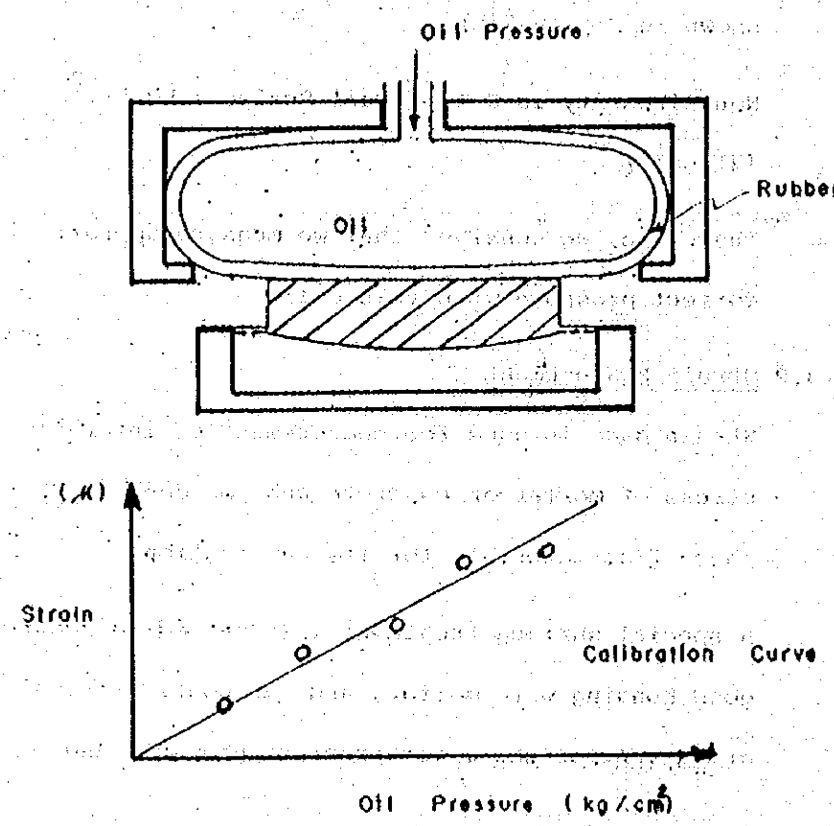

(b) Calibration

Fig. 8-7 Pressure Cell

as shown in Fig. B-8

In general, the elastic modulus of concrete is about 140,000 to 500,000 kg/cm^2 (2x10^6 - 71x10^6 psi.), while E of this kind of gage is 28,000 kg/cm^2 (40x10^4 psi.). So, the case of embedding it in concrete is no problem.

However, in this test, we have an attempt to embed it in the soil cement base. According to the results of Report No. MR. 85 the elastic modulus of soil-cement is about 5,000 to 15,000 lb/in^2 (352 to 1,054 kg/cm^2).

The Elastic modulus of the gage is bigger than that of soil cement. In this case, there is passibility that gage does not work or the slipping occurs around the gage. But there is not better kind of gage except this type of gage for embedding in soil cement in today's technology.

Let us emphasize that gage installation in soil-cement is trial.

In Analysis, if the deformation of soil cement is the same as that of gage material, stress can be calculated as follows.

$$\sigma = \varepsilon . E_s \qquad \text{..............(6)}$$

where σ = stress (kg/cm^2)

ε = strain (deformation)

E_s = Elastic modulus of soil cement (kg/cm^2)

In this test, the elastic modulus of the gage is bigger

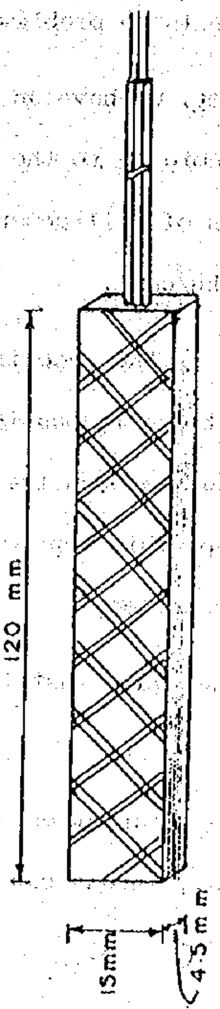

Fig. 8-8 Type KM embedment Gage.

than that soil cement, so, there is high possibility that the deformation where the gage's installation is smaller than that where no installation of the gage.

In calculating stress, the following idea is introduced. The stress in the gage is the same as the stress in soil-cement, so the stress in calculated as follows.

$$\sigma = \varepsilon E_G \quad \text{............(8)}$$

where σ = stress (kg/cm.^{2})

ε = strain

E_G = Elastic modulus of the gage (kg/cm.^{2})